Published in final edited form as:
*Adv Synth Catal*. 2014 July 7; 356(10): 2135–2196. doi:10.1002/adsc.201400017.

# Catalytic Isonitrile Insertions and Condensations Initiated by RNC–X Complexation

**Suravi Chakrabarty**[#a], **Shruti Choudhary**[#a], **Arpit Doshi**[#a], **Fa-Qiang Liu**[#a], **Rishabh Mohan**[#a], **Manasa P. Ravindra**[#a], **Dhruv Shah**[#a], **Xun Yang**[#b], and **Fraser F. Fleming**[b,*]

[a] Mylan School of Pharmacy, Graduate School of Pharmaceutical Sciences, Duquesne University, Pittsburgh, PA 15282-1530, USA

[b] Department of Chemistry, Duquesne University, Pittsburgh, PA 15282-1530, USA

[#] These authors contributed equally to this work.

## Abstract

Isonitriles are delicately poised chemical entities capable of being coaxed to react as nucleophiles or electrophiles. Directing this tunable reactivity with metal and non-metal catalysts provides rapid access to a large array of complex nitrogenous structures ideally functionalized for medicinal applications. Isonitrile insertion into transition metal complexes has featured in numerous synthetic and mechanistic studies, leading to rapid deployment of isonitriles in numerous catalytic processes, including multicomponent reactions (MCR). Covering the literature from 1990–2014, the present review collates reaction types to highlight reactivity trends and allow catalyst comparison.

### Keywords

catalysis; condensation; coupling; isocyanides; isonitriles

## 1 Introduction

Driven largely by an emphasis on multicomponent reactions,[1] the rich chemistry of isonitriles[2] is experiencing a renaissance.[3] The synthesis of isonitriles has blossomed because isonitriles provide a rapid entry into drug-like molecules, heterocycles,[4] and diverse molecular scaffolds.[5]

Isonitriles have a highly unusual structure. The isonitrile carbon bears a free electron-pair and is one of the few, naturally occurring stable carbenes.[6] Crystal-lographic analyses indicate that the isonitrile group is linear and not bent, suggesting structure **1″** as a better representation than implied by **1′** where the $sp^2$ N would suggest a trigonal structure (Figure 1). Infrared spectra are consistent with the isonitrile carbon–nitrogen unit having triple bond character. The IR resonance at ~2100 $cm^{-1}$ is only slightly less than those of the



* Fax: (+1)-412-396-5683; phone (+1)-412-396-6031; flemingf@duq.edu.

corresponding nitrile at ~2200 $cm^{-1}$. For simplicity, isonitriles are often drawn as in **1** with a triple bond but no charges.

The formal divalent character of isonitriles places them as carbene equivalents capable of sequentially adding a nucleophile and an electrophile. The carbon is weakly nucleophilic, and requires a potent electrophile partner such as the iminium ions that are intermediates in the Ugi reaction.[7] Dramatic progress in Ugi, Passerini, and related multicomponent additions has recently been reviewed.[1–3]

Isonitriles are emerging as key coupling partners in transition metal-catalyzed insertion reactions. Isonitriles readily associate with transition metals because of a strong s-donation from the lone pair on carbon with a simultaneous back donation into the excellent p*-acceptor orbitals of the NC unit.[7] Compared with their isoelectronic CO counterparts, isonitriles are stronger σ-donors which results in particularly strong complexes with metals in high oxidation states.[8] Conversely, the π-acceptor properties are weaker than those of CO resulting in poorer complexation to metals in low oxidation states.

A measure of the excellent ligating properties of isonitriles is gleaned from the ability of $CNCH_2CO_2Me$ to displace a tridentate pybox ligand from a palladium complex.[9] A similar ligand displacement with a pincer complex causes catalyst deactivation in one case and in another, modification of the catalyst through insertion, to form the true precatalyst.[10] Strong complexation of isonitriles through σ-donation and π-acceptance is exploited in hexakis(2-methoxyisobutylisonitrile)-$^{99m}$Tc(I), a radiotracer used for myocardial perfusion imaging.[11]

The excellent ligation of isonitriles to transition metals has been exploited to remove spent ruthenium from cross-metathesis reactions.[12] In many cases, metal coordination to isonitriles facilitates either internal or external nucleophilic attack to form carbene-ligated metal complexes.[13]

Catalytic turnover with isonitriles is challenging because of the strong coordination to transition metals. Metal coordination activates isonitriles toward nucleophilic attack and simultaneously retards dissociation. In some cases, adding the isonitrile slowly over the course of the reaction sufficiently retards isonitrile complexation to make catalysis viable.

Unlike catalytic cycles involving the insertion of CO, the analogous insertion of isoelectronic isonitriles is significantly less common. The challenge in catalyzing insertion reactions with isonitriles lies in preventing multiple insertions leading to polymers, and preventing irreversible complexation to the catalyst. Many catalytic cycles access medium-sized metallocycle intermediates in which an intramolecular reaction or reductive elimination is faster than further isonitrile insertion.

The most frequently used catalysts are palladium complexes. Several palladium complexes are capable of catalyzing reactions with isonitriles without ligand exchange or isonitrile insertion into the ligand.[14] Many reactions proceed through palladium(II) species, formed through oxidative addition, that react with isonitriles through an insertion into a palladium carbon bond. In several instances discrete palladium(II) complexes have been demonstrated

to react with isonitriles through an insertion mechanism to provide characterized intermediates.[14] Subsequent reductive elimination sequences close the catalytic cycle.

Facile coordination of isonitriles to metals increases the acidity of the adjacent protons. Deprotonation of metal-complexed isonitriles often proceeds with weak bases such as triethylamine.[15] Metallation affords nucleophiles that can react in stepwise alkylations and in concerted [3+2]cycloaddition with alkenes and alkynes.

This review surveys catalytic insertions of isonitriles into carbon-metal bonds and reactions catalyzed by activation of the isonitrile moiety. Although some catalysts function as Lewis acids, catalysts are only included if the isonitrile is activated rather than the electrophile. The catalysis therefore differs from Ugi and Passerini reactions where Lewis acid catalysts bind to the electrophile. Particularly interesting are several organic catalysts that activate isonitriles through hydrogen bonding. Only reactions with synthetically useful yields are included. An increased focus on isonitrile-activated reactions is loosely traced to 1990 which represents the earliest date of the articles included in the review.

The review is organized according to the product generated through the isonitrile condensation. In some cases the first-formed product is employed as an intermediate en route to a different target material, often a heterocycle. The categorization of catalytic methods by product type allows a direct comparison between different catalysts and catalytic cycles that is expected to facilitate future method development.

## 2 Aldol-Type Condensations

Lewis acidic metals activate isonitriles toward deprotonation. The resulting nucleophiles react with imines and aldehydes to form aldol-type intermediates, which typically react further by attacking the isonitrile function. Isocyanoacetates are easily deprotonated in the absence of a Lewis acid catalyst and often the background non-catalyzed condensation occurs at a similar rate. Overall the condensation provides a route to oxazolines and imidazolines.

During the multicomponent condensation of α-acidic isocyanides with ketones and primary amines, the formation of 2*H*-2-imidazolines was catalyzed by AgOAc [Eq. (1)].[16,17] Substituted isocyanoacetates **2**

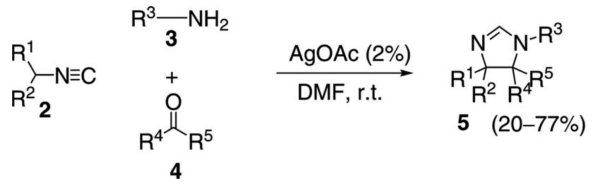


(1)

($R^1$=$CO_2R^6$) form 2-imidazolines **5** readily in DMF, but the conversion is incomplete in other solvents unless AgOAc is added. Isocyanoamides are similarly activated by AgOAc or CuI.

AgOAc activates isonitrile **2** toward deprotonation by complexing to the isonitrile carbon (Scheme 1). Deprotonation of the silver-isonitrile complex **6** by acetate yields the nucleophile **7**. Nucleophilic attack of **7** on iminium **8** affords **9**, possibly through an *anti* transition structure to minimize steric demand, which sets the *trans* stereochemistry in the imidazoline. Subsequent intramolecular attack by the amine onto the isonitrile affords argentate **10**. Proton transfer, formally within **10**, yields 2-imidazoline **5** and regenerates the catalyst.

CuCl and $PPh_3$ catalyze the condensation of methyl isocyanoacetate (**11a**) with aldehydes **12** [Eq. (2)].[18] The mechanism of this aldol-type condensation, like

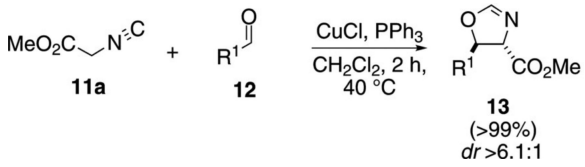


(2)

most similar condensations, directly follows Scheme 1 with aldehyde **12** substituting for the iminium **8**. All the reactions were quantitative and exhibited a high preference for the *trans*-oxazoline **13**.

Methyl isocyanoacetate (**11a**) was condensed with a series of ketones **4** to afford substituted oxazolines **14** [Eq. (3)]. Extensive base and catalyst screening

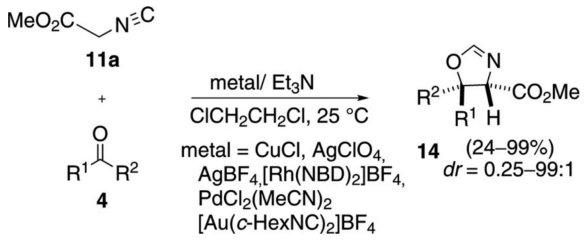


(3)

identified $AgClO_4$, $AgBF_4$, CuCl, and AgOAc as competent catalysts.[19] Methyl isocyanoacetate (**11a**) is easily enolized and the uncatalyzed aldol condensation is particularly favorable in polar solvents.[20] The condensation with electron-deficient ketones work well. Unactivated ketones such as acetophenone require heating to 50°C for 24 h. Aliphatic ketones fail to react completely, affording oxazolines **14** with yields less than 37%. Typically the *trans*-oxazoline **14** is the major diastereomer.[21]

A series of oxazolines **14** was prepared by condensing methyl isocyanoacetate (**11a**) with aldehydes **12** or ketones **4** [Eq. (4)].[22] The copper(I) salts CuCl and

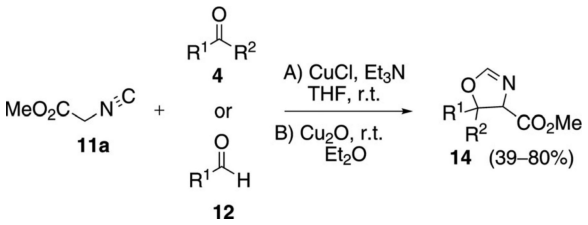


(4)

$Cu_2O$, were found to be more efficient than either *t*-BuOK or $ZnCl_2$, providing a direct comparison of catalytic and non-catalytic methods.

A hydroxyapatite-bound cationic ruthenium complex catalyzes the condensation of methyl isocyanoacetate (**11a**) with benzaldehyde (**12a**) [Eq. (5)].[23]

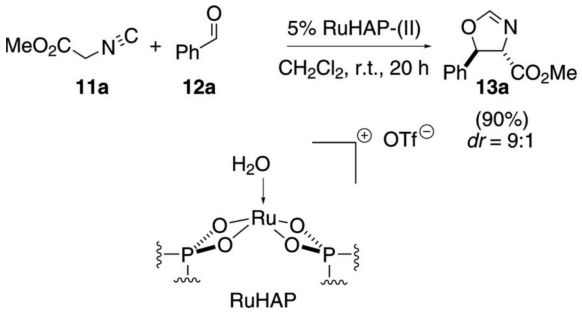


(5)

Copper iodide catalyzes the condensation of ethyl isocyanoacetate (**11b**) with *ortho*-hydroxyphenyl ketones **15** [Eq. (6)]. Methanol is the optimal solvent because the aminocoumarins **16** are insoluble and can

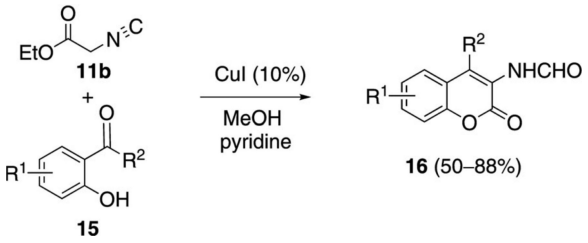


(6)

be isolated simply by filtration. The condensation is interesting in affording lactones rather than oxazolines.

The formation of aminocoumarin **16** involves inter- and intramolecular events. Copper iodide complexes to isonitrile **11b** and, in the presence of pyridine, forms the copper enolate

**17a** (Scheme 2).[24] The structure of the copper enolate **17a** has not been determined and although depicted with copper bound to carbon, the solution species could be an oxygen-bound enolate or an equilibrium mixture of the two species. Attack of **17a** on the carbonyl of **15** affords **18**. Proton transfer within **18** generates **19** which is poised for an intramolecular lactonization to afford **20**. Cyclization of the alkoxide **20** on the activated isonitrile affords **21**, a process which may precede closure of the lactone. Protonation of the copper-carbon bond of **21**, opening of the oxazoline **22**, and reprotonation, affords the aminocoumarin **16**.

Despite the wealth of catalysts developed for the isocyanoacetate aldol condensation, the synthesis of manzacidin B represents the first use of this reaction in total synthesis. A key step in the synthesis employed catalytic CuCl in the condensation of *tert*-butyl isocyanoacetate (**11c**) with oxazolidine aldehyde **12b** [Eq. (7)].[25] The facial attack on the aldehyde is dictated


(7)

by the aminal chirality whereas CuCl controls the diastereoselectivity, favoring the *trans*-oxazoline **13b**.[25]

The copper-catalyzed reaction of isocyano ester **11**, 2-(2-ethynylphenyl)oxirane **23** and sulfonyl azide **24**, [Eq. (8)] proceeds through two catalytic cycles to give

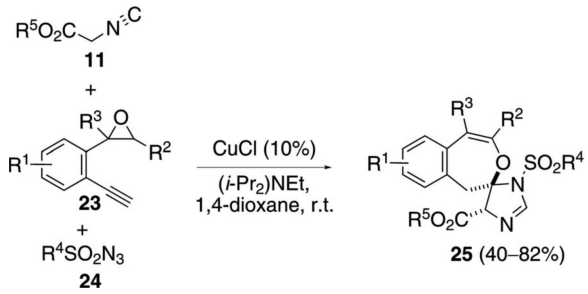


(8)

spirocyclic imidazolines **25** (Scheme 3 and Scheme 4).[26] Solvent and base were screened and the aromatic substituents ($R^1$=H, Cl, F, OMe) of the epoxide substrate were varied.

In the first catalytic cycle, CuCl catalyzes the condensation of epoxide **23** with the sulfonyl azide **24** to generate **30** (Scheme 3). Presumably the reaction proceeds *via* a copper-catalyzed deprotonation of **23** with (*i*-Pr)$_2$NEt followed by cycloaddition with **24**. Copper

migration and loss of nitrogen from **26** forms the ketenimine **27**. Intramolecular nucleophilic attack of the epoxide onto the ketenimine leads to **28** that engages in a ring opening proton transfer to furnish **29**. Protonation of **29** regenerates CuCl and releases imine **30**.

The condensation of imine **30** with isocyanoacetate **11** is formally a CuCl-catalyzed [3+2]cycloaddition (Scheme 4). CuCl-assisted deprotonation of isocyano acetate **11** affords **17** that attacks imine **30** to form **31**. Intramolecular cyclization of **31** to **32** and protonation of the carbon-copper bond affords the imidazoline **25** and regenerates CuCl and $(i\text{-Pr})_2$NEt.

Screening various ligands with CuCl identified complex **34** as an effective catalyst for the condensation of methyl isocyanoacetate (**11a**) with imines **33** [Eq. (9)]. The yield was quantitative with a high preference for *trans*-imidazolines **35**.[27]

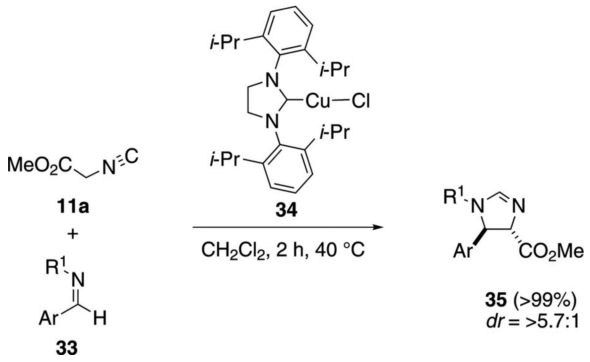


(9)

The ruthenium-catalyzed reaction of isocyanoacetamide **36a** with *N*-sulfonylimines **37** affords *trans*-2-imidazolines **38** [Eq. (10)].[28] When less than

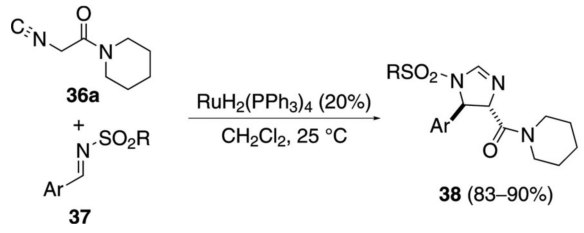


(10)

20 mol% catalyst is used, the yield of 2-imidazoline **38** decreases and an oxazole is formed competitively.

Although the mechanism of the ruthenium condensation is not known, the catalytic cycle likely follows the general isonitrile-aldol sequence (Scheme 1). Isonitrile activation by ruthenium presumably generates a metallated isonitrile or an enolate that condenses with the imine through either a [3+2]cycloaddition or by sequential addition–cyclization and protonation.

$RuH_2(PPh_3)_4$ catalyzes a similar condensation of methyl isocyanoacetate (**11a**) with *N*-sulfonylimines **39** to afford *trans*-imidazolines **40** [Eq. (11)].[29] A methanol-dichloromethane solvent mixture provided the optimal diastereoselectivity and chemical yield. Tosyl- and phenylsulfonylimines having aliphatic and aromatic substituents react equally well.

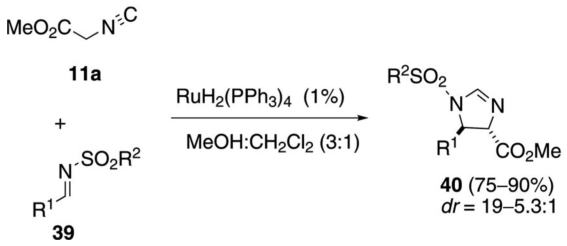


(11)

The active catalyst **42a**, for the condensation of methyl isocyanoacetate (**11a**) with **39**, is presumed to form *via* hydrogen extrusion from $RuH_2(PPh_3)_4$ and coordination of $Ru(PPh_3)_4$ to **11a** (Scheme 5). Oxidative addition of ruthenium into one of the acidic methylene protons affords the enolate **43a** that attacks imine **39** to afford the ruthenacycle **44**. Migration of the metal-nitrogen bond with concomitant attack on the isonitrile carbon affords **45**. Coordination of another isonitrile **11a** and reductive elimination regenerates active catalyst **42a** and affords the *trans*-imidazoline **40**.

An aldol condensation of the chiral isonitrile-amide **36b** with the chiral aldehydes **12c** or **12d** was highly stereoselective (Scheme 6).[30] Screening copper sources identified a copper salen complex as the most diastereoselective metal. The selectivity is rationalized by assuming that the copper-complexed isonitrile eno-late **46**, selectively attacks the aldehydes **12c** or **12d** from the top face.

Catalytic copper iodide promotes the reaction of activated isonitriles **49** with oxazolones **50** to form bisoxazoles **51** [Eq. (12)].[31] The isonitrile activating

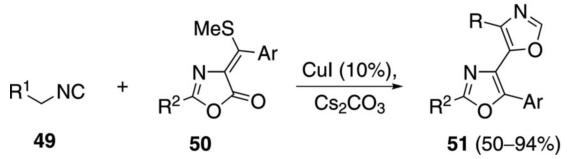


(12)

group can be sulfonyl, ester, pyridyl, amide, or a substituted phenyl group.

As with many copper-catalyzed reactions with activated isonitriles, the copper facilitates deprotonation to afford an isocyano enolate (**49**→**17**, Scheme 7). Attack of enolate **17** onto the carbonyl of **50** generates enolate **52** which engages in a proton transfer to form enolate **53**. Cyclization of **53** leads to **54**. Protonation of **54** by the activated isonitrile releases **55**

that reacts with a copper(I) species accompanied with deprotonation by $Cs_2CO_3$ to afford **56**. Reductive elimination from **56** releases the copper(I) species and the bisoxazole **51**.

Pincer metal complexes **59** have been used extensively in platinum- and palladium-catalyzed aldol condensations to afford oxazolines **13** and imidazolines **58** [Eq. (13)]. The condensations exhibit a high preference

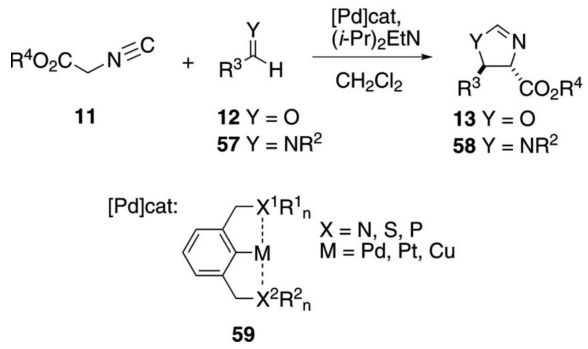


(13)

for the *trans*-diastereomer in which the alkyl group $R^3$ and the ester reside on opposite sides of the oxazoline or imidazoline ring.

All pincer complexes catalyze the aldol condensation of isocyanoacetates *via* essentially the same catalytic cycle (Scheme 8). The pincer precatalyst typically has a labile ligand (halide, water, triflate), providing a vacant coordinating site for isocyanoacetate **11** to bind to. Mechanistic studies show that the isonitrile binds particularly strongly to the metal center, implying that the palladium-isonitrile bond is best considered as a covalent bond.[32] Deprotonation of the metal-bound isonitrile is facile and does not necessarily require added base to form the enolate **61**. The slow step of the pincer-catalyzed aldol condensation is the attack of the coordinated isonitrile enolate **61** on the aldehyde or imine.[33] Subsequent internal attack on the isonitrile transforms **62** to the metallated heterocycle **63**. Coordination of **11** and concomitant protonation of **63**, releases the heterocycle and the pincer complex **60**.

Pincer complexes vary primarily in the nature of the ligated heteroatom coordinated with the metal ion and in the substituents on this ligand. Although the metal ion can be varied, palladium is the most common metal used in pincer complexes for isocyanoacetate condensations. Usually the diastereoselectivity is very high. Many catalysts incorporate a deep binding pocket at the metal site to create a chiral environment for imparting enantioselectivity. Despite much variation, high enantioselectivity remains elusive.[34]

### 2.1 Aldol Condensations with $C_2$-Symmetrical NCN Pincer Complexes

The oxazoline-derived pincer complexes **64a–c** catalyze the condensation of methyl isocyanoacetate (**11a**) with benzaldehyde (**12a**) to form the *trans*-oxazoline **13a** [Eq. (14)].[34] No enantioselectivity was reported, which is typical for this type of pincer-catalyzed condensation. The iminocyclohexane pincer complex **64b** exhibits a very similar

profile affording **13a** with a dr of 4:1. Similarly, the chiral bis-pyridine complex **64c** catalyzes the formation of **13a** (*dr*=3:1) but the background reaction accounts for at least 50% of the conversion. Not surprisingly, the isoxazole **13a** was racemic.[35] The corresponding platinum complex exhibits the same diastereoselectivity profile.

Pincer-catalyzed condensations of TosMIC (**49a**, $R^2$=$SO_2$Tol) with various aldehydes exhibited the best selectivity with the cationic aqua platinum catalyst **66** (M=Pt) [Eq. (15)].[36] The *tert*-butyl-substituted complex **66** ($R^3$=*t*-Bu) was virtually inactive whereas the enantioselectivities using Ph, Bn, and *s*-Bu alkyl substituents were distinctly lower than that

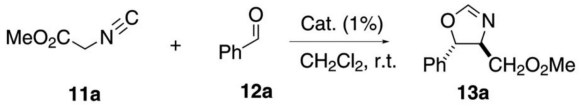


**11a** **12a** **13a**

Catalysts:

(14)

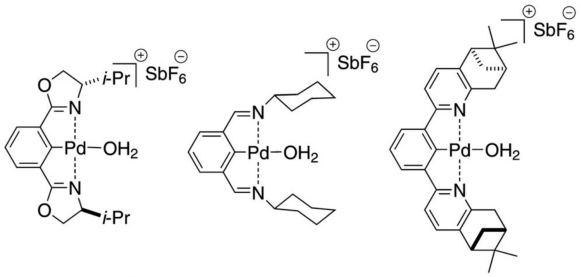


**64a** (95%) *dr* = 4:1 **64b** (75%) *dr* = 4:1 **64c** (70%) *dr* = 3:1 *er* = 56:44

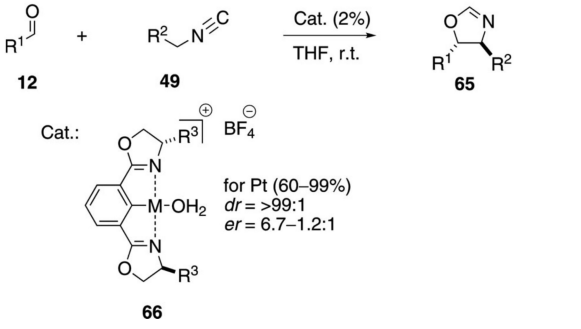


**12** **49** **65** **66**

(15)

of the corresponding *i*-Pr complex. Only the *trans*-diastereomer was detected with reasonable levels of enantioselectivity. Analogous condensations of methyl isocyanoacetate (**11a**) with aldehyde **12** and catalyst **66** (M=Pt, $R^3$=*i*-Pr) were distinctly less selective than for the corresponding condensation with TosMIC.

The diphenylhydroxymethylpyrolidinyl pincer complex **67a** catalyzes the condensation of methyl isocyanoacetate (**11a**) with aromatic aldehydes **12** [Eq. (16)].[36] Although the preference for the *trans* diastereomer

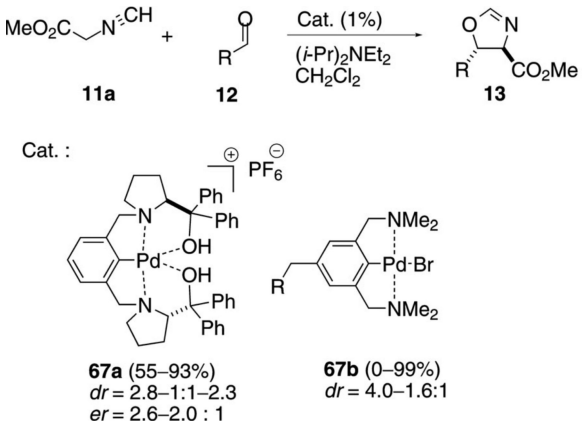


(16)

is modest, there is a changeover with *ortho*-methoxybenzaldehyde in favoring the *cis* diastereomer. Most interesting is a modest enantioselectivity in the condensation, which is higher for the *cis* diastereomer than for the *trans* diastereomer. There is essentially no change in the diastereoselectivity when the counter ion $PF_6$ is replaced by $BF_4$.

A series of complexes **67b** was prepared in which the substituent R contained an amino acid linked through an amide or ester.[37] No enantioselectivity was observed for the **67b**-catalyzed condensation of **11a** with benzaldehyde, and the diastereoselectivity was modest.

The pincer complexes **67c** and **68** coordinate one hydroxy or carbonyl group to fully saturate the coordination sphere of the cationic palladium complexes (Figure 2).[34,38] Fast coordination and dissociation takes place in solution, allowing the isonitrile to coordinate and be activated by the metal center. The catalysts afforded oxazolines with modest *dr* and *er*.

## 2.2 Aldol Condensations with PCP and SCP Pincer Complexes

The generally poor stereoselectivity with chiral pincer complexes such as **64a–c** stimulated shifting the chirality from a nitrogenous ligand to a phosphine ligand. The $C_2$-symmetrical phosphine pincer **69** was used to condense methyl isocyanoacetate (**11a**) with an aldehyde [Eq. (17)]. The diastereoselectivity was high but

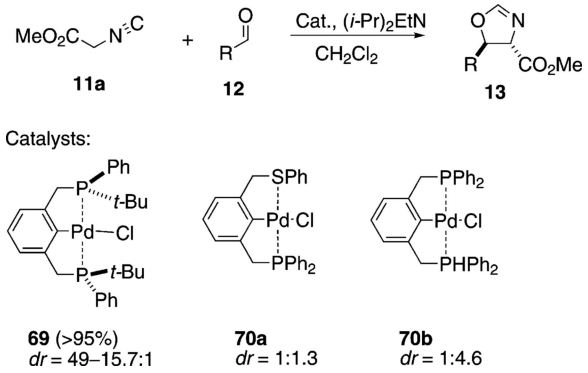


(17)

the enantioselectivity was never greater than 1.3:1. The platinum analogue of **69** exhibited no catalytic activity.[39]

The non-symmetrical, achiral pincer complex **71a** was prepared and the catalytic activity compared with that of the symmetrical pincer complex **71b** [Eq. (17)].[40] Both complexes are *trans*-selective with non-symmetrical **71a** being the least selective and most reactive.

Complexes **71a** and **71b** are precatalysts which incorporate isocyanoacetate to afford active catalyst **72a** or **72b**, respectively [Eq. (18)]. The insertion

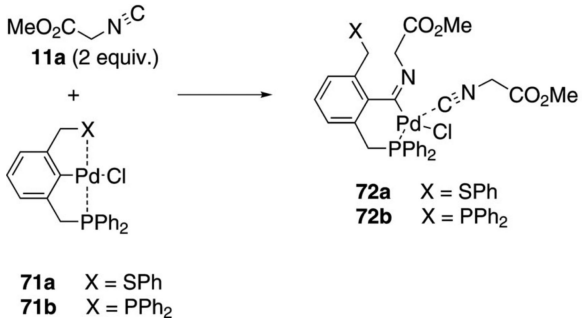


(18)

occurs by dissociation of one ligand, isonitrile coordination, followed by isonitrile insertion. For the un-symmetrical complex **72a**, the phosphine remains coordinated while the PhS ligand is free.

Extensive optimization with the chiral pincer complex **71c** was rewarded with the highest enantiomeric ratio in a pincer-catalyzed aldol condensation [Eq. (19)].[41] Treating **71c** with silver chloride provided

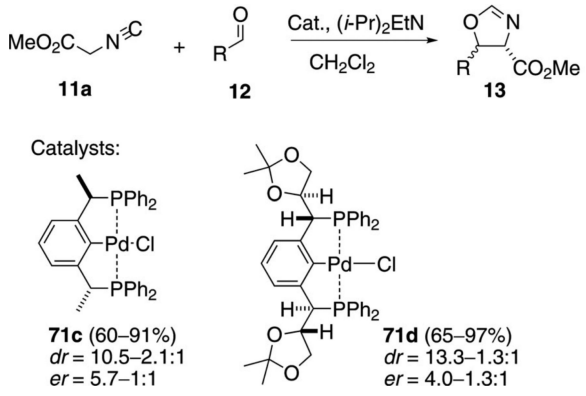


(19)

a catalyst with significantly more activity than the platinum analogue. The aldol condensations of methyl isocyanoacetate (**11a**) and diverse aldehydes **12** afford mixtures of *trans*- and *cis*-oxazolines **13**. The highest *er* was obtained with mesityl aldehyde (*er*=5.7:1) indicating that installing chirality on the benzylic carbon is a feasible strategy for stereocontrol with pincer complexes. Catalyst **71d**, bearing a chiral benzylic substituent, also reacts with a variety of aldehydes to afford *trans*-oxazolines with good diastereo-selectivity and similar enantioselectivity.[42]

Palladium complexes **73a–c** catalyze the condensation of methyl isocyanoacetate (**11a**) with sulfinylimines **39a** [Eq. (20)].[43] The biphenanthrol catalyst

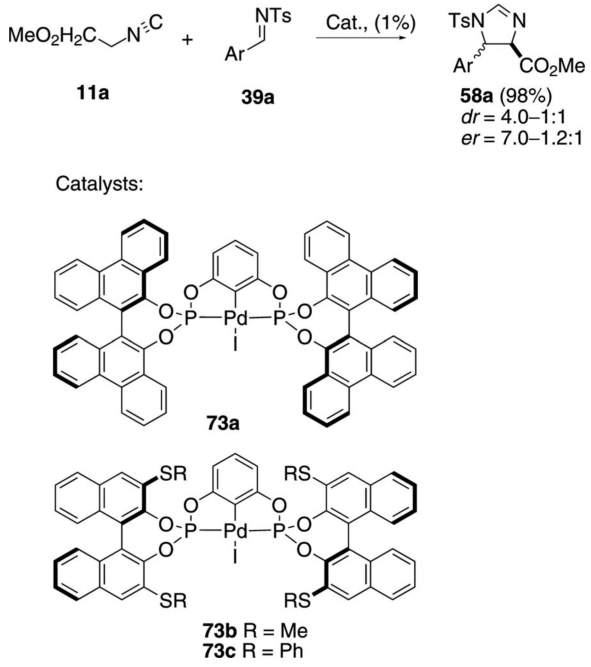


(20)

**73a** provided higher selectivity than the binol complexes **73b** and **73c**, although the diastereoselectivity is modest with both catalysts (4.0–1.0:1). The enantioselectivity was higher with the sterically more demanding catalyst **73a** than for the corresponding binol complex **73b**, affording a 7:1 enantiomeric ratio with the imine derived from benzaldehyde. All catalysts gave better enantioselectivity for the minor *cis*-imidazoline diastereomer.

## 2.3 Immobilized Pincer Complexes

Bimetallic palladium complex **73d** catalyzes the aldol condensation of methyl isocyanoacetate (**11a**) with aldehydes **12** to form oxazolines **13** [Eq. (21)].[44] Each palladium atom is coordinated to an SCS-type ligand with the two pincer units linked by a chiral spacer. There is no cooperativity between the metal centers. The enantioselectivity is virtually non-existent as expected for such remote chirality. The chiral acetal was used to link the catalyst to silica to form a catalyst which showed essentially the same profile as catalyst **73d**.

The NCN-pincer complex **73e** incorporates a pyrene unit as a fluorescent tag [Eq. (22)].[45] The

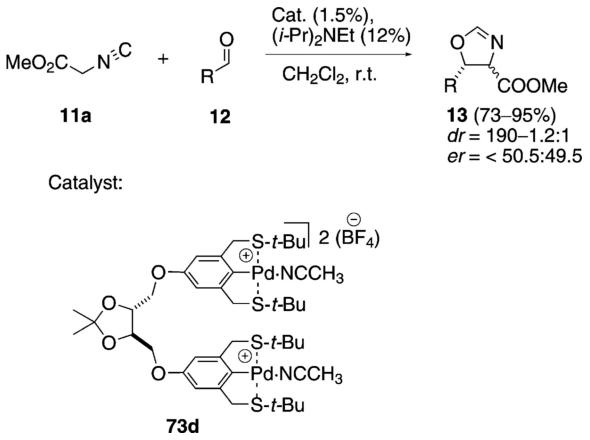


(21)

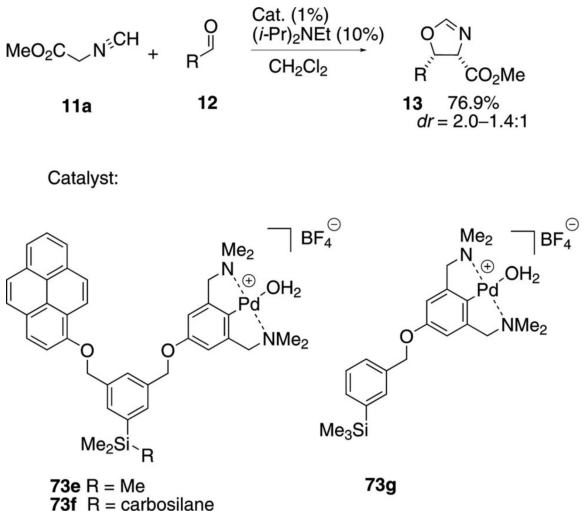


(22)

trimethylsilyl substituent on **73e** and **73g** provides a solution mimic for the carbosilane-immobilized analogue **73f**.[46] A related silicon tether strategy allows pincer complexes to be incorporated within dendrimers.[47] The carbosilane allows for catalyst recycling by nanofiltration. The tweezer-pincer complex **73e** has a small rate enhancement relative to **73g** indicating possible cation-π interaction perhaps because of a faster isonitrile ligation or association with the aromatic aldehyde. The silane complex **73f** catalyzes a slower condensation than **73e**, although the total turnover numbers are similar for the two catalysts.[48] The diastereoselectivity was the same with all three catalysts.

Palladium(II) bis(amino)aryl NCN pincers **73h–j** were attached to $C_{60}$ through three different linkers [Eq. (23)].[40] All three immobilized catalysts, and the parent **73k**, gave very similar rates and diastereoselectivity. The large size of the $C_{60}$-linked complexes provides retention in continuous-flow processes.

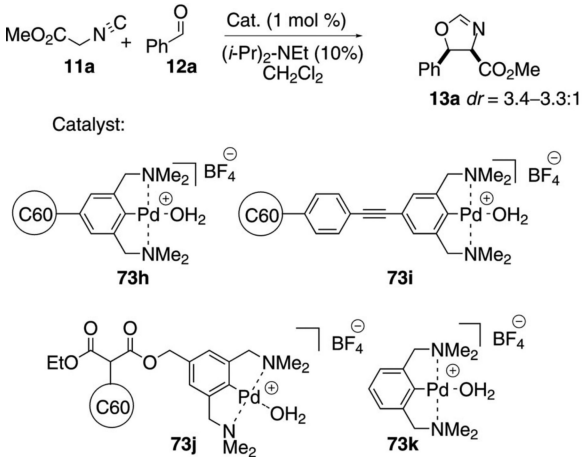

(23)

The non-symmetrical cyclometallated platinum complex **73l** provides excellent diastereoselectivity in the aldol condensation of methyl isocyanoacetate (**11a**) with aldehydes **12** [Eq. (24)].[42] In contrast, there is virtually no enantioselectivity.

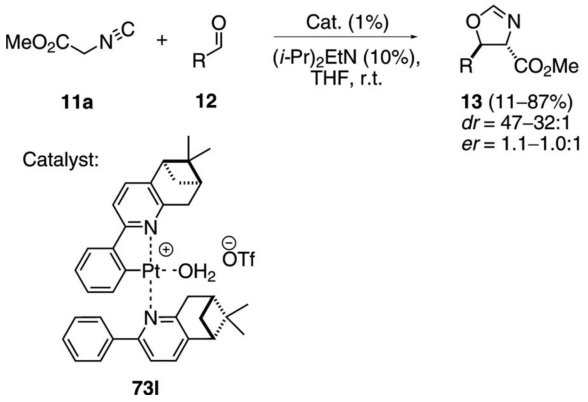


73l

(24)

## 2.4 Aldol Reactions Promoted by Cooperative Catalysts

Cooperative catalysis, in which a multifunctional organic scaffold is combined with a transition metal, is emerging as a powerful tool in asymmetric synthesis. The diastereoselective condensation of methyl isocyanoacetate (**11a**) with aldehydes (**12**) is representative [Eq. (25)].[50] The condensation employs $CoI_2$, chiral ligand **74**, and the thiourea organocatalyst **75**. NMR analysis indicates that **75** binds to the isonitrile. Although the reaction is catalyzed by $CoI_2$ alone, the thiourea improves the diastereomeric ratio from 1.2 to 5.7:1. Dioxane is added as a co-solvent to improve the solubility of the cobalt catalyst.

The catalytic cycle engages a thiourea-complexed isonitrile **77** with the cobalt catalyst-ligand complex **76** (Scheme 9). A downfield shift of the thiourea NH

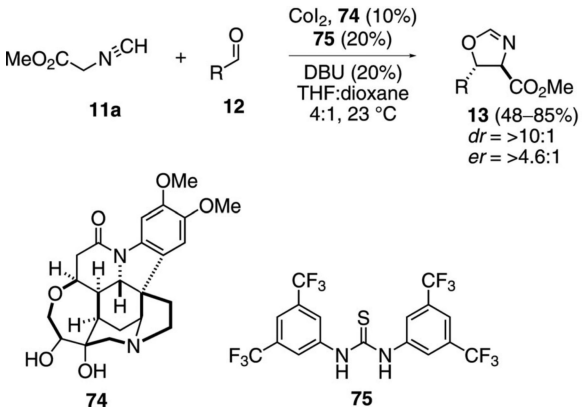


74 75

(25)

signal occurs on adding the isonitrile **11a** to the thiourea **75**, suggesting formation of complex **77** prior to deprotonation by DBU. Side products include an aldol arising from condensation without cyclization, consistent with isonitrile activation by the thiourea and not the metal center. Ligation of the enolate to cobalt complex **76** forms **78** in which a key hydrogen bond between the hydroxy and the enolate oxygens anchors the two groups in a specific orientation. Condensation within the preorganized complex **78** leads to **79** that cyclizes internally to provide **80**. Protonation of **80** releases the oxazoline **13** and regenerates the cobalt catalyst. In addition to high selectivities, the reaction provides a high yield with both aromatic and aliphatic aldehydes.

Several organocatalysts incorporate two different functional groups to bind and activate a substrate. The chiral thiourea **82** functions as a bifunctional organocatalyst in catalyzing the addition of isocyanoacetate **81** to imines **39b** [Eq. (26)].[51] Extensive optimization

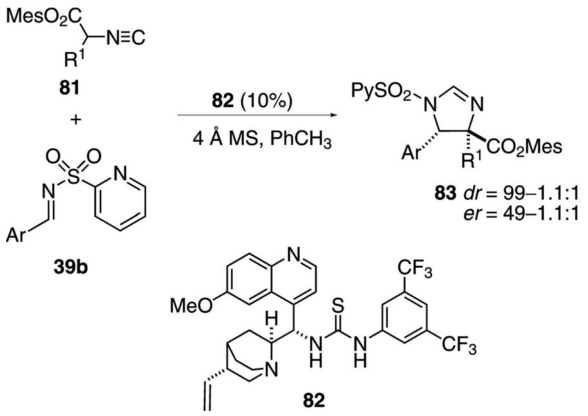


(26)

identified the requirement for the pyridylsulfonyl imine **39b** suggesting a two point binding between the catalyst and the pyridine and imine nitrogens. The reaction tolerates diverse substituents in the imine, with an aromatic substituent $R^1$ in the isonitrile affording the best stereoselectivity.

A key design feature of organocatalyst **82** is the presence of the thiourea for hydrogen bonding to the isonitrile (Scheme 10).[52] Hydrogen bonding between the isonitrile **81** and the organocatalyst **82** aligns the complex **84** for internal deprotonation. The enolate reorganizes to **85** with the enolate oxygen complexed to the thiourea. Anchoring of the imine to the ammonium ion by the two nitrogens within **85** is speculated to control the geometry and set the stereochemistry in imidazoline **83**. Attack of the sulfonamide nitrogen of **86** onto the isonitrile followed by protonation, affords **83** and regenerates catalyst **82**.

Organocatalyst **82** effectively catalyzes the condensation of phenyl isocyanoacetate **87** with protected methyleneindolinones **88** [Eq. (27)].[53] The reaction tolerates halogen and alkyl substituents in the indolinones. α-Alkyl isocyanoacetates are not sufficiently acidic to participate in the reaction. Subtle interactions control the stereoselectivity, with the phenyl amide-protected indoles **88a** affording *anti*-diastereomers and Boc-protected indoles **88b**

favoring *syn* diastereomers. The catalytic cycle is presumably analogous to that for imine condensations (Scheme 10).

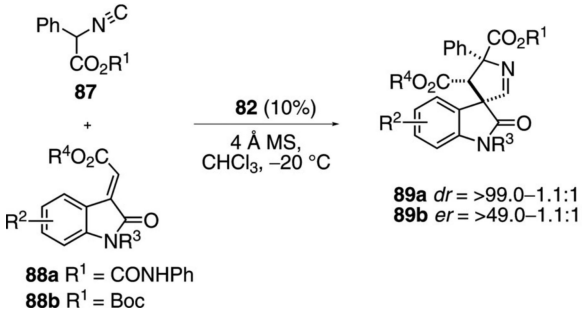


(27)

Silver oxide complexed with the chiral aminophosphine ligand **91**, catalyzes the condensation of isocyanoacetate **90** with aldehydes **12** to form oxazolines **13** or **92** [Eq. (28)].[54] Control experiments establish that both silver and the ligand are required for catalysis. Aromatic aldehydes and sterically hindered aliphatic aldehydes give high selectivities. Non-substituted isocyanoacetates (**90**, $R^2$=H) afford *trans*-oxazolines **13** whereas substituted isocyanoacetates **90** afford the *cis*-diastereomers **92**.

The chiral phosphine ligand **91** contains a coordination site for complexing silver and a bridgehead nitrogen

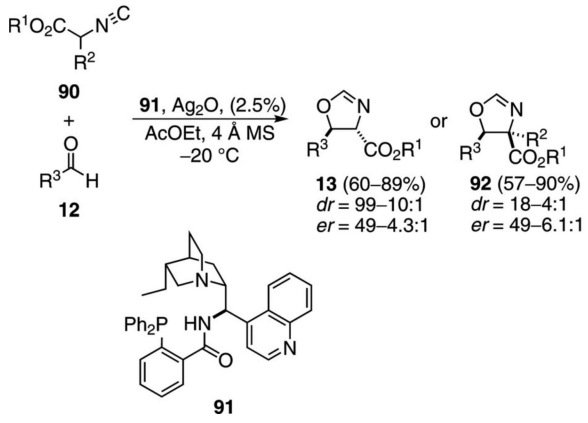


(28)

capable of deprotonating the activated isonitrile (Scheme 11). Complexation of silver oxide to the phosphine **91** likely creates the active catalyst **93** *in situ* (Scheme 11). Isonitrile complexation to **93** allows internal deprotonation by the tertiary amine, forming an ammonium ion that associates with the enolate in **94**. Attack on the aldehyde is directed by the chiral environment created through complexation, leading to the alkoxide **95**. Cyclization of **95** affords **96**. Protonation of the silver-carbon bond by the ammonium ion releases the oxazoline **13** or **92** and allows the catalyst to re-enter the catalytic cycle.

One of the first catalytic isonitrile-type aldol reactions was the condensation of methyl isocyanoacetate (**11a**) and aldehydes **12** promoted by the bifunctional gold ferrocenylphosphine complex formed with ligand **97** [Eq. (29)].[55] Modification of the terminal amino

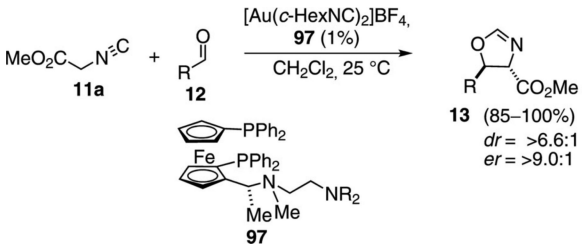


(29)

group has a significant influence on the diastereoselectivity.[56] Solution NMR analysis of analogues in which the stereochemistry of the secondary methyl group is varied indicate that the substituent controls the conformation required for catalysis.[57] Changing the length of the tether decreases the selectivity.

The gold-catalyzed condensation of isocyanoacetate with aldehydes requires the planar chirality induced by the ferrocene and the chirality in the amine side chain (Scheme 12). Gold binds to the phosphorus atoms of the ferrocenyl ligand[58] to form complex **98** having a vacant coordination site that binds methyl isocyanoacetate (**11a**). Once bound, the activated isonitrile **99** is deprotonated by the distal amine, which NMR experiments show is in close proximity to the methylene protons (**99**→**100**). Experiments with catalysts in which the benzylic amine is replaced by a sulfide give very similar enantioselectivities, implying that the optimal chain conformation requires a heteroatom.[59] Enolate **100** remains in close proximity to the ammonium ion, exposing only the *si* face of the enolate for attack on the incoming aldehyde. Following condensation, **100**→**101**, the alkoxide adds to the isonitrile carbon to form the oxazoline-gold complex **102**. Protonation within **102** releases the catalyst and ejects the oxazoline **13**.

Silver-ferrocenyl catalysts condense methyl isocyanoacetate (**11a**)[60] and tosylmethyl isocyanide (**49a**)[61] with aldehydes [Eq. (30)]. The silver complex **105a** catalyzes the condensation of activated methyl isonitrile with substituted aromatic, saturated aliphatic, and α,β-unsaturated aldehydes. The selectivity is

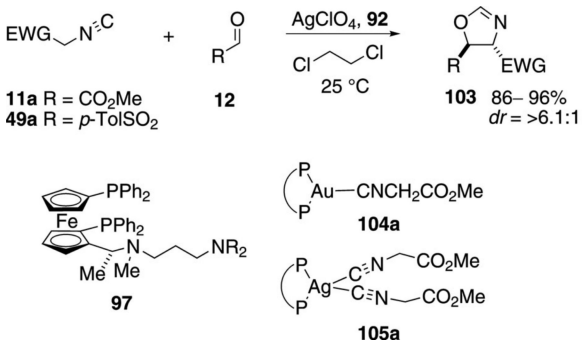


(30)

lower than for the gold complex **104a** but adding methyl isocyanoacetate (**11a**) slowly by syringe pump gives comparable selectivity. IR and kinetic data indicate that the gold catalyst adopts a tricoordinate structure **104a** in which gold is bound to two phosphorus atoms and the carbon of methyl isocyanoacetate (**11a**). The corresponding silver complex **105a** binds to the same ligand and two molecules of methyl isocyanoacetate (**11a**).[60] Limiting the available methyl isocyanoacetate (**11a**), or increasing the temperature from –10°C to 25°C, favors a tricoordinate silver structure, similar to **104a**, which affords the oxazoline **103** more selectively.

The neutral gold complex formed from $Me_2S{\cdot}AuCl$ and the ferrocene ligand **97** catalyzes the condensation of **11b** with imines **39a**, suggesting that the same catalytic species is formed as in the aldol condesation. The catalyst condenses ethyl isocyanoacetate (**11b**) with imines **39a** to generate *cis*-imidazolines **58b** [Eq. (31)].[62] The enantioselectivity is not influenced by changing the electronic nature of the aromatic imine.

Bis(cyclohexyl isocyanide)gold(I) tetrafluoroborate, is distinctly less selective in the condensation of **11a**

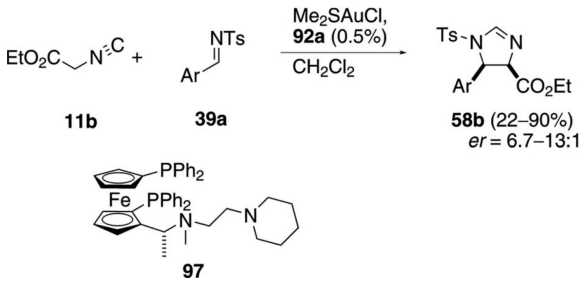


(31)

with aldehydes **12**. Electron deficient aromatic benzaldehydes are less selective whereas tetra- and pentafluorinated benzaldehyde form *cis*-oxazolines with high enentioselectivity [Eq. (32)].[63] With less than

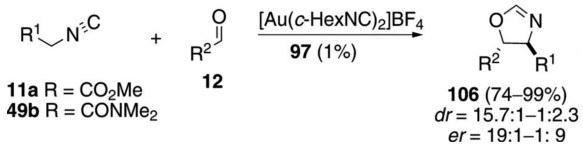


(32)

four fluorine atoms in the aromatic ring of the aldehyde, the diastereoselectivity and enantioselectivity are modest. The analogous condensation of isocyanoacetamide **49b** with aldehydes does not exhibit the same stereoselectivity, affording primarily *trans*-oxazolines **106**.[64]

The gold-catalyzed condensations of isocyanoacetate and isocyanoacetamide proceed with the same facial selectivity on the enolate but differ in the facial selectivity on the aldehyde. For fluorinated aldehydes the usual transition structure **107** is posited to be less favorable than **108** because of an electrostatic attraction between the enolate oxygen and the electron-deficient fluoroaromatic ring (Figure 3). Possibly the enolate derived from the isocyanoacetamide suffers from steric compression in **108** and so reacts through TS **107**.

## 3 Condensations Leading to Pyrroles and Indoles

Isonitriles have featured prominently as precursors in pyrrole syntheses.[65] In most instances the isonitrile nitrogen becomes embedded within the pyrrole as the aromatic nitrogen.

$CpCo(CO)_2$ was found to catalyze the condensation of *tert*-butyl isonitrile **1a**, trimethylsilyl cyanide (**109**), and 4-octyne (**110a**) to give the substituted pyrrole **111a** [Eq. (33)].[66] Unfortunately the reaction is not

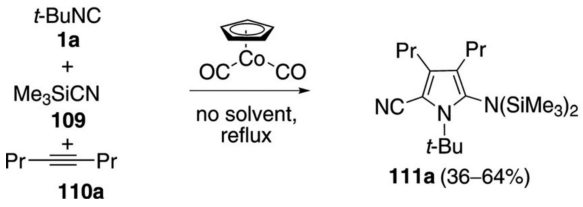


(33)

general as variation of the isonitrile and alkyne leads to numerous pyrroles in low yield. The mechanism of this unusual reaction is not known.

Silver acetate catalyzes the addition of methyl isocyanoacetate (**11a**) to activated olefins **112** leading to substituted pyrrolines **113** [Eq. (34)].[67] The reaction

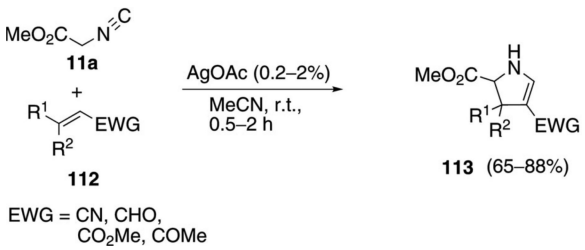


(34)

exhibits a high chemoselectivity in prefering conjugate addition to carbonyl addition, even with enals and enones. Mono-, di-, and trisubstituted Michael acceptors work equally well, providing variability in the number and nature of the pyrroline substituents.

Mechanistically, silver acetate catalyzes the reaction by first coordinating to methyl isocyanoacetate (**11a**, Scheme 13). The resulting complex **114** is activated towards deprotonation by acetate which affords the enolate **115**. Michael addition of **115** to the activated olefin **112** affords a second enolate **116** which is poised for a formal 5-*endo-dig* cyclization. Protonation of the resulting pyrroline **117** by interaction with methyl isocyanoacetate (**11a**) gives the pyrroline **118** and regenerates the silver complex **114**. Subsequent tautomerization of $\Delta^1$-pyrroline **118** generates the more stable $\Delta^2$-pyrroline **113**.

A chiral variant of the $\Delta^2$-pyrroline synthesis has been developed using a catalyst formed by complexing silver nitrate with the chiral bifunctional catalyst **120** [Eq. (35)].[68] Several silver salts promote the reaction

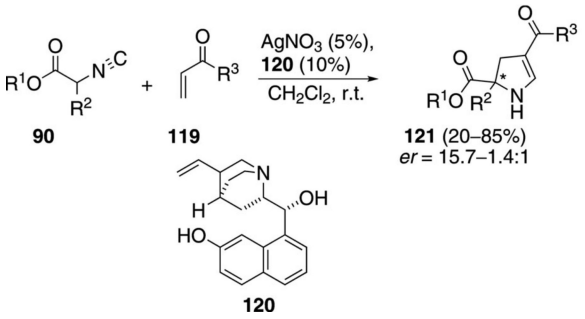


(35)

in the absence of a quinuclidine catalyst. Only $AgNO_3$ suppressed the background condensation while facilitating the reaction with **120**. The enantioselectivity and yield are modest, though the reaction does install quaternary centers.

The catalytic cycle involves isonitrile activation by silver and chiral recognition by interaction with bi-functional catalyst **120** (Scheme 14). Complexation of isonitrile **90** with silver nitrate activates the isonitrile complex **122** toward deprotonation. Deprotonation of **122** by the quinuclidine nitrogen of **120** forms the enolate complex **123** in which an

electrostatic attraction holds the enolate in a chiral environment. Facial selectivity in the attack on the Michael acceptor is attributed to H-bonding with the aromatic hydroxy group that concommitently activates the enone toward attack **123**→**124+125**. Subsequent 5-*endo-dig* cyclization of enol **125** leads to pyrroline **126** which protonates and tautomerizes to the 2,3-dihydro-1*H*-pyrrole **121**.

Modified *Cinchona* alkaloids such as **128** catalyze the cycloaddition of isocyano esters **90** with nitroolefins **127** to form 2,3-dihydropyrroles **129** [Eq. (36)].[69]

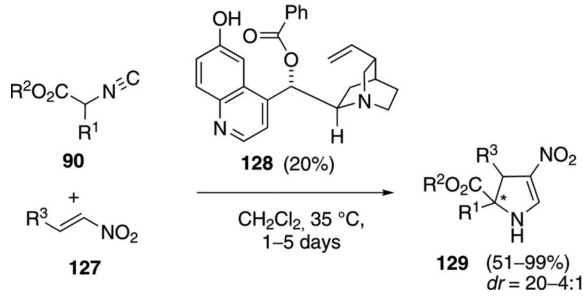


(36)

The tertiary amine and the aromatic hydroxy group of **128** are essential for high selectivity. The functional group requirements of the catalyst suggest a mechanism similar to that of catalyst **120** (Scheme 14) in which the chiral base promotes the Michael addition. Diverse electronic substituents are tolerated in the nitroolefin and in the isocyano ester. Unsubstituted isocyano esters are one of the few substrates that do not react.

The quinolone-derived thiourea **131** catalyzes the [3+2]cycloaddition of α-phenyl isonitrile esters **87** with methyleneindolinones **130** to afford 3,3′-pyrrolinidyl spirooxindoles **132** [Eq. (37)].[70] By varying the

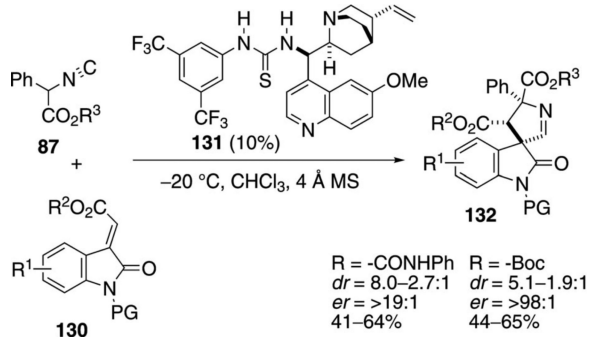


(37)

protecting group on the methyleneindolinone, the *syn*- or *anti*-spiroindole is generated with moderate to good diastereoselectivity and with high enantioselectivity. *N*-Phenylamide-protected indolinones give *anti*-spirooxindoles in which the two ester substituents lie on

opposite sides of the indoline ring. *N*-Boc protected indoles give primarily *syn*-adducts. Diverse substitution on the aromatic ring of the indolinone is tolerated.

Although a mechanism has not been proposed, surveys of similar organocatalyzed reactions establish the basic control elements likely to operate in this reaction.[71] The quinuclidine nitrogen of the catalyst **131** likely abstracts a proton from the activated isonitrile **87** to generate enolate **133** that remains close to the ammonium ion through an electrostatic interaction (Scheme 15). Internal conjugate addition of the enolate is likely directed by subtle conformational features induced by the protecting groups and the quinoline ring (**133**→**134**). Attack of the enolate **134** onto the isonitrile followed by protonation from the ammonium ion regenerates the catalyst and releases the spiroindole **132**.

The chiral complex **137**, generated from silver acetate and (*S*)-(2′-hydroxy-1,1′-binaphthyl-2-yl)diphenylphosphine, catalyzes the formal [3+2]cyclization of α-aryl isocyano esters **135** with 2-oxobutanoate esters **136** to afford 2,3-dihydropyrroles **138** [Eq. (38)].[72] A

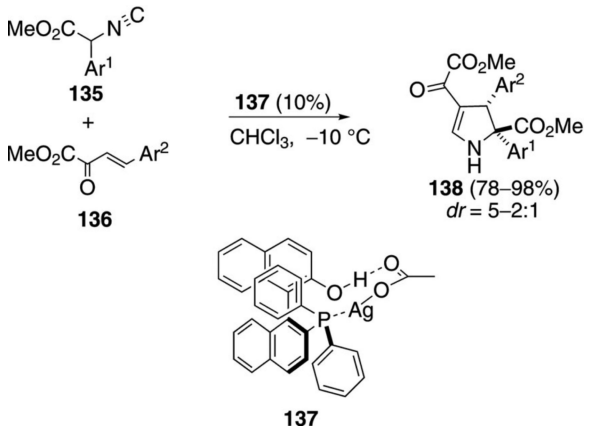


(38)

variety of aromatic substituents is tolerated within the 2-oxobutanoate and the isocyanoacetate.

The active catalyst is **137** that crystallizes when phosphine is added to AgOAc (Scheme 16). Complexation of **137** to isonitrile **135** leads to ejection of acetate and facilitates deprotonation of isocyanoacetate to generate the stabilized enol complex **139**. Coordination of the oxobutanoate **136** to the central silver sets the orientation for the conjugate addition and subsequent cyclization **140**→**141**. Chelation of the 2-butanoate carbonyls with the central silver enhances the electrophilicity of the double bond and orients the substrate for Michael addition to the *re* face. Protonation of the carbon-silver bond in **141** releases the pyrrole **138** and regenerates the silver catalyst.

$Rh_4(CO)_{12}$ catalyzes the condensation of ethyl isocyanoacetate (**11b**) with ketones **4** to give unsaturated formamides **142** [Eq. (39)]and with diketones **143** to

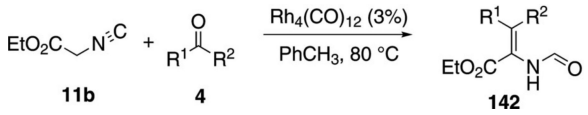


(39)

give substituted pyrroles **144** [Eq. (40)].[73] The regio-selectivity is dictated largely by steric compression.

The rhodium catalyst initiates the catalytic cycle by co-ordinating to ethyl isocyanoacetate (**11b**) and inserting into the C–H bond **145**→**146** (Scheme 17).

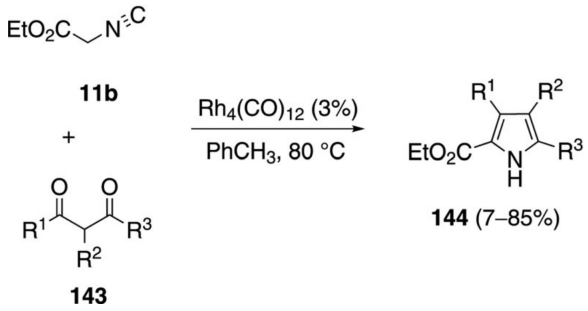


(40)

Nucleophilic attack of **146** on the 1,3-diketone **143** gives the alkoxide **147**. Protonation of **147** by ethyl isocyanoactate **11b** gives the alcohol **148** and regenerates the rhodium catalyst **146**. Isonitrile **148** eliminates water which subsequently hydrolyzes the isonitrile group to give formamide **149**. Decarbonylation of **149** by the rhodium catalyst affords **150** which suffers internal condensation to give the pyrrole **144**.

Substituted pyrroles **151** were synthesized through the copper-catalyzed addition of activated isonitriles **49** to electron-deficient alkynes **110** [Eq. (41)].[74] The reaction is catalyzed by $Cu_2O$, CuSPh, CuBr, or copper nanoparticles. Reactions catalyzed by $Cu_2O$

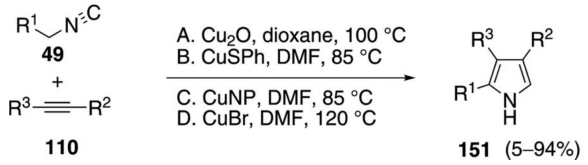


(41)

require two mol equivalents of phenanthroline and are distinctly more efficient with acetylenic esters than with acetylenic ketones, nitriles, amides, or sulfones. Copper(I)benzenethiolate and copper nanoparticles were employed in DMF at 85°C. An

additional catalyst-base[74a] combination of CuBr and $Cs_2CO_3$ (120°C) is effective with terminal alkynes not having an electron-withdrawing group.

The catalytic cycle involves metallation, cyclization and release of the copper catalyst (Scheme 18). Activation of the isonitrile **49** by copper allows facile metallation resulting in the cuprated isonitrile **17**. Carbo-metallation of alkyne **110** or a Michael-type addition by cuprated isonitrile **17**, leads to the vinyl-copper **152**. Intramolecular cyclization of **152** generates the copper 2*H*-pyrrolenine **153** which undergoes a 1,5 hydride shift to afford the copper pyrrole **154**. Protonation of 154 likely proceeds by coordination of the isonitrile **49**, facilitating the protonation, to form the pyrrole **151** and regenerating **17**. Experiments with copper catalysts and terminal alkynes implicate a similar mechanism.[74a] Recent experiments with $Ag_2CO_3$ and terminal alkynes are suggested to proceed through a [3+2]cycloaddition.[75]

The titanium complex **155** catalyzes the condensation of *t*-BuNC (**1a**) with an amine **3** and an alkyne **110** to form pyrroles **156** [Eq. (42)].[76] Terminal alkynes **110** ($R^3$=H) react more efficiently than internal

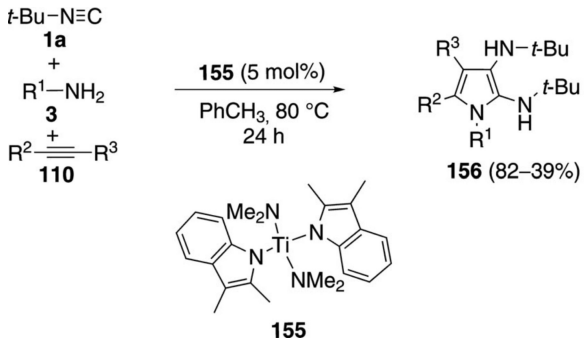


(42)

alkynes **110**. Only aromatic amines engage in catalysis.

An essential feature of the cataylic cycle is formation of a formal titanium nitrene **157**, which allows [2+2]cycloaddition to form titanocycle **158**, and insertion of *t*-BuNC (**1a**) to form **159** (Scheme 19). Using indolyl titanium pre-catalyst **155**, a second isonitrile insertion occurs after formation of **159**, transforming **159** to **160**. Further isonitrile insertions are disfavored because they involve formation of a 7-membered titanocycle. Coordination of amine **3** causes protonation of the metal bonds, delivering the catalyst **157** and releasing imine **161**. Intramolecular cyclization **161**→**162**, proton transfer, and tautomerization deliver the pyrrole **156**.

Palladium acetate catalyzes the formation of 5-iminopyrrolones **164** from two equivalents of an isonitrile **163** and a bromoalkyne **110b** [Eq. (43)].[77] Performing the reaction in a stepwise fashion allows control

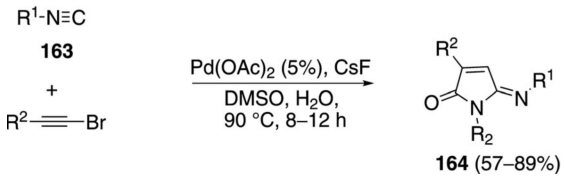


(43)

over the iminopyrroline substituents. Alkyl and aryl substituents are tolerated in both the alkyne and the isonitrile. Isocyanobenzene and isocyanoacetate gave low yields.

The catalytic cycle rests on the *in situ* formation of bromoacrylamide **166** from bromoalkyne **110b** and isonitrile **163** (Scheme 20). The reaction proceeds in two stages; CsF promotes the addition of the isonitrile **163** to the bromoalkyne **110b** and the subsequent hydrolysis to the β-bromoacrylamide **166**, whereas $Pd(OAc)_2$ catalyzes the insertion and cyclization reaction. Oxidative addition of zero-valent palladium species **165** to the bromoacrylamide **166** affords the vinyl-palladium complex **167** which inserts an equivalent of isonitrile **163** to afford **168**. Internal complexation of palladium to the amine facilitates deprotonation which transforms **168** to palladacycle **169**. Reductive elimination of palladium from **169** affords the 5-iminopyrrolidinone **164** and regenerates the catalyst.

Several iodoaryl Michael acceptors were coupled with activated isonitriles to afford oxindeno[1,2-*b*]pyrroles. Copper iodide catalyzes the coupling of isonitriles **49** and 1-(2-iodoaryl)-2-yn-1-ones **170** to give 4-oxoindeno[1,2-*b*]pyrroles **171** [Eq. (44)].[78] Alkyl and aryl substituents $R^2$ are tolerated on the alkyne

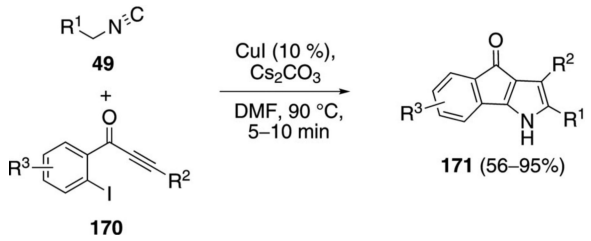


(44)

whereas the isonitrile substituent $R^1$ must be an electron-withdrawing group.

The key catalytic species is the cuprated isonitrile **17** formed by complexation of CuI to **49** followed by deprotonation (Scheme 21). Formal [3+2]cycloaddition of **17** onto ynone **170** gives the arylcopper **172**. Intramolecular insertion of copper into the aryl C–I bond likely affords the copper(III) species **173**. Reductive elimination from **173** ejects **174** that subsequently tautomerizes to the 4-oxoindeno[1,2-*b*]pyrrole **171**. The copper(I) species generated during the reductive elimination, engages with the isonitrile to reform the catalyst **17**.

Using the same catalyst system, 4-oxoindeno[1,3-*b*]pyrroles **171** are synthesized by coupling activated isonitriles **49** with 1-(2-haloaryl)enones **175** (Scheme 22).[79] An initial cycloaddition **175**→**176** is followed by cyclization **176**→**177** that follows the same copper catalytic cycle as with **170** (Scheme 22). An air oxidation aromatizes **177** to afford **171**.

The same copper coupling stategy was employed with *N*-(2-haloaryl)propiolamide **178** and the activated isonitrile **49** to yield pyrrolo[3,2-*c*]quinolin-4-ones **179** [Eq. (45)].[80] The analogous coupling with alkynoates

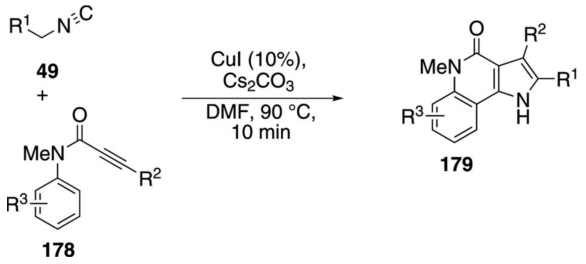


(45)

was unsuccesful. Alkyl and aryl substituents $R^2$ are well tolerated on the alkyne side chain of **178** as are electron-withdrawing or donating groups $R^3$ on the aromatic ring. Electron-withdrawing groups on the aryl group of propiolamide **178** activate the substrates in the coupling process.

The ruthenium complex **180** catalyzes an unusual synthesis of 7-methylindole **181a** from 2,6-xylyl isonitrile **163a** [Eq. (46)].[81] The reaction is limited to 2,6-xylyl

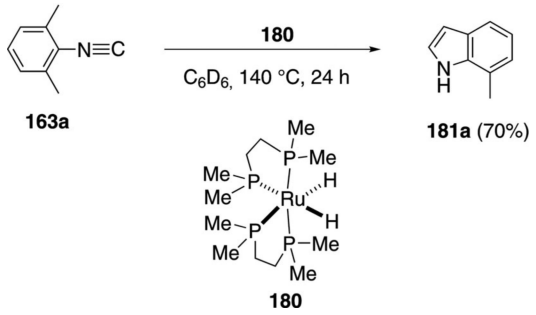


(46)

isonitrile because less substituted isonitriles remain complexed to the catalyst. High temperatures are required for the reductive elimination and catalyst turnover.

The mechanism involves loss of hydrogen gas from the ruthenium precatalyst **180** to give the true catalyst **182** (Scheme 23). Ligation of catalyst **182** to isonitrile **163a** affords **183**. Release of one of the phosphines (**183**→**184**) exposes two free coordination sites, allowing ruthenium insertion into the benzylic C–H bond to give the ruthenacycle **185**. Alkyl migration within **185** to the isonitrile group forms the heterocycle **186** which tautomerizes to

form the indole **187**. A *trans*-to *cis*-isomerization allows the reductive elimination from *cis*-**188** to afford the indole **181a**.

In C–H activation couplings with isonitriles, palladium catalysts generally have a greater substrate scope than the ruthenium catalyst **180**. $Pd(OAc)_2$ and $Ad_2PBu$ form a complex that catalyzes the coupling of *ortho*-alkylaryl isonitriles **189** with aryl iodides or bromides **190** to afford indoles **191** [Eq. (47)].[82] Electron-donating

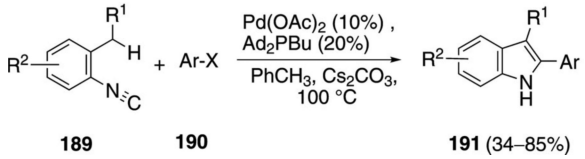


**189** **190** **191** (34–85%)

(47)

and electron-withdrawing substituents $R^2$ are tolerated at the *para*-position of the isonitrile.

The catalytic cycle is initiated by an oxidative addition of zerovalent palladium species **165** into the aryl halide **190** (Scheme 24). Isocyanide insertion into **192** gives the palladium imine **193** which is poised for insertion into the benzylic C($sp^3$)–H bond **193**→**194**. Reductive elimination from **194** and tautomerization affords the 2-substituted indole **191** and regenerates the palladium catalyst **165**.

The same palladium-catalyzed C–H insertion strategy provides tetracyclic carbazoles **199** from *ortho*-alkynylphenyl isonitriles **195** (Scheme 25).[82] Following oxidative addition of palladium(0) into the aryl halide **190**→**192**, isonitrile insertion affords **196**. Internal carbopalladation of **196** generates **197**. Insertion of the palladium(II) to the proximal benzylic C–H bond transforms **197** into **198** which reductively eliminates and tautomerizes to form **199**.

Camptothecins are accessable through a palladium-catalyzed C–H insertion process (Scheme 26).[83] Zerovalent palladium species **165** inserts into 6-iodo-*N*-propargylpyridone **200** to afford **201** that coordinates and inserts isonitrile **202** to form **203**. Close proximity of palladium to the alkyne triggers carbopalladation to **204**. C–H insertion **204**→**205** and reductive elimination then gives 11*H*-indolizino[1,2-*b*]quinolin-9-ones **206**. Sterically encumbered substituents are tolerated at the acetylenic terminus of **200** whereas unsubstituted acetylenic pyridines are un-reactive.

$Pd(Ph_3P)_2Cl_2$ catalyzes the condensation of isonitriles **163** with *N*-tosylaziridines **207** and 2-iodophenols **208** to form 1,4-benzoxazepines **209** [Eq. (48)].[84]

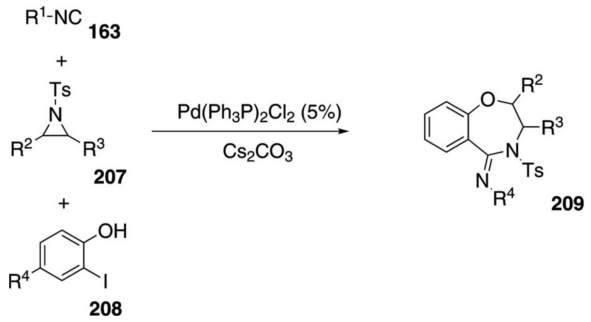


(48)

Tertiary isonitriles are most effective in the condensation, with cyclohexyl isonitrile affording the corresponding benzoxazepine distinctly less efficiently. Chloro, methyl, and phenyl substituents are tolerated in the iodophenol in equally effective condensations with cyclic or acyclic aziridines.

The condensation proceeds through base-promoted aziridine ring opening, uniting the phenol **208** and aziridine **207** into the ether **210** (Scheme 27). Insertion of palladium species **165** into the aryl iodide is proposed to afford **211** followed by isonitrile insertion and dehydrohalogenation of **212** to afford **213**. Given the likely coordination in **211**, which decreases the amine acidity, the dehydrohalogenation may occur prior to isonitrile insertion. Reductive elimination from **213** affords **209** and regenerates the active catalyst.

Palladium acetate catalyzes the condensation of isonitriles **163** with 2-alkynylanilines **214** to afford 3-amidylindoles **215** [Eq. (49)].[85] Primary, secondary,

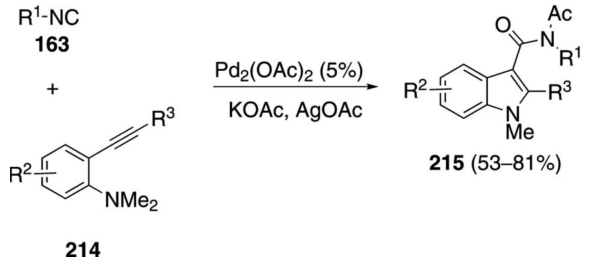


(49)

and tertiary aliphatic isonitriles react well but 2,6-dimethylphenyl isocyanide failed to react. All of the successful substrates contained an aromatic or aliphatic substituent $R^3$ on the alkyne.

Conversion of the aminoacetylene **214** into indole **215** proceeds through an initial aminopalladation (**214**→**215**, Scheme 28). Isonitrile insertion into the palladium complex **216** affords **217** that suffers demethylation and reductive elimination to generate indole **218** that subsequently tautomerizes to **215**. Subjecting independently prepared **216** to the reaction conditions affords **215**, providing support for the proposed mechanism.

Palladium trifluoroacetate catalyzes the condensation of isonitriles **163** with aminoalkynes **214** to afford cyanoindoles **219** [Eq. (50)].[86] *tert*-Butyl isonitrile

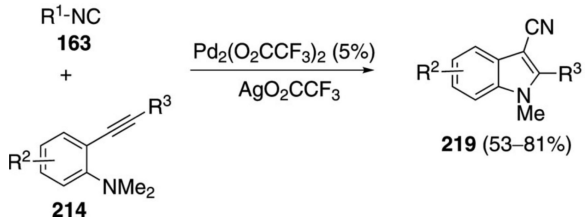


(50)

and cyclohexyl isonitrile react equally well, whereas 2,6-dimethylphenyl isonitrile does not participate in the reaction. Alkyl- and arylacetylene substituents react well.

The reaction mechanism presumably parallels the acylation process (Scheme 28) except for **217** suffering reductive dealkylation and a fragmentation with release of nitrile **219** rather than a reductive elimination.

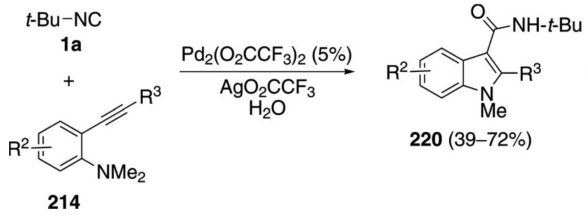


(51)

Supporting this change in mechanism is the addition of water to the reaction mixture which, with *tert*-butyl isonitrile (**1a**), results in formation of the corresponding amide **220** [Eq. (51)].

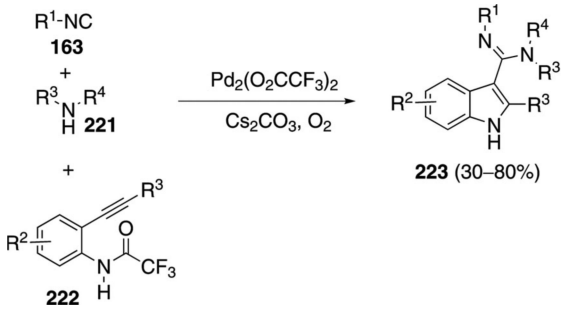


(52)

Palladium trifluoroacetate catalyzes a related condensation of isonitriles **163** with 2-alkynylamides **222** and an amine **221** to afford indoles **223** [Eq. (52)].[87] Tertiary isonitriles react best with the isonitriles cyclohexyl isocyanide and pentyl isonitrile providing the

corresponding indoles in 39–45% yield. The reaction tolerates electron-withdrawing and electron-donating substituents in the benzene ring and aliphatic and aromatic acetylenic substituents.

Mechanistically, the reaction is initiated through an oxidative condensation of palladium with the isonitrile **163** and amine **221** to afford **224** (Scheme 29). Coordination of palladium complex **224** to the acetylene of **222** activates the system toward cyclization, perhaps through the deprotonated amide **225**. Reductive elimination from the resulting indole **226**, accompanied by loss of the trifluoroacetamide, affords **223** and releases zerovalent palladium species **165**.

Catalytic palladium acetate condenses *ortho*-acetylenic isonitriles **228** with aryl iodides **227a** to afford substituted indoles **229** [Eq. (53)].[88] Electron-donating groups and chlorine substituents within the aryl iodide **227a**, have minimal effects on the reaction. Electron-withdrawing substituents cause a distinct decrease in the yield of the indole **229**. Aryl iodides

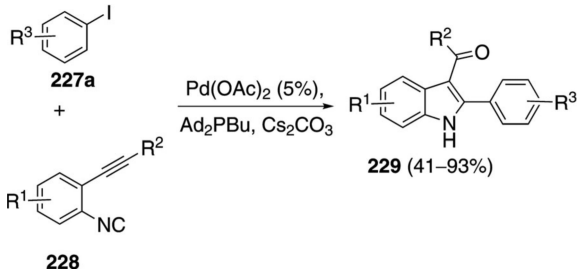


(53)

bearing nucleophilic *ortho* subtituents react further with the ketone to afford tetracyclic indoles.

The catalytic cycle is initiated through insertion of zerovalent palladium into the aryl iodide **227a** to form **230**. Insertion of the isonitrile **228** into the palladium-carbon bond of **230** generates **231** that is poised for cyclization (Scheme 30). Activation of the pendant alkyne by palladium complexation facilitates nucleophilic attack by hydroxide, acetate, or carbonate to afford **232**. Reductive elimination from **232** and hydrolysis or enolization leads to the indole **229** and regenerates zerovalent palladium **165**.

The combination of $Pd(OAc)_2$, $Ph_3P$, and CsOPiv catalyzes the coupling of 2,6-disubstituted phenyl isocyanides **233** with 2-halobiaryls **234** to afford iminofulvenes **235** [Eq. (54)].[89] The optimal isonitrile proved to be 2,6-diisopropylphenyl isocyanide (**233**); aliphatic isonitriles are unsuitable reaction partners. A wide range of biaryls, electron-deficient pyridines,

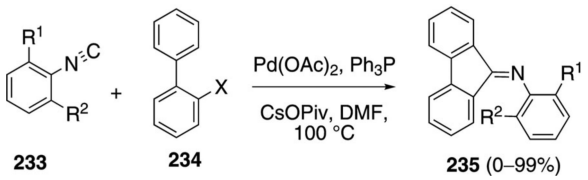


(54)

and similar substrates, effectively participate in the coupling. The reaction exhibits good functional group tolerance.

Labelling studies demonstrate that the turnover-limiting step of the reaction is C–H insertion (Scheme 31). Initial C–X insertion of zerovalent palladium into **234** affords **236**. Isonitrile insertion into **236** affords **237** bearing the pivolate ligand. Palladation of the aromatic ring may proceed through concerted metallation–deprotonation (**237**) or electrophilic addition; the precise mechanism is not known. Subsequent reductive elimination from the iminopalladium species **238** affords imine **235** and regenerates the catalyst.

Borylindoles **240**, valuable substrates for Suzuki–Miyaura coupling, were prepared through a copper-catalyzed borylation–cyclization of 2-alkenylphenyl isonitrile **239** [Eq. (55)].[90] The coupling proceeds at room temperature and, after filtration, the boryl imine can be used directly in a subsequent Suzuki–Miyaura coupling.

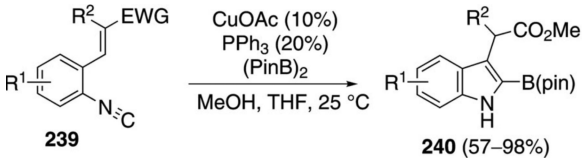


(55)

The coupling is initiated by reaction of $(BPin)_2$ (**242**) with the copper-phosphine complex **241** to form the active copper catalyst **243** (Scheme 32). Insertion of isonitrile **239** into the copper-boron bond of **243** leads to the organocopper-containing imine **244** triggering an internal 1,4-conjugate addition **244**→**245**. Protonation of **245** by methanol releases CuOMe and **247** that then tautomerizes to indole **240**. CuOMe then reacts readily with $(PinB)_2$ to regenerate the catalyst **243**.

An analogous silylation sequence employs isonitrile **248**, the same catalyst system, and a silylboronate to generate silylindoles **249** [Eq. (56)].[90] An electron-withdrawing

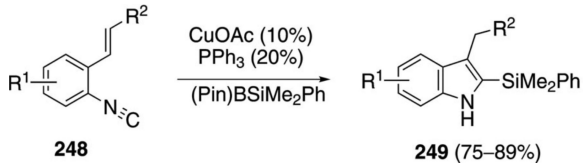


(56)

olefinic substituent $R^2$ is required: an ester, an amide, or a nitrile. The donor and acceptor groups OMe, Me and $MeO_2C$ groups are tolerated as substituents $R^1$ in the aromatic ring.

Copper iodide catalyzes the condensation of ethyl isocyanoacetate **11b** and 2-haloaryl aldehydes or ketones **250** and **251** to afford indole-2-carboxylic acid esters **252** [Eq. (57)].[91] The aromatic ring tolerates

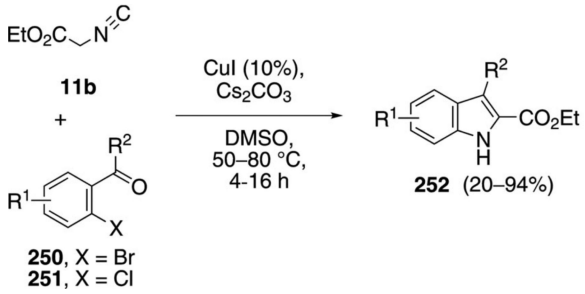


(57)

diverse electronic substituents. Ketones react more efficiently than aldehydes.

Although the mechanism has not been determined, the sequence likely involves a Knovenagel condensation of the cuprated isonitrile **17a** with the carbonyl halide **250**/**251** (Scheme 33). Hydrolysis of the unsaturated isonitrile **253** by the liberated water then generates the corresponding formamide **254**. Copper-catalyzed cyclization **254**→**255**, reductive elimination, deformylation, and protonation from ethyl isocyanoacetate (**11b**) complete the catalytic cycle.

Palladium acetate catalyzes the synthesis of 2,3-substituted indoles **258** from *ortho*-alkenylphenyl isonitrile **256a**, aryl iodides **257**, and diethylamine **221a** [Eq. (58)]. Although the yields are modest, the isonitrile

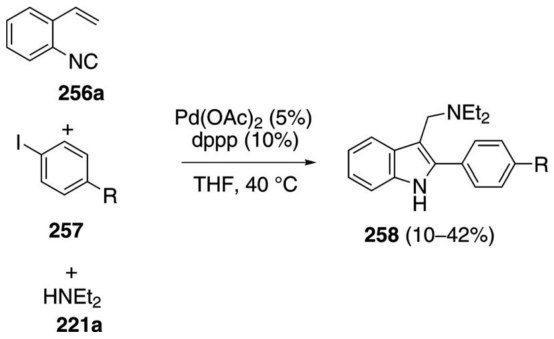


(58)

tolerates diverse electronic substituents and the reaction assembles a functionalized indole in a single step.[92]

Mechanistically, insertion of the palladium catalyst **259** into the aryl iodide **257** gives **260** (Scheme 34). Complex **260** inserts isonitrile **256a** with the palladium then adding onto the pendant olefin to give **261**. Nucleophilic attack of diethylamine onto the palladium complex followed by reductive elimination and tautomerization gives the indole **258** and the palladium hydride complex **262**. Base-induced reductive elimination of **262** by diethylamine regenerates the palladium catalyst **259**.

## 4 Condensations Affording Imidazoles

CuI catalyzes the condensation of isocyanoacetates **11** with carbodiimides **263** to form benzoimidazo[1,5-*a*]imidazoles **264** [Eq. (59)].[93] The condensation is

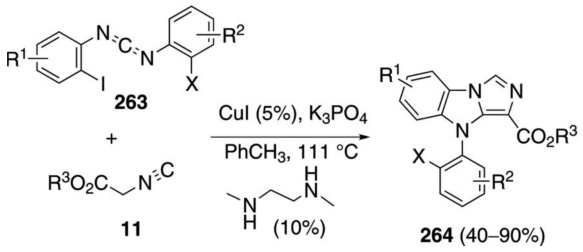


(59)

formally a [3+2]cycloaddition followed by a copper-catalyzed amination with the aryl iodide. A variety of amine ligands was screened with $N^1$,$N^2$-dimethylethane-1,2-diamine proving optimal. An isocyano ester is required for good yields; the sulfonyl isonitrile, TosMIC, provides **264** in only 40% yield. Me, Cl, I or H substituents are tolerated in the diimide **263**.

Activation of isonitrile **11** by the CuI-amine catalyst forms the metallated isonitrile **17** (Scheme 35). A formal [3+2]cycloaddition of **17** with the diimide **263** generates **265**, although a stepwise attack of **17** onto the C=N bond, followed by cyclization, may be more

likely because the process directly parallels related reactions of imines. Tautomerization of **265** to **266**, followed by a copper-assisted protonation by **11** yields **267** and regenerates the cuprated isonitrile **17**. Copper-catalyzed intramolecular C–N coupling[94] of **267** leads to the benzoimidazo[1,5-*a*] imidazole **264**.

The first cross-condensation of isonitriles to form imidazoles was discovered during an attempted synthesis of pyrroles [Eq. (60)].[95] The $Cu_2O$-catalyzed

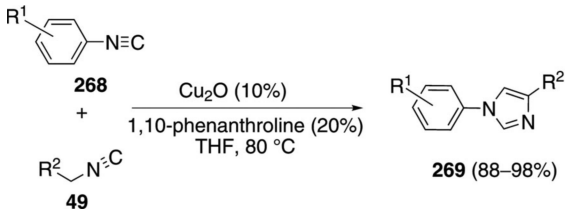


(60)

reaction effectively condenses a variety of electron-rich and electron-deficient aryl isonitriles **268** with isonitriles **49** bearing an adjacent electron-withdrawing group $R^2$. The reaction proceeds at 80°C in THF. Aliphatic isonitriles do not participate in the reaction.

Copper oxide activates the C–H bond of the isonitrile **49** to generate cuprated isonitrile **270** (Scheme 36). Nucleophilic addition of **270** onto aryl isonitrile **268** forms the copper imine **271** with subsequent attack of the aryl nitrogen onto the isonitrile carbon to give **272**. Proton transfers transform **272** to imidazole **273**. Protonation of the C–Cu bond of **273** by **49** yields the 1,4-disubstituted imidazole **269** and regenerates the true catalyst **270**.

An almost identical cross-condensation of ethyl isocyanoacetate (**11b**) with aryl isonitriles **268** was performed with catalytic $Cu_2O$ and proline to form *N*-arylimidazoles **274** [Eq. (61)].[96] The isonitriles were

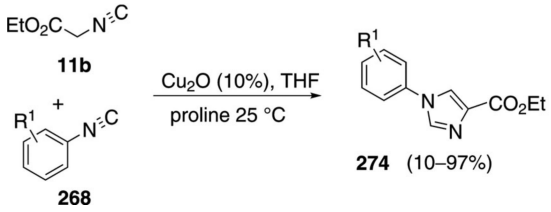


(61)

prepared from the corresponding formamides, dehydrated with $POCl_3$ and $Et_3N$, and used without purification. Proline was found to be the best ligand when the reaction was performed at room temperature, although 1,10-phenanthroline is equally efficient if the reaction is performed in refluxing THF. The reaction tolerates electron-withdrawing and electron-rich substituents in the aromatic ring. Considerable functional group tolerance was demonstrated through reactions of acetylated isonitrile-containing glycosides.

Copper(I) oxide is a weak base that combines with proline and isocyanoacetate **11b** to form complex **275** (Scheme 37). Complex **275** chelates to the isonitrile **268** to form **276** with a π interaction that facilitates an intramolecular nucleophilic attack to yield **277**. The precedented complexation explains why cross-condensation is favored over homodimerization. Intramolecular attack within isonitrile **277** affords zwitterion **278** from which subsequent proton transfers afford **279**. Coordination of isocyanoacetate **11**, and protonation of the copper-carbon bond, closes the catalytic cycle and releases the *N*-arylimidazole **274**.

Various oxazoles and benzoxazoles **281** are readily assembled through a three-component coupling of aryl iodides and bromides **227** with *tert*-butyl isonitrile (**1a**) and an amino alcohol or *ortho*-aminophenol **280** [Eq. (62)].[97] Only the isonitrile carbon is incorporated

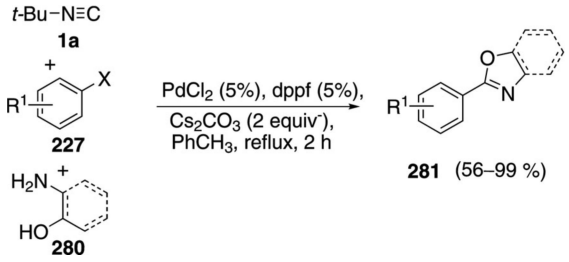


(62)

into the oxazoline **281**, with aminoethanol acting to displace *tert*-butylamine. The coupling is equally efficient with electron-rich and electron-deficient aryl bromides, iodides, and triflates.

The same $PdCl_2$-dppf combination allows the conversion of diamines **282** to imidazoles **283** [Eq (63)].[98] In some cases the combination of $PdCl_2$ and dppp is superior to $PdCl_2$ and dppf. Extending the reaction to 1,3-diaminopropane affords a tetrahydropyrimidine in 95% yield.

The two reactions involve essentially the same mechanism. Palladium oxidatively adds to the aryl halide **227** to generate the aryl palladium halide **284** which then inserts *tert*-butyl isonitrile (**1a**) to yield **285** (Scheme 38). Attack of aminoethanol on **285** affords **286** and releases the catalyst. The amidine **286**

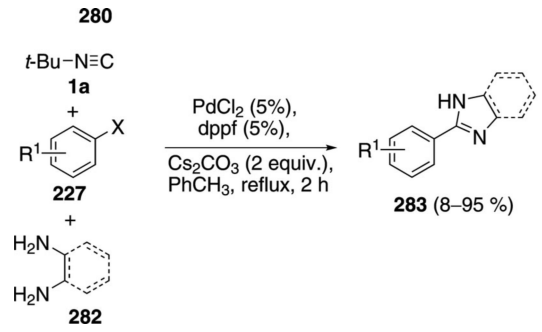


(63)

suffers internal cyclization with loss of *tert*-butylamine to provide the oxazoline **281**. Aminophenols and diamines react through an analogous sequence.

$Pd(OAc)_2$ in 2-methyltetrahydrofuran catalyzes the condensation of isonitriles **163** with *ortho*-phenylenediamines **282**, and similar bis-nucleophiles, to afford 2-aminobenzimidazole **287** [Eq. (64)].[99] The

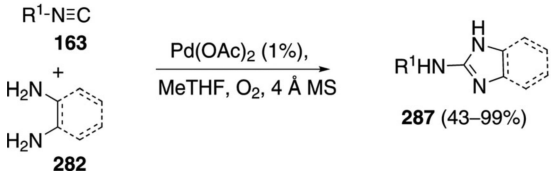


(64)

$Pd(OAc)_2$ system has wide substrate scope both in the diamine and in allowing condensations with primary, secondary and tertiary isonitriles. In some instances, diamines bearing strong electron-withdrawing groups require higher catalyst loadings for complete conversion.

Palladium acetate is proposed to react with isonitrile **163** to form the active catalyst **288** (Scheme 39). Reaction of the diamine **282** with **288** affords **289** which suffers isonitrile insertion from the coordinated isonitrile. Additional isonitrile then complexes the open coordination site. Reductive elimination from **290** releases the benzimidazole **287** with concomitant formation of the zerovalent palladium complex **291**. Reoxidation of **291** with molecular oxygen regenerates the catalyst and releases water.

Tetrakis(triphenylphospine)palladium catalyzes the condensation of several isonitriles **163** with *ortho*-aminophenols **292** to generate 2-aminobenzoxazoles 293 [Eq. (65)].[100] Electron-rich *ortho*-aminophenols **292**

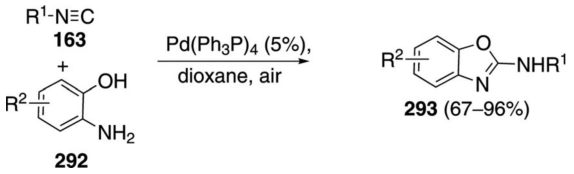


(65)

react smoothly whereas aromatics with electron-withdrawing groups require higher temperatures and longer reaction times. Primary, secondary, and tertiary isonitriles react equally well. Ethyl isocyanoacetate (**11b**) was the only substrate reported not to react.

Switching the catalyst from $Pd(Ph_3P)_4$ to $PdCl_2$ redirects the isonitrile–*ortho*-aminophenol condensation to afford 3-aminobenzoxazines **294** [Eq. (66)].[100] The double insertion process tolerates primary, secondary, and tertiary isonitriles.

Palladium acetate catalyzes the reaction of isonitriles 163 with anthranilic acids 295 to afford bioactive

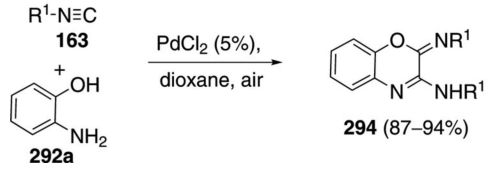


(66)

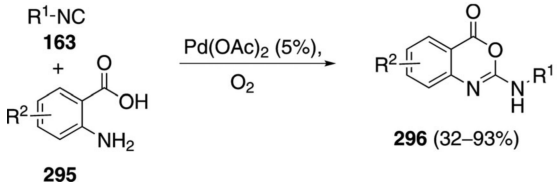


(67)

2-aminobenzoxazinones **296** [Eq. (67)].[101] Primary, secondary, and tertiary isonitriles participate in the reaction although the yield with butyl isonitrile was distinctly reduced. The condensation tolerates electronically diverse substituents in the anthranilic acid without adversely affecting the reaction efficiency.

The excellent ligation of isonitriles is thought to result in the conversion of palladium acetate into complex **288** incorporating two isonitrile groups. Condensation of **288** with anthranilic acid **295** leads to **297** which undergoes migratory insertion of an isonitrile ligand followed by ligation of another isonitrile to the vacant coordination site (Scheme 40).

Reductive elimination from **298** releases **296** and a palladium(0) complex **299** that is reoxidized to **288**.

## 5 Condensations Affording Imines

Over twenty years ago styrene (**300a**) was hydroiminoformylated with cyclohexyl isonitrile (**163b**) [Eq. (68)].[102]

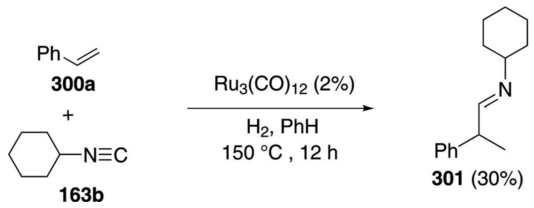


(68)

$Ru_3(CO)_{12}$ catalyzes the reaction, through an unknown mechanism, to afford imine **301** in a modest 30% yield. Although the reaction with pentene only gave 14% of the corresponding imine, the reaction seems ripe for development.

$Pd(PPh_3)_4$ catalyzes the iminocarbonylative cross-coupling reaction between *tert*-butyl isonitrile (**1a**), 9-alkyl-9-BBN **302** derivatives, and haloarenes **190** to afford imines **303** [Eq. (69)].[103] Strong bases and

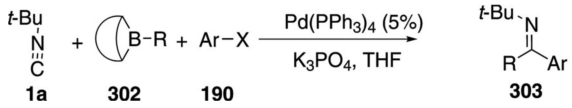


(69)

polar solvents lower the yield as do electron-withdrawing substituents on the iodoarene. The reaction is sensitive to the stoichiometry of the isonitrile and the 9-alkyl-9-BBN derivative; a 1:1 ratio being optimal. A boron–isonitrile complex appears to provide a reservoir of isonitrile while minimizing the concentration of free isonitrile.

Zerovalent palladium species **165** initiates the catalytic cycle through an insertion into the aryl halide **190** to generate **192** (Scheme 41). Delivery of the isonitrile *via* the borane complex **304** allows insertion into the aryl-palladium bond of **192** to form **305**. Base activation of the free borane facilitates the alkyl transfer from boron to palladium **305**→**306**. Reductive elimination from **306** releases the imine **303** and completes the catalytic cycle.

C–H bond insertion of isonitrile **163** into benzene (**307**) with $RhCl(PR_3)R^1NC$ (**308**) affords iminobenzaldehyde **309** [Eq. (70)].[104] A mechanism-oriented

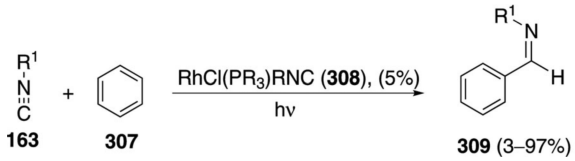


(70)

study demonstrated the feasability of catalysis under UV irradiation, measuring conversion rather than isolated yield.

The precise mechanism for the C–H and isonitrile insertion is not clear. UV irradiation of **308** is thought to promote dissociation of either a phosphine or an isonitrile ligand to create the electrophilic rhodium complex **310** (Scheme 42). Insertion of **310** into benzene generates the complex **311** which coordinates isonitrile **163** and triggers an insertion of the ligated isonitrile group **312**→**313**. Reductive elimination from **313** releases the benzaldimine **309** and the active catalyst **310**. Excess isonitrile forms a bisphosphine–bisisonitrile rhodium complex which precipitates from solution. Under UV irradiation the complex is able to release sufficient amounts of a catalytically active species to promote the reaction.

A scandium imide complex **315** catalyzes the C–H insertion into pyridine (**314**) and subsequent isonitrile

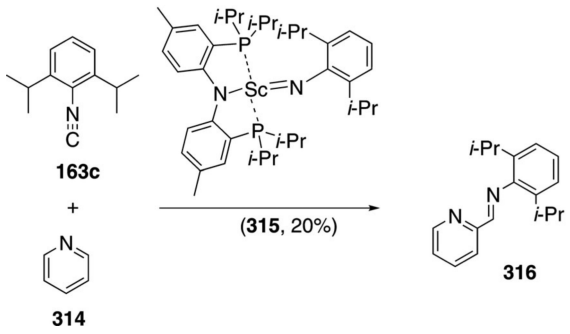


(71)

insertion to form the imino-substituted pyridine **316** [Eq. (71)].[105] The catalytic reaction was not performed preparatively but gives complete conversion after 4 h. Only the hindered isonitrile **163c** engages in catalysis; less hindered isonitriles bind irreversably to the catalyst.

Isolation of several scandium complexes supports the proposed catalytic cycle (Scheme 43). Complex **317**, generated by addition of pyridine to **315**, is the active form of the catalyst which undergoes C–H insertion to form **318**. Insertion of the isonitrile **163c** into the scandium-carbon bond of **318** generates **319**; an intermediate that can be crystallized from solution (Scheme 43). Proton transfer within **319** affords tautomer **320** that releases the iminopyridine **316**, binds additional pyridine, and regenerates the catalyst.

α-Iminophosphine oxides **322** are synthesized by the palladium-catalyzed insertion of isonitriles **163** into secondary phosphine oxides **321** [Eq. (72)].[106]

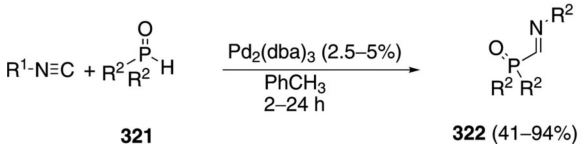


**321** **322** (41–94%)

(72)

Aromatic and aliphatic substituents on the isonitrile are tolerated, even with sterically hindered substrates. Both aliphatic and aromatic substituents are tolerated, but highly branched phosphines are unreactive.

An initial insertion of $Pd_2(dba)_3$ into the P–H bond of the phosphine oxide **321** is thought to initiate the catalytic cycle. The resulting hydropalladium complex **323** inserts isonitrile **163** into the Pd–H bond to form complex **324** (Scheme 44). Subsequent reductive elimination from **324** affords the α-iminophosphine oxide **322** and regenerates the palladium catalyst.

Several rhodium(I) complexes catalyze the condensation of isonitriles **163** with secondary phosphine oxides **321** to afford bisphosphinoyl(amino)methanes **325** [Eq. (73)].[106] Presumably the mechanism parallels that of the palladium-catalyzed sythesis of α-iminophosphine

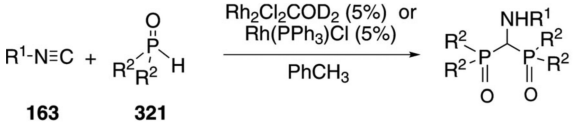


**163** **321** **325** (47–95%)

(73)

oxides [Scheme 44] but includes a second phosphine oxide insertion followed by an attack on the initially formed iminophosphine oxide **322**.

Palladium acetate catalyzes the insertion of aryl isonitriles **326** into the Si–Si bond of disilanes **327**. [Eq. (74)].[107] The insertion was performed with a series of

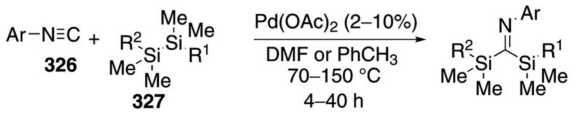


**326** **327**

**a** Ar = 2,6-xylyl (Xy)
**b** A r= 2,5-diisopropylphenyl (Dip)

**328** (28–81%)

(74)

oligomeric silanes resulting in silylimines of varying molecular weights.

Mechanistically, the palladium(II) catalyst is reduced by isonitrile ligation[108] to the palladium(0) complex **329**. Oxidative addition of **329** into the oligosilane **327** forms complex **330** (Scheme 45). Attack of the Pd–Si bond on the isonitrile **326** affords imine **331** which reductively eliminates to form **328** and regenerate the Pd(0) catalyst.

Copper oxide catalyzes the cyclization of isocyanobenzyl alcohols **332** [Eq. (75)].[109] 4*H*-3,1-Benzoxazines **333** are generated when the carbinol substituent $R^1$ is 4-$MeOC_6H_4$, Ph, 4-Cl-$C_6H_4$, 4-pyridyl, or a *tert*-butyl group whereas tetrahydrofuranimines **334** are generated when the substituent $R^1$ is a 2-(5-methylfural) or an isopropyl group. The reason for the changeover in product formation is unknown but is independant of the metal.

Copper oxide cyclizes isocyanobenzyl alcohols **332** by coordinating and activating the isonitrile carbon (Scheme 46).[110] Coordination of copper to the isonitrile **332** forms complex **336** which is activated toward

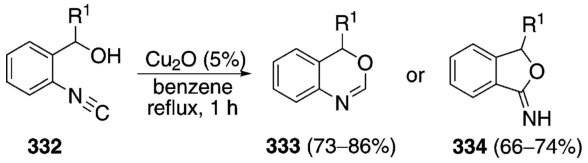


**332** **333** (73–86%) **334** (66–74%)

(75)

internal attack by the hydroxy group. Cyclization and subsequent deprotonation affords **337**. Protonation of **337** forms **333**. Alternatively the benzoxazine **337** can undergo a formal 1,2-rearrangement to afford the isobenzofuranimine **338**. Protonation of the iminocopper bond in **338** yields the tetrahydrofuranimine **334** and regenerates the copper catalyst.

Aromatic and aliphatic isonitriles **163** are condensed with bromoacrylamides **166** and catalytic palladium acetate to form 2,5-diiminofurans **339** [Eq. (76)].[111] The reaction is essentially the same as a previously

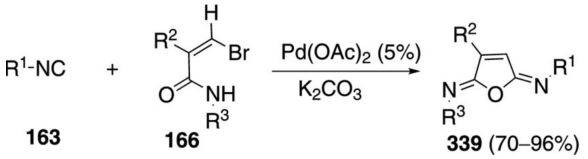


**163** **166** **339** (70–96%)

(76)

reported furan sequence in which the bromoacrylamide is generated *in situ* from a bromoalkyne (*cf.* Scheme 20). The difference lies in the use of $K_2CO_3$ rather than CsF which presumably redirects the reaction to **339** rather than an iminopyrrolidinone.

Mechanistically the reaction likely begins with an oxidative addition of the palladium(0) species (**165**) into the vinyl bromide to afford **167** (Scheme 47). Insertion of the isonitrile **163** into the palladium-carbon bond is followed by attack of the more nucleophilic oxygen onto the metal center of **168**. Presumably the different ligands on palladium, compared to

that in the iminopyrrolidinone reaction, are responsible for the preferential closure to **340** which reductively eliminates to afford **339**.

Palladium acetate, in combination with DPEPhos, catalyzes the condensation of **tert**-butyl isonitrile (**1a**) with ketone **341** to generate iminolactones that were hydrolyzed to the corresponding isocoumarins **342** [Eq. (77)].[112] Aromatic ketones (**341**, $R^3$=Ar) work

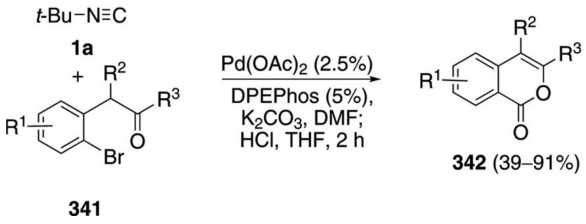


(77)

particularly well with minimal dependence on the electronic nature of the aromatic ring. $NiCl_2$ (2.5%), DPPE, and $K_2CO_3$ catalyze the same condensation of *tert*-butyl isonitrile with ketones **341** to afford iminolactones (52–91%) with the advantage of employing a less expensive metal.[113]

Palladium acetate with DPEPhos[112] and $NiCl_2$, DPPE[113] both catalyze the condensation of the regioisomeric bromo ketones **343** with *tert*-butyl isonitrile to afford iminophthalides that were hydrolyzed to the corresponding phthalides **344** [Eq. (78)]. The ketone substituents $R^2$ can be aliphatic or aromatic.

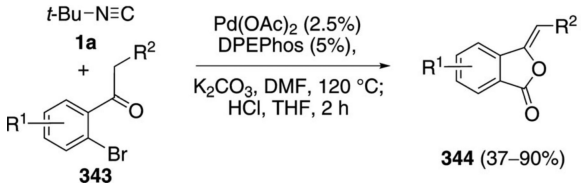


(78)

Electron-rich aromatics are efficient substrates while electron-deficient aromatics are distinctly less effective substrates.

The mechanisms for the isocoumarin and phthalide syntheses are very similar. In the case of isocoumarins, oxidative addition of zerovalent palladium species **165** into the aryl bromide **341** affords complex **345** (Scheme 48). Sequential isonitrile coordination and insertion leads to the coordinated enol **346** that is activated toward deprotonation **346**→**347**. Reductive elimination from **347** generates the iminocoumarin **348** that is hydrolyzed in a separate step to afford **342**.

The rhodium complex $[RhCl_2Cp^*]_2$ catalyzes the synthesis of 3-(imino)isoindolines **350** from isonitriles **163** and *N*-benzoylsulfonamides **349** [Eq. (79)].[114]

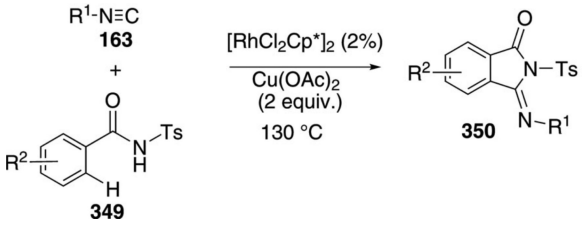


(79)

C–H insertion adjacent to the sulfonamide is followed by isonitrile insertion and ring closure. The sulfon-amide is necessary for the reaction; less acidic benz-amides are unreactive. $Cu(OAc)_2$ is required as an oxidant. Aliphatic and aromatic isonitriles react equally well but substituted aromatic isonitriles polymerize.

Several mechanistic experiments provide insight into the individual steps of the catalytic cycle. Rhodium insertion into the *ortho*-position of the benzamide is facile, implicating C–H insertion and cyclization as the first steps of the catalytic cycle (**349**→**351**, Scheme 49). Isonitrile complexation to rhodacycle **351** affords **352** as a prelude to insertion into the Rh–C bond (**352**→**353**). Reductive elimination from **353** generates the 3-(imino)isoindoline **350** and a rhodium(I) complex which is reoxidized to the rhodium(III) catalyst.

Tertiary isonitriles **163** react with *o*-haloamides **354** to form 3-(imino)isoindolines **355** in the presence of catalytic palladium acetate [Eq. (80)].[115] Several aromatic,

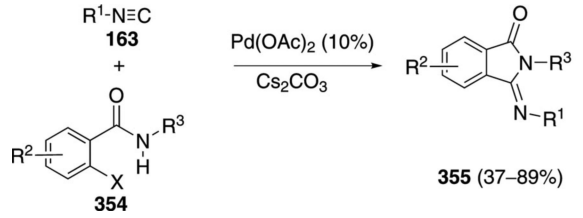


(80)

benzylic, and cyclopropyl substituents are tolerated as substituents on the amide. Iodobenzamides react most efficiently (**354** X=I). A chlorobenzamide affords the corresponding 3-(imino)isoindoline 355 less efficiently (44%) than the corresponding bromide.

Insertion of the benzamide **354** into zerovalent palladium species **165** affords **356** with an interaction between palladium and the amide nitrogen (Scheme 50). Isonitrile insertion into the palladium-carbon bond affords **357** that ejects HBr to afford **358**. The elimination of HBr may occur at **356** prior to isonitrile insertion as the precise order of steps is currently unknown. Reductive elimination from **358** affords **355**, releasing palladium for further catalysis.

A related palladium-catalyzed double insertion of isonitrile **163** into carbonate **359** generates iminolactone **360** [Eq. (81)].[116] The mechanism is uncertain,

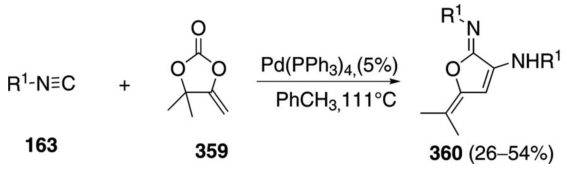


(81)

although it may involve successive isonitrile insertion into a π-allyl palladium complex.

Heating 1,2,3-benzotriazin-4(3*H*)-ones **361** in the presence of catalytic PdCp($\eta^3$-$C_3H_6$) and an isonitrile **163** triggers nitrogen extrusion and isonitrile insertion to afford 3-(imino)isoindolines **362** [Eq. (82)].[117]

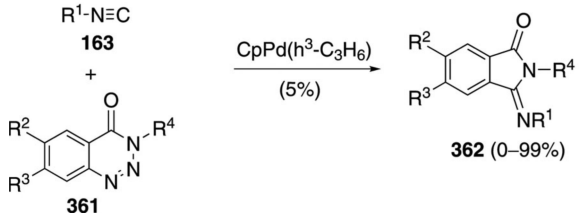


(82)

Electron-rich and electron-deficient substituents are tolerated in the 1,2,3-benzotriazin-4(3*H*)-ones **362** as are both aliphatic and aromatic isonitriles.

The diazosulfones **363** react with aryl isonitriles **326** to afford **364** [Eq. (83)]. The yields are slightly better than for the corresponding 1,2,3-benzotriazin-4(3*H*)-ones **361**.

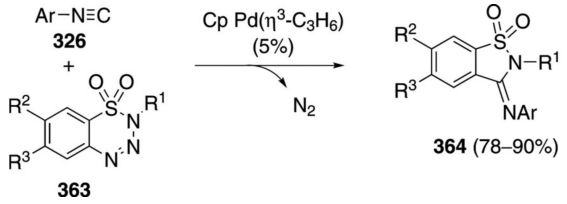


(83)

The catalyst is believed to be a zerovalent palladium complex **165**, which is consistent with the high catalytic activity of $Pd(dba)_2$. 1,2,3-Benzotriazin-4(3*H*)-ones **361** insert palladium(0) and release nitrogen gas to afford palladium(II) complex *365* (Scheme 51). Sequential binding of the isonitrile **165** to the palladacycle **365** and insertion into the Pd–C bond affords **366**. Reductive elimination from **366** releases the 3-(imino)isoindoline **362** and the zerovalent palladium catalyst.

$Pd(Ph_3)_4$ catalyzes the formation of conjugated cyclopenteneimines **368** from isonitriles **163** and γ-methylidene-δ-valerolactones **367** [Eq. (84)].[118] Aromatic isonitriles having bulky substituents work best; 4-$MeOC_6H_4NC$ requires a different catalyst generated from $PdCp(\eta^3\text{-}C_3H_5)$ and dppf. Preliminary experiments to achieve asymmetric induction with $PdCp(\eta^3\text{-}C_3H_5)$

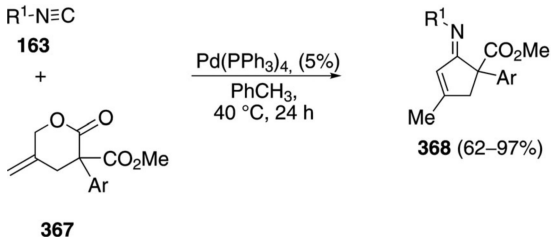


(84)

and the chiral ligand (*R*)-DTM-Segphos provided the cyclopentenimine **368** with an *er* of 9:1.

The proposed mechanism involves insertion of zerovalent palladium **165** into the allylic lactone **367** triggering decarboxylation to the π-allyl zwitterion **369** (Scheme 52). Attack of the enolate onto the isonitrile **163** gives imine anion **370** which cyclizes onto the electrophilic π-allyl to complete the catalytic cycle **370**→**368**. Given the electrophilicity of the π-allyl palladium moiety, the sequence may well be inverted: isonitrile attack on the π-allyl followed by ring closure through attack of the enolate on a nitrilium intermediate. The cyclopenteneimines **368** are readily hydrolyzed to the corresponding enones **371**.

Several nickel complexes promote the intramolecular co-cyclization of silyl cyanides **373** and enynes or dienes **372** to form iminocyclopentenes **374**.[119] $Cp_2Ti(PMe_3)_2$, or $Ni(COD)_2$ with ligand **375**, both catalyze the reaction [Eq. (85)].[120] In solution silyl cyanides exist as the major component in equilibrium with the corresponding isonitriles,[121] providing a low

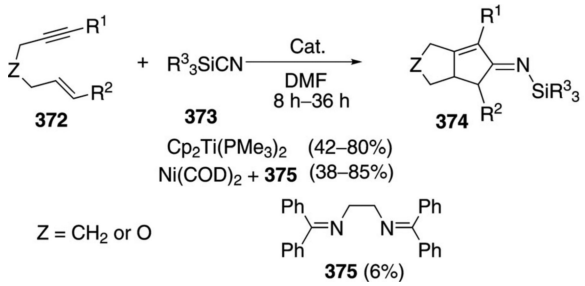


(85)

concentration of the isonitrile which minimizes irreversible binding to the catalyst. Optimizations with $Cp_2Ti(PMe_3)_2$ identified $Et_3SiCN$ and *t*-$BuMe_2SiCN$ as the best isonitrile sources. The imines **374**, obtained in close to quantitative yield, were hydrolyzed

to the corresponding ketones. Several substituents are tolerated in the tether. Terminal alkynes **372** ($R^1$=H) are not viable substrates.

$Ni(COD)_2$ in combination with the diimine ligand **375**, catalyzes the same addition of enynes to silyl cyanides to form iminocyclopentenes [Eq. (85)].[122] The $Ni(COD)_2$ method is more functional group-tolerant than the $Cp_2Ti(PMe_3)_2$-catalyzed cyclization. The mechanism is presumably analogous to that of the titanium-catalyzed cyclization except proceeding through a Ni(0)–Ni(II) catalytic cycle.

Mechanistically, the active titanium catalyst **376**, formed by ligand dissociation from $Cp_2Ti(PMe_3)_2$, cyclizes the enyne **372** to titanocycle **377** (Scheme 53). Insertion of the isonitrile into the $sp^3$ Ti–C bond affords **378** from which reductive elimination delivers the iminocyclopentene **374** and the catalyst **376**.

$[RhCl(COD)]_2$ catalyzes the coupling of aromatic isonitriles **326** with diynes **379** to afford iminocyclopentadienes **380** [Eq. (86)].[123] Ester and ether functionality is tolerated in the tether linking the two alkynes.

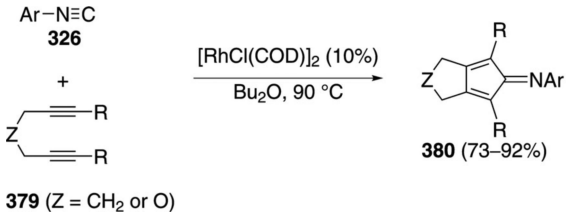


(86)

Portionwise isonitrile addition in coordinating solvents was required for the coupling. A rapid addition was required for 4-methoxyphenyl isonitrile, presumably to prevent catalyst deactivation.

The catalytic cycle involves two key steps, cyclometallation and isonitrile insertion (Scheme 54). Rh-catalyzed cyclometallation of diyne **379** affords rhodacycle **381**. Subsequent isonitrile insertion into one of the Rh-carbon bonds affords **382** from which reductive elimination generates the iminocyclopentadiene **380**. For the catalytic cycle to operate, the rhodium catalyst must react faster with the diyne than with the isonitrile. Reversable complexation to the isonitrile appears unlikely.

Several transition metal catalysts condense alkynes and an isonitrile to form azadienes and aza-1,3-diynes.[124] In some cases the bifunctional imines are isolated while in other cases they are converted to heterocycles *in situ*.

$Rh_4(CO)_{12}$ catalyzes the addition of a tertiary alkyl (**163**) or aryl isonitrile **326**, a terminal alkyne **383**, and a hydrosilane **384** to afford *Z*- or *E*-azadienes *Z*-**385** and *E*-**386**, respectively [Eq. (87)].[125] The nature of the isonitrile dictates the stereochemistry; tertiary alkyl isonitriles afford (*Z*)-β-silyl-α,β-unsaturated imines **385** whereas aromatic isonitriles afford (*E*)-β-silyl-α,β-unsaturated imines **386**. Alkynes bearing

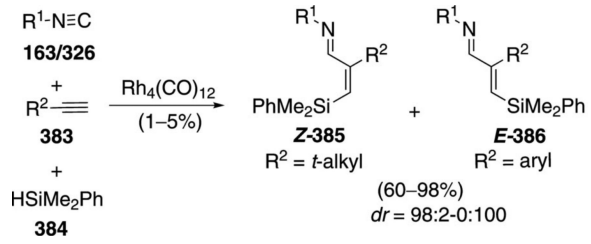


(87)

electron-withdrawing groups or sterically demanding groups diminish the reaction rate.

The catalytic cycle hinges on $Rh_4(CO)_{12}$ reacting with $HSiMe_2Ph$ to form complex **387** (Scheme 55). *syn*-Addition of **387** to the alkyne **383** affords the (*Z*)-β-silylvinyl rhodium complex **388** which inserts an isonitrile **163/326** to form the imino-rhodium intermediate **389**. When the imino substituent has a tertiary alkyl group, the complex reacts with $HSiMe_2Ph$ to give **389** and regenerate the catalyst **387**. Aromatic substituents $R^1$ on the isonitrile allow a rapid *Z*→*E* equilibration **389**→**390**→**391** prior to reaction with the hydrosilane.

The titanium pyrrolyl complex **392** catalyzes the union of an isonitrile **163** and an alkyl- or arylamine **3** with an alkyne **110** to form azadienes **393** [Eq. (88)].[126] Terminal and internal alkynes are equally effective, although the reaction is only modestly regio-selective with internal alkynes. Quaternary, sterically hindered isonitriles react well, but phenyl isonitrile and cyclohexyl isonitrile do not react to afford azadienes.

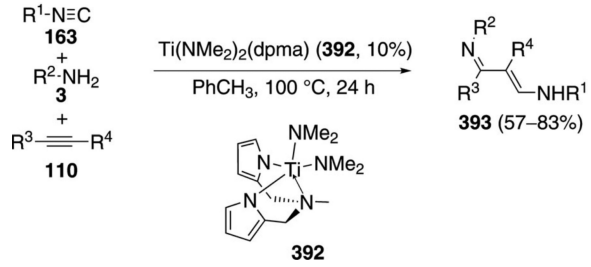


(88)

The pyrrolyl complex **392** is thought to be the pre-catalyst en route to the active titanium imido catalyst **394** (Scheme 56). Reversible [2+2]addition of **394** to the alkyne **110** forms **395** that inserts the isonitrile **163** into the titanium-carbon bond. The resulting iminoacyl complex **396** binds the amine **3** which protonates the titanium-carbon and titanium-nitrogen bonds to release the azadiene **393** and regenerate the titanium imido complex **394**.

The related titanium pyrrolyl complexes **398** and **399** catalyze the three-component coupling of an isonitrile **163**, an alkyne **110** and a hydrazine **397** to form hydrazones **400** [Eq. (89)].[127] Internal and terminal alkynes **110**, alkyl and aryl isonitriles **163**, and alkyl-and

aryl-containing 1,1-disubsituted hydrazines **397** give the unsaturated β-aminohydrazones **400**. Yields vary from 12–73%, suggesting that further advances are required for the reaction to be robust.

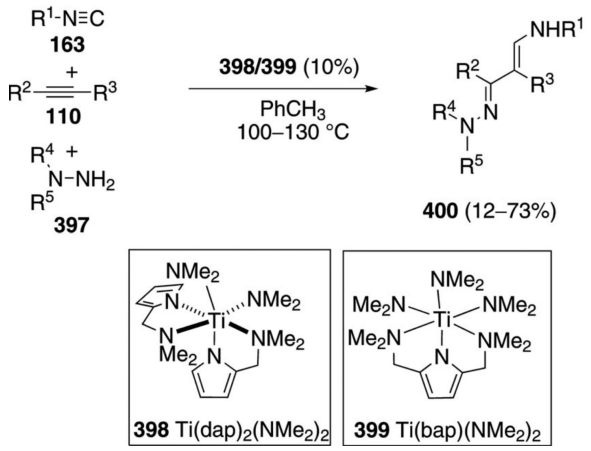


(89)

Catalyst **398**, containing two 2-(*N*,*N*-dimethylaminomethyl)pyrrolyl ligands, is the best catalyst in all but one case. Mechanistic studies indentify dissociation of one ligand as the first step. Subsequent coordination and deprotonation of the hydrazine **397** then generate the active catalyst **401** (Scheme 57). Reversible [2+2]cycloaddition with the alkyne **110** generates the azacyclobutyl titanacycle **402** whose formation sets the regioselectively of the coupling. Isonitrile insertion into the titanium-carbon leads to **403** which binds hydrazine that subsequently protonates the titanium-carbon and titanium-nitrogen bonds. The bound azadiene **400** is released and the Ti=N catalyst **401** reenters the catalytic cycle.

Palladium acetate catalyzes the condensation of hindered aromatic and aliphatic isonitriles with tosylimines **404** and ethyl diazoacetate **405** to form acrylamidines **406** [Eq. (90)].[128] Tosylimines **404** derived


(90)

from aromatic aldehydes react well whereas aliphatic aldehydes lead to complex mixtures with minimal acrylamide.

Palladium catalysts effectively couple latent carbenes such as **405** with isonitriles **163** to generate ketenimines **407** (see Scheme 79). The ketenimine **407** is proposed to react with tosylimine **404** to form the formal [2+2]azetidine **408** (Scheme 58). Proton-transfer and ring opening of **408** generate **406**. Several mechanistic experiments are consistent with the proposed sequence.

## 6 Condensations Affording Yneimines

The half-sandwich, rare earth complex **409** catalyzes the cross-coupling of isonitriles **163** with terminal alkynes **383** to yield (*E*)-1-aza-1,3-enynes **410** [Eq. (91)].[129] Aromatic and aliphatic substituents are tolerated equally well in the alkyne. Electron-rich arylacetylenes

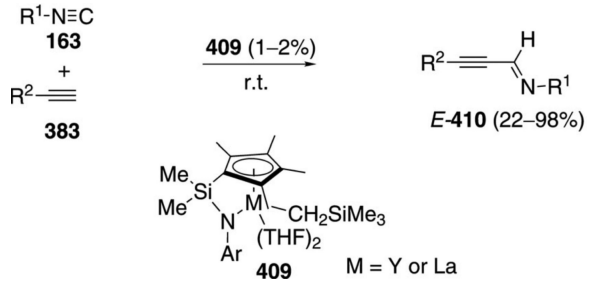


(91)

**383** do not react well with catalyst **409** (M=Y) but do react with the corresponding lanthanum catalyst **409** (M=La).

Adding the lanthanide complex **409** to a terminal alkyne **383** generates the bridged catalyst **412** (Scheme 59). On coordination of the isonitrile **163**, the complex dissociates to the open dimetallate **413**. Internal attack of the terminal alkynide onto the isonitrile leads to **414** which binds the alkyne **383** and protonates to form the (*E*)-1-aza-1,3-enynes **410** and regenerate **412**.

Organoactinide complexes catalyze the insertion of isonitriles **163** into terminal alkynes **383** to yield (*Z*)-1-aza-1,3-enynes **418** [Eq. (92)].[130] Three different actinide

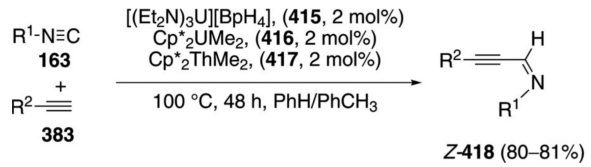


(92)

complexes catalyze the condensation, varying in the ratios of accompanying dimeric and oligomeric imines. All three catalysts require heating to 90–100°C and sterically demanding

substituents on the acetylene. $(Cp^*)_2UMe_2$ has a propensity to form multiple isonitrile insertion products, although moderating the ratio of alkyne to isonitrile diminishes the propensity toward oligomerization.

Organoactinide complexes **415–417** are protonated on coordination of the terminal acetylene **383** generating the active catalyst **419** (Scheme 60). Isonitrile insertion into the actinide-carbon bond, to form **420**, is the rate-determing step in the sequence. Protonation of **420** by the terminal acetylene **383** releases the acetylenic aldimine **418** and regenerates the catalyst **419**.[131] Kinetic studies show that **419** is the resting state of the catalyst.

The uranium pre-catalyst $(Cp^*)_2UMe_2$ **416** affords a significant amount of double insertion product **422** *via* **421**. Insertion of isonitrile **163** into the uranium complex **420** is favored with excess isonitrile **163** and with acetylenes **383** bearing small subsitutuents. The insertion to afford Z-imines Z-**418** retards the formation of double insertion product **422**, because of steric compression between the isonitrile and terminal acetylene substituents.

The organothorium catalyst **417** promotes the conjugate addition of the terminal acetylene **383** to the acetylenic imine **410** (Scheme 61). Deprotonation of terminal acetylene **383** by the precatalyst **417** affords the true catalyst **423**. Coordination of the acetylenic imine **410** is followed by conjugate addition to give **424**. The conjuage addition is favored with less sterically demanding acetylenes, presumably because the conjugate addition is sterically and electronically retarded with large substituents. Sterically demanding subsitutuents may prevent complexing to the actinide **423**. Complex **424** binds additional alkyne **383**, allowing protonation and release of **425** and the thorium catalyst **423**.

Samarium silylamides catalyze the insertion of isonitriles into terminal alkynes [Eq. (93)].[132] A doubly subsituted phenyl isonitrile is essential, even *t*-BuNC

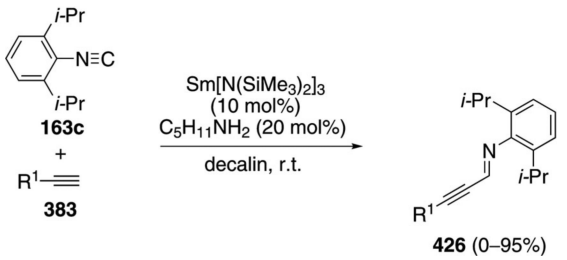


(93)

is unreactive. The most effective isonitrile is 2,6-diisopropylphenyl isonitrile **163c** which likely inhibits oligomerization because of the severe steric compression. Terminal alkynes **383** tolerate remote ether, tertiary amine, and an alkyl chloride functionality. Aromatic alkynes are more reactive than aliphatic alkynes.[133]

Mechanistic studies indicate that primary amines are essential proton transfer agents for the silylamide-catalyzed isonitrile condensation (Scheme 62). Although the precise structure of the catalyst is uncertain, evidence suggests an initial protonation of $Sm[N(SiMe_3)_2]_3$ to form

**427**. Alkyne coordination and deprotonation generate the Sm-acetylide **428** and release the amine **3a**. Insertion of the isonitrile **163c** into the organosamarium bond forms the imine **429**. Protonation of **429** may be from the amine co-catalyst **3a** or the terminal acetylene. Monitoring the reaction identified the *Z*-acetylenic imine as the intial product that slowly isomerizes to the more stable *E*-diastereomer **426**.

A catalyst-ligand combination composed of $Pd(OAc)_2$ and DPEPhos condenses *tert*-butyl isonitrile (**1a**), an aryl bromide **190a**, and a terminal alkyne **383** to afford yneimines **430** [Eq. (94)].[134] Subsequent

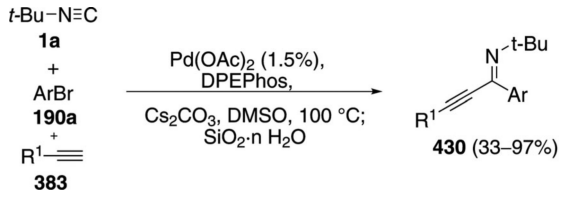


(94)

hydrolysis on silica gel affords alkynones. The reaction tolerates aromatic and heterocyclic bromides having diverse substituents. Alkynes bearing aromatic substituents are distinctly better substrates than their aliphatic counterparts. Overall the isonitrile functions as a carbon monoxide equivalent.

The catalytic cycle proceeds *via* insertion of zerovalent palladium species **165** into the aryl bromide **190a** to afford the Pd(II) complex **192a** (Scheme 63). Isonitrile insertion into the palladium-carbon bond, probably through prior coordination, then affords **431**. Alkyne complexation and deprotonation by $Cs_2CO_3$ generates **432** from which reductive elimination delivers ynimine **430**.

## 7 Quinazoline, Quinolone and Isoquinoline Syntheses

A series of isoquinolines **434** was prepared by the palladium-catalyzed insertion of *tert*-butyl isonitrile (**1a**) into bromo amides **433** [Eq. (95)]. The bromo amides

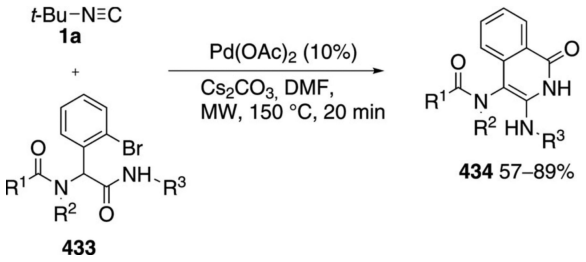


(95)

**433** were prepared by a microwave-accelerated Ugi multicomponent condensation.[135] Variation in the amide is tolerated but no variation in the aryl bromide was reported.

Catalysis is initiated by palladium insertion into the aryl bromide **433** (Scheme 64). The authors propose insertion of *tert*-butyl isonitrile (**1a**) into **435** to afford **436** and a base-assisted cyclization to give **437**. Given the proximity of the amide to the electrophilic palladium in **435**, a more likely sequence is cyclization followed by isonitrile insertion. Reductive elimination from **437** affords **438**. Tautomerization and protonation of **438** to **439** (Scheme 64, *lower segment*), followed by fragmentation, affords **440** that loses isobutylene en route to the isoquinoline-1(2*H*)-one **434**.

The palladium-catalyzed intramolecular imidoylative cross-coupling of isonitriles **163** with *N*-(2-bromoaryl)amidines **441** produces 4-aminoquinazolines **442** [Eq. (96)].[136] Catalyst optimization identified an inexpensive phosphine ligand (DPCB), and $Pd(OAc)_2$ as the optimal combination. In difficult cases, the re-

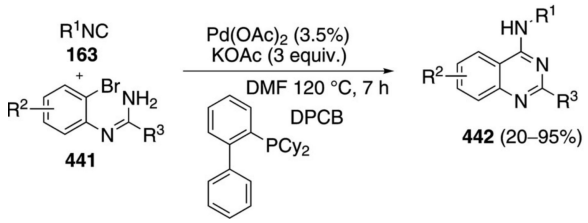


(96)

action temperature can be increased to 160°C and the catalyst loading increased to 5 mol%. Halides are tolerated in the aromatic ring, and any dehalogenation can be suppressed by performing the reaction at lower temperatures. The reactions with alkyl isonitriles are efficient but aryl isonitriles cannot be employed.

The key mechanistic steps are oxidative addition, isonitrile insertion and cyclization. Oxidative addition of palladium(0) species **165** into **441** is followed by coordination to the amidine moiety leading to the palladium complex **443** (Scheme 65). Isonitrile insertion into **443** produces **444** which is deprotonated with KOAc to afford the seven-membered palladacycle **445**. Reductive elimination of palladium from **445** yields **446** which aromatizes to afford 4-aminoquinazoline **442**.

A related palladium-catalyzed amidation employs direct C–H insertion followed by isonitrile insertion to generate 4-amino-2-aryl(alkyl) quinazoline **448** [Eq. (97)].[137] The reaction is performed in an oxygen

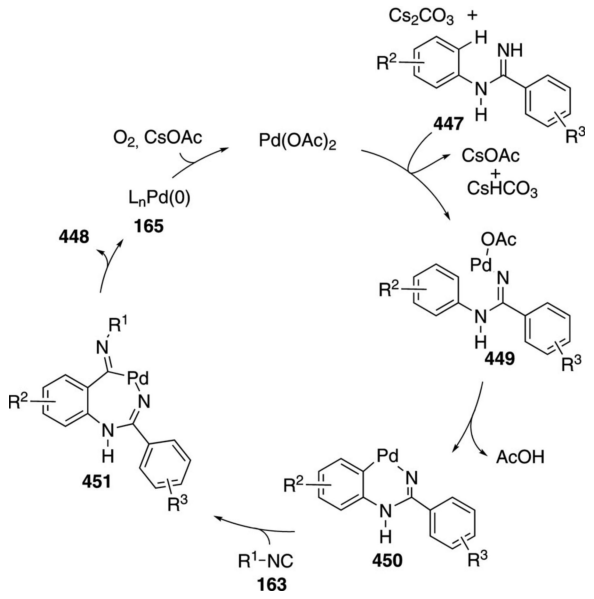


(97)

atmosphere to reoxidize the palladium catalyst. Electron-donating groups on the benzamidine ring of **447** are more efficient than electron-withdrawing groups. Sterically encumbered aryl isonitriles **163** and *t*-BuNC (**1a**) give higher yields than their less hindered counterparts, which correlates with the thermal stability of isonitriles.

The benzamide cyclization begins with coordination of $Pd(OAc)_2$ to the amidine nitrogen of **447** which promotes deprotonation by cesium carbonate to form **449** (Scheme 66). Nucleophilic attack of the aromatic ring on palladium provides cyclopalladated **450**. Isonitrile insertion into **450** affords **451** that reductively eliminates an imine that tautomerizes to produce the quinazoline **448**. Subsequent oxidation of palladium(0) **165** regenerates palladium acetate.

Quinazolines **452** are formed in the palladium-catalyzed multicomponent addition of two equivalents of *tert*-butyl isonitrile (**1a**) and an amine **3**, to bis(2-iodoaryl)carbodiimides **263** [Eq. (98)].[138] Reaction optimization identified toluene as the best solvent and $Cs_2CO_3$ as the best base. Electron-rich and electron-deficient carbodiimides work equally efficiently.

Oxidative addition of palladium(0) to the aryl iodide **263** and nucleophilic addition of the amine **3** to the carbodiimide generate the palladium(II) complex

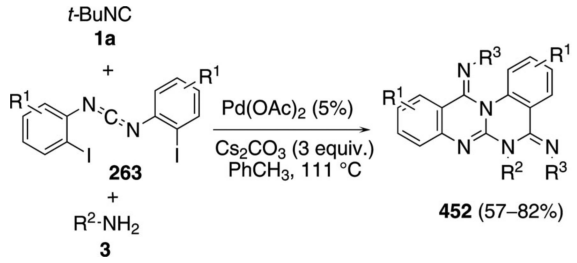


(98)

**453** (Scheme 67). Deprotonation by $Cs_2CO_3$ leads to a transient six-membered palladium complex that inserts *tert*-butyl isonitrile (**1a**) to give palladacycle **454**. Reductive elimination of **454** is followed by a second oxidative addition into the other aryl iodide. The resulting palladium(II) complex **455** engages in the same type of addition–cyclization sequence: **455**→**456**→**457**. Reductive elimination from **457** produces the quinazolino[3,2-*a*]quinazoline **452** and regenerates palladium(0).

Quinazolin-4(3*H*)-imines **459** are formed in the palladium-catalyzed condensation of isonitrile **163**, the carbodimide **458**, and the amine **221** [Eq. (99)].[139]

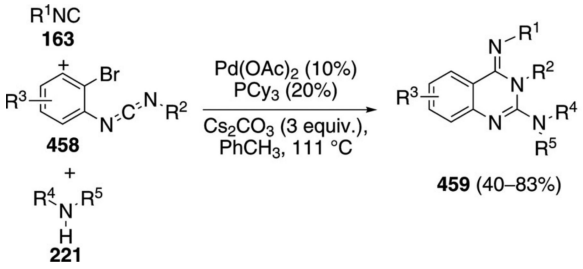


(99)

The amine **221** can be primary or secondary and the isonitrile **163** can be primary or tertiary. Modest substitution in the aromatic ring is tolerated (Me, Cl, F). The sequence was also performed by replacing the amine with benzyl alcohol and *tert*-butylphenol to afford oxygen-substituted quinazolin-4(3*H*)-imines; substitution of the amine for diethyl phosphite affords 4-imino-3,4-dihydroquinazolin-2-ylphosphonates.[140] In the latter case, *tert*-butyl isonitrile (**1a**) is the best isonitrile partner, although cyclohexyl and butyl isonitrile are serviceable substrates.

Mechanistically, oxidative addition of zerovalent palladium species **165** to carbodiimide **458** generates the palladium(II) complex **460** that undergoes isonitrile insertion to afford **461** (Scheme 68). Nucleophilic addition of the amine to the carbodiimide triggers cyclization to **462** with reductive elimination leading to the quinazolin-4(3*H*)-imine **459**. The precise order of the steps is uncertain and may involve nucleophilic attack on the carbodiimide prior to oxidative addition by the palladium catalyst.

Aromatic and aliphatic primary, secondary, and tertiary isonitriles **163** are condensed with ortho-acetylenic anilines **463** under palladium catalysis to afford quinolines **464** [Eq. (100)].[141] Using $PdCl_2$ as the catalyst

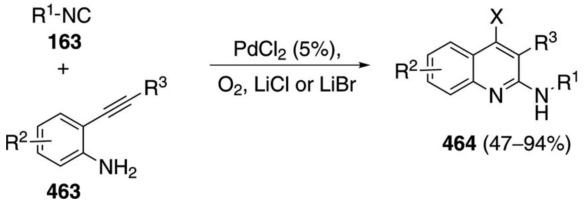


(100)

and stoichiometric LiCl affords the chloroquino-line whereas use of $PdBr_2$ and LiBr generates the corresponding bromoquinoline. Diverse substituents are tolerated within the aromatic ring without influencing the reaction efficiency.

Coordination of the palladium catalyst to the alkyne and the amine is proposed to activate **463** to a *trans*-halopalladation (Scheme 69). The close proximity of the amine to the palladium center likely results in ligation as indicated in **465**. Isonitrile insertion into **465** affords **466** that loses HX to afford **467**. The precise order of the cyclization, insertion, and dehydrohalogenation may be different in the conversion of **465** to **467**. Reductive elimination of **467** to afford **468** is followed by isomerization to the quinoline **464**. Palladium(0) is reoxidized in air to the palladium(II) catalyst.

Palladium acetate catalyzes the condensation of *tert*-butyl isonitrile (**1a**) and cyclohexyl isonitrile (**163b**) with **469** to afford phthalazino[1,2-b]quinazolinones **470** [Eq. (101)].[142] Me and Cl substituents in

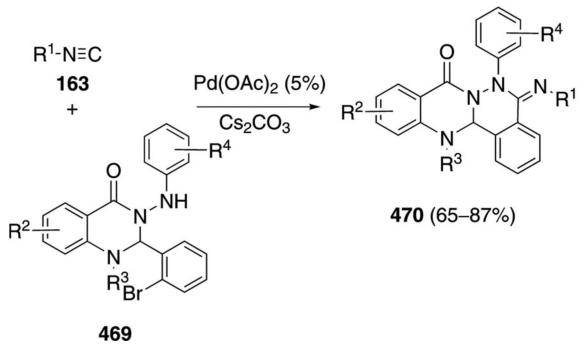


(101)

the aromatic rings are tolerated. Substrates with prop-argyllic substituents $R^3$ on the aniline nitrogen were cleaved during the reaction.

Oxidative addition of palladium into the aryl bromide **469** initiates the catalytic cycle (Scheme 70). The resulting palladium complex **471** complexes to the proximal nitrogen

facilitating deprotonation of the amine nitrogen. The sequence depicted posits isonitrile insertion into **471** followed by dehydrohalogenation of **472** to afford **473**, although the precise sequence of steps is unknown. Reductive elimination from **473** releases **470** and allows zerovalent palladium to reenter the catalytic cycle.

## 8 Urea, Amide, and Amidine Syntheses

Gold(I) forms strong complexes with isonitriles because of the strong s-donation by the carbon electron pair.[143] Gold powder catalyzes the condensation of isonitriles **163** with secondary amines **221** in the presence of oxygen or a tertiary amine oxide to afford ureas **474** [Eq. (102)].[144] Electron-rich amines react

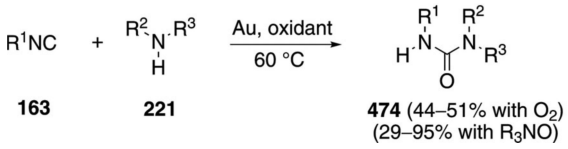


(102)

fastest with increasing steric demand diminishing the reaction rate.

Organic isonitriles **163** bind to the gold surface through a σ donation of the electron pair, with minimal π back donation from the metal, to form **475** (Scheme 71).[145] The complexation effectively activates the $\eta^1$ bound isonitrile toward nucleophilic addition which, for secondary amine **221**, affords **476**. Interaction of the amine hydrogens with the gold surface may facilitate migration of the amine proton to the imine nitrogen and formation of the gold carbene **477**. Subsequent oxidation releases the urea **474**. Although the oxidation mechanism remains uncertain, rate studies suggest that the oxidation is not rate-limiting.

An analogous gold-catalyzed condensation of butyl isonitrile **163d** with the primary amine, butylamine (**3b**), affords the carbodiimide **478a** [Eq. (103)].[146]

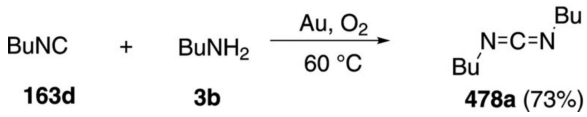


(103)

The mechanism is thought to proceed through a similar catalytic cycle as for secondary amines (Scheme 71), although the oxidation sequence is unknown.

A mechanistically distinct, gold-catalyzed coupling between isonitriles **163**, primary or secondary amines, and amine *N*-oxides **479** affords ureas **474** (Scheme 72).[147] The reaction efficiency correlates with the isonitrile cone angle;[148] more hindered isonitriles react less efficiently. Secondary and primary amines react equally well, and appear not to be subject to the same steric demands as the isonitrile component.

Mechanistically, absorption of the isonitrile onto the gold surface to give **475** is followed by attack of the amine oxide oxygen onto the activated isonitrile carbon (**475+479→480**), (Scheme 72). The resulting complex **480** ejects the tertiary amine **481** to form the gold-complexed isocyanate **482**. Attack of the secondary amine on the isocyanate **482** releases the urea **474** with concommitant formation of the active gold catalyst.

Cobalt acetate is found to catalyze the condensation of isonitriles with anilines **483** to form ureas **484** under ultrasonic irradiation [Eq. (104)].[149] Primary,

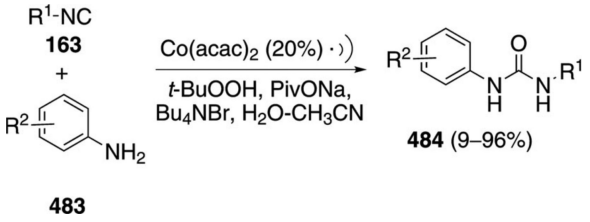


(104)

secondary, and tertiary alkyl isonitriles and 2,6-dime-thylphenyl isonitrile function effectively in reactions with electron-rich anilines. Performing the reaction with sublimed sulfur affords the corresponding thioamide. Primary and secondary amines can be substituted for anilines to afford the corresponding ureas,

Cobalt acetate catalyzes the condensation of *tert*-butyl isonitrile (**1a**) with 2-aminophenols (**485**, Y=O), 2-aminothiophenols (**485**, Y=S), and 1,2-diaminobenzenes (**485**, Y=NH) to afford the corresponding heterocycles **486** [Eq. (105)].[150]

The proposed mechanism incorporates radical and ionic intermediates (Scheme 73). Sequential addition

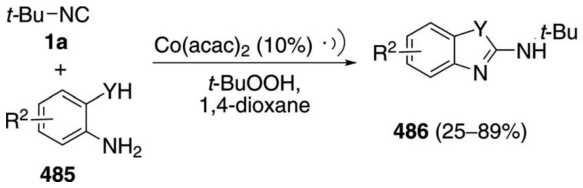


(105)

of two equivalents of isonitrile **163** to $Co(acac)_2$ first gives **487** through displacement of one coordination within an acac ligand and then **488** through displacement of a second acac ligand. Nucleophilic attack on the coordinated isonitrile gives **489**. Addition of *t*-BuO radical causes oxidation of cobalt to give the cobalt carbene **490** which ejects *t*-$BuO^-$ and the radical fragment **491**. Subsequent oxidation of **491** and interception by the appropriate nucleophile afford the amidine-type core **492**.

Palladium catalyzes the condensation of isonitriles **163** and amines **3** to form *N*,*N*-dialkylcarbodiimides **478** [Eq. (106)].[151] Cyclohexyl and *tert*-butyl isonitrile

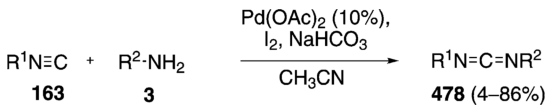


(106)

react equally well with aliphatic amines or an electron-rich aniline. Stoichiometric iodine and oxygen are integral components of the reaction. The mechanism is uncertain, but may involve the reaction of an isonitrile-complexed palladium catalyst either with the amine or with an *N*-iodoamine.

$NiCl_2$ catalyzes the condensation of tertiary isonitriles **1** with primary amines **3** to afford carbodiimides **493** [Eq. (107)].[152] Oxygen or air is required to reoxidize

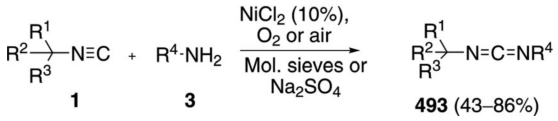


(107)

the catalyst and either molecular sieves or $Na_2SO_4$ is required as a dessicant. Amines bearing electron-rich substituents react more efficiently than those with electron-deficient substituents, although greater efficiency can be achieved by switching to $Ag_2O$ as the oxidant. In one case $(Ph_3P)_4Pd$ was substituted for $NiCl_2$ and found to only slightly reduce the reaction efficiency.

Isonitriles feature in a palladium-catalyzed carbox-amidation of indoles [Eq. (108)].[153] Unprotected or

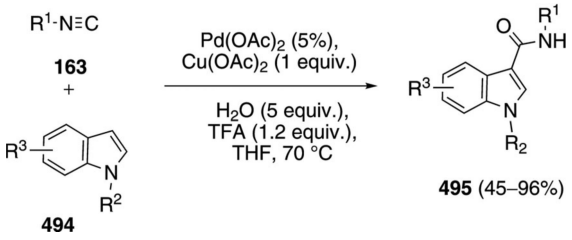


(108)

*N*-alkyl-substituted indoles **494** work equally well in reactions with *tert*-butyl, isopropyl, cyclohexyl, adamantyl, and 2,6-dimethylphenyl isonitriles. Indoles protected with electron-withdrawing groups do not react. The C-3 substituted indoles redirect the carboxamidation to C-2 while 2-methylindole reacts, but only in 45% yield.

$Pd(OAc)_2$ is thought to initiate the condensation through an electrophilic palladation of indole **494** at C-3 (Scheme 74). Isonitrile complexation to the palla-dated indole **496** followed by migratory insertion is thought to afford imidoyl palladium **497**. In the absence of water, **497** suffers reductive elimination to yield **500** which rearranges to **495**. In the presence of water, which is the case for most reactions, acetate is displaced from complex **497** to afford **498**. Reductive elimination of palladium from **498** and tautomerization of 499 affords **495**. Labelling experiments with $H_2{}^{18}O$ are consistent with incorporation of $^{18}O$ into the amide carbonyl oxygen.

Palladium chloride catalyzes a related indole-3-carboxamide synthesis through the condensation of isonitriles **163** with *ortho*-alkynylanilides **501** [Eq. (109)].[154] *tert*-butyl isonitrile and adamantly isonitrile

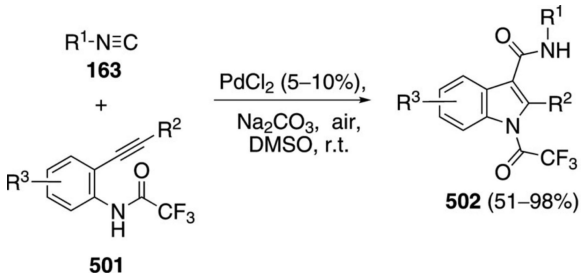


(109)

react well, whereas butyl, isopropyl, cyclohexyl, and 2,6-dimethylphenyl isonitriles afford indoles less efficiently. Electron-donating substituents in the aromatic ring facilitate the reaction. Reactions with electron-withdrawing substituents require heating to 50°C to drive the process to completion. Switching the base from $Na_2CO_3$ to KOAc affords the corresponding *N*-acylindolecarboxamide (**502** $R^1$=OAc).

The catalytic cycle is likely initiated by coordination of palladium to alkyne **501**, activating the alkyne toward amidopalladation (**503**, Scheme 75). Base-assisted nucleophilic attack of the amide onto the activated alkyne creates the palladated indole **504**. Isonitrile insertion to **504**, followed by reductive elimination from **505** generates the imidoyl chloride **506** which, upon hydrolysis with adventitious water and cleavage of the trifluoroacetamide, affords **502**.

Isonitriles **163** couple with aryl bromides **227** in the presence of catalytic $PdCl_2$ to efficiently afford amides **507** [Eq. (**110**)].[155] Triphenylphosphine and

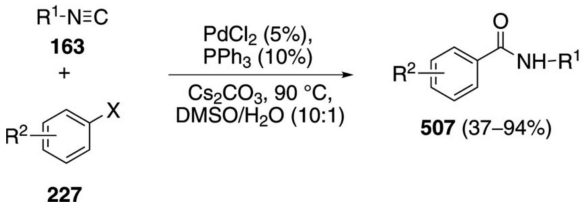


(110)

$Cs_2CO_3$ are essential for the reaction. Electron-withdrawing substituents in the aryl halide afford higher yields and the reaction proceeds in less time than for reactions with electron-donating substituents. Secondary, tertiary, and aromatic isonitriles react equally well. Alkenyl bromides, benzyl bromides, and aryl iodides react as well as aryl bromides. Not all aryl chlorides react and an elevated temperature, 90–110°C, is required for those that do.

Amidation of the aryl halides most likely occurs through an initial oxidative addition of zerovalent palladium species **165** into **227** to afford **192** (Scheme 76). Sequential coordination of the isonitrile **163** followed by migratory insertion affords the iminopalladium complex **508**. Experiments with $^{18}O$-labelled water show incorporation of the label into the carbonyl oxygen suggesting that addition of water to **508** occurs through ligand displacement **508**→**509**, reductive elimination (**509**→**510**), and tautomerization of **510** to amide **507**.

Carboxylic acids engage in a decarboxylative coupling with 1-ethyl-4-isocyanobenzene (**326b**) to afford amides [Eq. (111)].[156] Several coinage metals catalyze

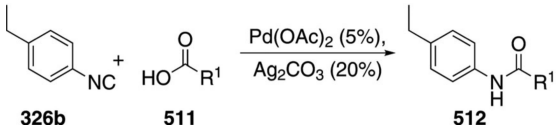


**326b** **511** **512**

(111)

the reaction with catalytic $Pd(OAc)_2$ or $Pd(O_2CCF_3)_2$ and $Ag_2CO_3$ affording the best yields. Diverse aromatic carboxylic acids are suitable substrates, although *para*-methoxybenzoic acid was not reactive, and several aliphatic and unsaturated acids afford good yields of the corresponding amides. Aliphatic isonitriles are incompatible with the reaction conditions.

Mechanistic experiments with $^{13}C$-labelled benzoic acid demonstrate that the amide carbonyl carbon is derived from the carboxylic acid. Palladium acetate is proposed to bind to isonitrile **326b** to form **513** which adds silver carboxylate **514** formed *in situ* from silver carbonate and the carboxylic acid **511** (Scheme 77). The resulting complex **515** suffers an acyl transfer to form the acyl palladium **516** that decarbonylates to form **517**. Protonation of **517** and metal exchange affords the silver carboxylate, releases the amide **512**, and regenerates palladium acetate.

$PdCl_2$ and $Pd(OAc)_2$ catalyze the three-component coupling of *tert*-butyl isonitrile (**1a**) with aryl[157] or alkenyl[158] bromides **190a** and primary or secondary amines **221** to afford amidines **518** [Eq. (112)]. The

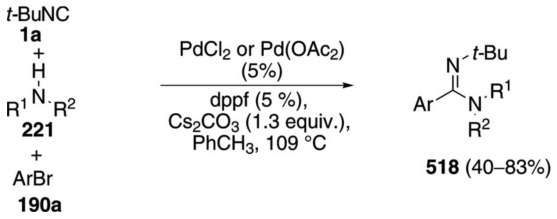


(112)

reaction uses *tert*-butyl isonitrile (**1a**) as the isonitrile component because other isonitriles gave significantly reduced yields and required slow addition over 8 h. Electron-rich aryl bromides and 3-bromopyridine couple equally well. (Aminoalkyl)aryl bromides react to afford cyclic amidines.[159]

An analogous palladium-catalyzed coupling of isonitriles **163** with aryl bromides **190a** and sodium alk-oxides or sulfenylates **519**, affords imidates and thio-imidates **520** [Eq. (113)].[160] Alkenyl bromides and sodium alkoxides afford α,β-unsaturated imidates.[158] Some diversity in the isonitrile is tolerated, with cyclohexyl

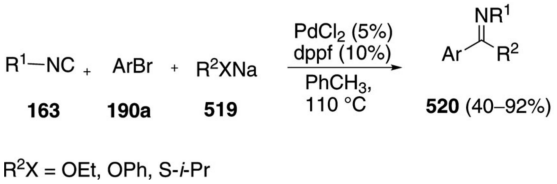


(113)

and butyl isonitriles reacting as well as *tert*-butyl isonitrile. Intramolecular cyclizations with hydroxyalkyl-substituted aryl bromides afford cyclic imidates.[159]

In some instances double isonitrile insertion occurs during the palladium-catalyzed coupling of isonitriles with alkoxides [Eq. (114)]. Multiple insertion is diminished


(114)

through the slow addition of the isonitrile, or by using a five-fold excess of the alcohol, *t*-BuOK as the base, and dioxane as the solvent.[161]

The palladium-catalyzed isonitrile condensations to form amidines **518**, imidates **520**, and iminoimidates **522** proceed through the same mechanism (Scheme 78). Insertion of zerovalent palladium into the aryl bromide **190a** forms complex **192a** which reacts with the

isonitrile **163** to afford the iminoyl palladium complex **523**. Nucleophilic attack on **523** affords palladium complex **524** that suffers reductive elimination to afford the amidine or imidate **518**/**520**/**522**. Double insertion reactions presumably arise through competitive addition of a second isonitrile to **523** or **524** prior to reductive elimination.

$(Ph_3P)_4Pd$ catalyzes the condensation of isonitriles **163** with carbenes derived from *N*-tosylhydrazones **525** [Eq. (115)].[162] The coupling of two formal carbenoids affords ketenimines that are hydrolyzed *in situ* to formamides **526**. Aromatic *N*-tosylhydrazones **525** ($R^1$=Ar) react efficiently when bearing electron-donating

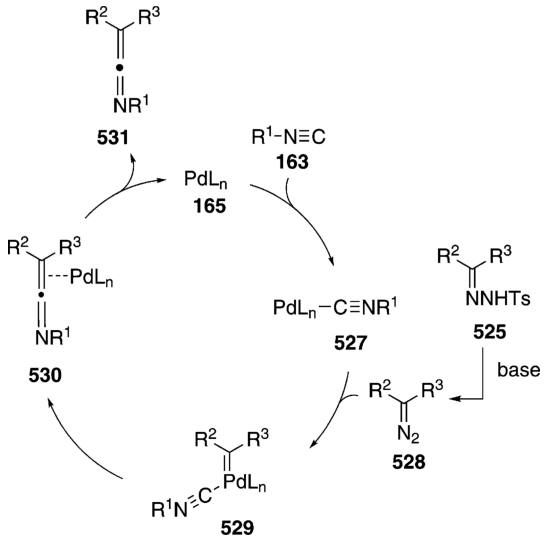


(115)

groups. Electron-withdrawing groups are 20–30% less efficient, possibly because the carbene is destabilized. Primary, and hindered tertiary, isonitriles react equally well. *N*-Tosylhydrazones **525** having alkyl substituents require heating, preferably in dioxane, for acceptable yields.

The mechanistic proposal assumes that the active catalyst **527** is a complex formed between palladium(0) and the isonitrile (Scheme 79). Condensation of **527** with the diazo compound **528** derived by base-induced elimination from the *N*-tosylhydrazone **525**, generates the palladium carbene **529**. Migratory insertion within **529** affords the palladium-complexed ketenimine **530** that is released to regenerate the palladium catalyst. Subsequent hydrolysis of the ketenimine **531** affords the amide **526**.

Sequential palladium-catalyzed C–H insertion–isonitrile insertion provides a facile entry to 6-aminoindolo[3,2-*c*]quinolines **533** and related hetero-cycles [Eq. (116)].[**163**] The strategy is illustrated with 2-(2-aminophenyl)indoles **532** that cyclize to **533** in

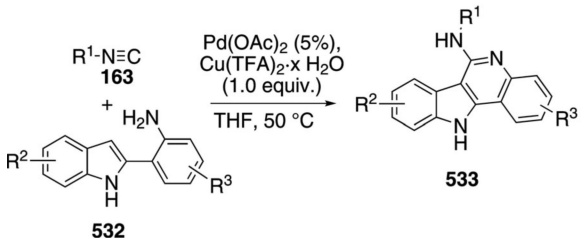


(116)

the presence of $Pd(OAc)_2$ and copper trifluoroacetate as an oxidant. A range of primary, secondary, tertiary and aromatic isonitriles **163** is effectively coupled. A chiral benzyl isonitrile forms **533** with complete stereochemical fidelity. Strong electron-withdrawing groups in the indole reduce the reaction efficiency but otherwise a diverse range of substituents is tolerated. The strategy has been extended to 2-(2-aminophenyl)-pyrroles and related substrates.

Mechanistically, coordination of the aniline nitrogen of **532** to the palladium catalyst is thought to initiate the catalytic cycle (Scheme 80). Electrophilic palladation of complex **534** furnishes the palladium(II) complex **535** that suffers complexation and migratory insertion of an isonitrile group **535**→**536**. Reductive elimination from **536** and subsequent tautomerization affords **533**. The zerovalent palladium is reoxidized by copper(II) to regenerate the active catalyst.

## 9 Miscellaneous Isonitrile Condensations

Many reactions of isonitriles proceed through the formal [3+2]cycloaddition of a metallated isonitrile to an alkene or alkyne. Additions to activated π-systems are more prevalent and proceed under much milder conditions than comparable additions to unactivated alkenes and alkynes. In the absence of an electron-withdrawing group, the mechanism may be through a [3+2] cycloaddition or through a carbometallation.

A highly efficient gold-catalyzed, formal [3+2]addition of substituted isocyanoacetates **90** to *N*-phenylmaleimide **537** affords chiral pyrrolidines **539** [Eq. (117)].[164] The enantioselectivity is higher with substituted

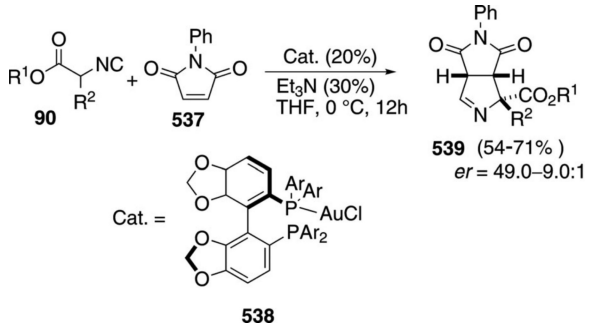

isocyanoacetates and is highest with sterically demanding alkyl-substituted isonitriles. The reaction proceeds *via* a metallated isonitrile generated from the isocyanoacetate **90**, a gold-ligand complex, and triethylamine. Mechanistic experiments identify the active catalyst as a cationic gold species **538**. Although the overall condensation represents a [3+2]cycloaddition, the reaction may involve a stepwise conjugate addition to maleimide followed by cyclization.

Titanium complexes **540** and **541** catalyze the iminoamination of isonitrile **163**, an amine **3**, and alkyne **110** to afford azadienes **542** (see Scheme 56) that can be transformed to heterocycles **543** and **544** depending on the work-up (Scheme 81).[**165**] Simple addition of hydoxylamine hydrochloride in ethanol and heating the reaction mixture for 16 h, regioselectively provides the oxazole **544**.

Catalyst **540** in combination with cyclohexylamine is the most general catalyst, whereas catalyst **541** works best for less reactive substrates. The regioselectivity is excellent with monosubstituted alkynes and can be tuned with internal alkynes through judiciuous choice of solvent and amine co-catalyst. Typically, after the iminoamination is complete, the solvent is removed, pyridine is added, and the reaction mixture is heated to 150°C for 24 h. The isolated yields with terminal alkynes (35–50%) are higher than those for internal alkynes (24–41%).

Performing the iminoamination with titanium catalyst **541**, alkyne **110**, *t*-BuNC (**1a**), and an aromatic amine generates *N*-aryl-1,3-diamines **545** (Scheme 82). Treating **545** with acetic acid generates quinoline **546**. The coupling reaction proceeds well with electron-rich anilines, aminonaphthalenes, and heterocyclic amines, which subsequently cyclize to afford fused heterocycles.[166] Typically the reaction is performed in two steps: the azadiene is formed and then the solvent is removed, acetic acid is added, and the reaction mixture is heated to 150°C for 24–48 h.

A novel copper oxide-catalyzed annelation of activated isonitriles **2** with fullerene (**547**) provides the corresponding 1-pyrrolines **548** [Eq. (118)].[167] Copper oxide is a more effective catalyst than amines, which also promote the reaction. Although no mechanistic

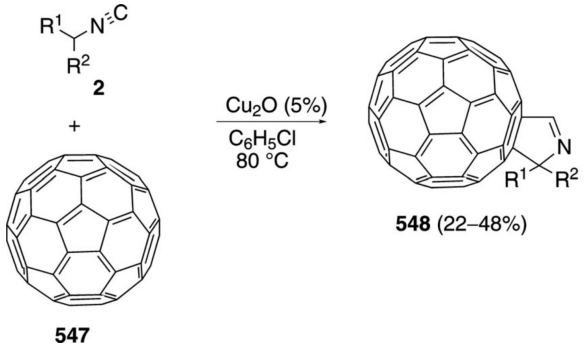


(118)

experiments were performed, the reaction is thought to proceed by a sequential nucleophilic addition followed by cyclization, rather than a direct [3+2]cycloaddition.

Two rhodium complexes catalyze the conversion of aromatic and aliphatic isonitriles **163** to isothiocyanates **551** [Eq. (119)].[168] Elemental sulfur is the best

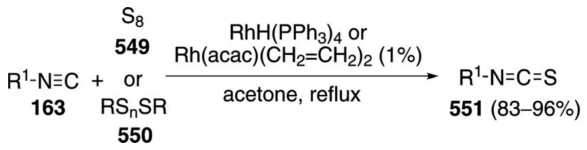


(119)

sulfur source with aryl tri- and tetrasulfides being somewhat less efficient; di- and trisulfides are not effective.

The active catalyst is thought to be the rhodiumisonitrile complex **552** because catalytic activity is only observed if the isonitrile is added prior to addition of sulfur (Scheme 83). An induction period occurs during the first 40 min of the reaction that can be avoided by refluxing sulfur in acetone prior to adding it to the catalyst. Transfer of sulfur to the catalyst **552**→**549**→**553** is followed by an internal sulfur transfer to the isonitrile to form isothiocyanate **551**. Rhodium complex **554** then binds an equivalent of isonitrile **163** to regenerate the catalyst **552**.

The molybdenum complex **556** catalyzes a similar sulfur atom transfer to isonitriles [Eq. (120)].[169]

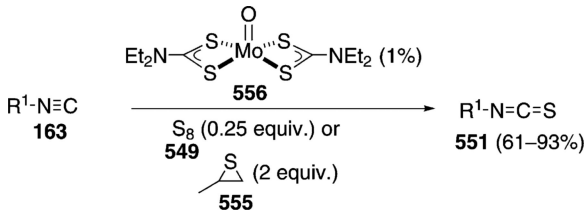


(120)

Either elemental sulfur or propylene sulfide (**555**) are competent sulfur sources. Propylene sulfide exhibits a greater functional group tolerence for alcohol, TMS ether, ester, and alkene functionalities.

The molybdenum complex **556** loads sulfur to afford the disulfide complex **557** (Scheme 84). Sulfur transfer most likely occurs by a nucleophilic attack of isonitrile **163** on **557** to afford the molybdenum(VII) oxosulfide **558** and isothiocyanate **551**. Independent synthesis of complex **558** and reaction with isonitrile **163**, established that both sulfur atoms are transferable. Molybdenum complex **558** participates in a second transfer **558**→**551**+**556**.

[(η-$C_3H_5$)$Pd_2Cl_2$] catalyzes the conversion of isonitriles **163** and $TMSN_3$ (**559**) into the corresponding cyanamide **560** [Eq.(121)].[170] Aromatic and aliphatic

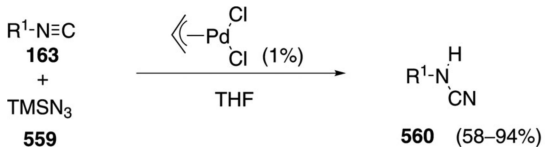


(121)

isonitriles participate, with electron-deficient aromatic isonitriles reacting fastest. Reactions with aryl isonitriles tolerate nitrile, ester, halogen, and alkyne substituents, as well as substitutents at both *ortho* positions.

Mechanistically, oxidative addition of palladium to $TMSN_3$ (**559**) affords the palladium(II) complex **561** that inserts the isonitrile **163** into the Pd–N bond to afford **562** (Scheme 85). A Curtius-type rearrangement of **562** expells nitrogen to afford **563** which tautomerizes to **564**. Reductive elimination from **564** regenerates palladium(0) and releases the silyl cyanamide **565**. During purification on silica gel the nitrogen-silicon bond is cleaved to provide cyanamide **560**.

The palladium-catalyzed condensation of aromatic isonitriles **268** with $TMSN_3$ (**559**) takes a different course in the presence of allyl methyl carbonate (**566**), affording allyl cyanamides **567** [Eq. (122)].[171] The reaction requires $Pd_2(dba)_2{\cdot}CH_3Cl$ or $Pd_2(OAc)_2$,

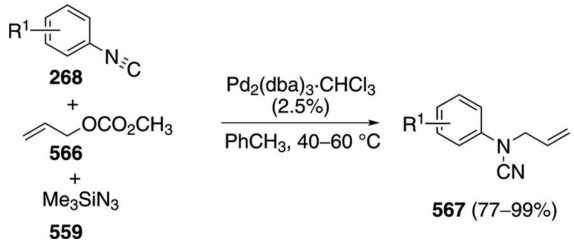


(122)

$TMSN_3$, and an aromatic isonitrile. Electron-withdrawing groups on the aromatic ring accelerate the reaction, which is even efficient with 2,6-disubstituted isocyanobenzenes.

The reaction mechanism involves palladium(0) insertion into allyl methyl carbonate (**566**) and reaction with $TMSN_3$ **559** to afford the π-allyl palladium azide **568** (Scheme 86). Isonitrile insertion into the Pd–N bond affords **569** that engages in a π-allyl palladium Curtius-type rearrangement to afford **570**. Tautomerization of **570** to **571** is followed by reductive elimination to install the allyl substituent in **567**. Independent preparation of a complex analogous to **571** ($R^2$=*p*-MeO) results in isomerization to the corresponding allyl cyanamide **567**, consistent with the proposed catalytic cycle.

Performing the allylation with $TMSN_3$ (**559**) and phenyl isonitriles **572** bearing an *ortho*-acetylene provides a concise route to *N*-cyanoindoles **573** [Eq. (123)].[172] The acetylene can be substituted or terminal, providing control over the C-2 indole substituent. Diverse substituents are tolerated in the benzene ring.

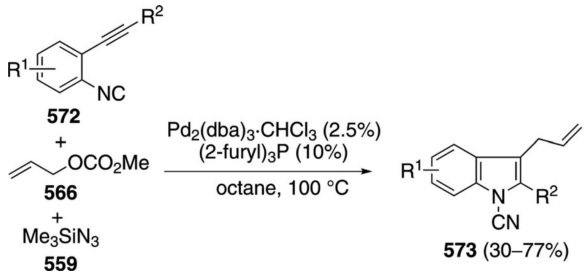


(123)

Electron-withdrawing groups distinctly reduce the yield and, in some cases, excess allyl methyl carbonate is required.

The mechanism parallels the formation of alkyl cyanamides. Insertion of palladium to the allyl carbonate **566** and reaction with $TMSN_3$ (**559**) affords the pallyl palladium azide **568** (Scheme 87). Isonitrile insertion into the palladium-nitrogen bond of **568** affords **574** triggering a Curtius-type rearrangement **574**→**575**. Tautomerization of **575** to **576** aligns the metal for a favorable amino palladation. Subsequent reductive allylation affords the indole **573**.

$[PdCl(allyl)]_2$ catalyzes one of the few isonitrile allylations in which the isonitrile group is retained [Eq. (124)].[173] The palladium-catalyzed addition of the activated isonitrile **90** to the carbonate **577** affords mixtures of regioisomeric isonitriles **578** and **579**. The bidentate ligand diphenylphosphinoethane (dppe) promotes the reaction, possibly by preventing irreversible coordination of the isonitrile to the palladium center. Allylic, benzylic carbonates are poor substrates whereas allylic phosphates react well but are not stable and must be generated, and used, *in situ*.

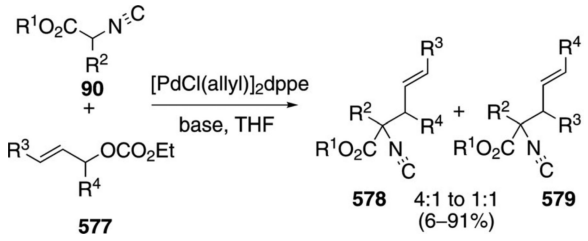


(124)

A palladium acetate-XantPhos combination catalyzes the condensation of tertiary isonitriles **163** with *ortho*-halobenzoates **580** and hydrazines **581** to afford 4-aminophthalazin-1(2*H*)-ones **582** [Eq. (125)].[174] Only tertiary isonitriles participate, possibly because sterically

demanding isonitriles, in combination with the large bidentate Xanthos, are required to prevent the irreversible complexation of the isonitrile to the palladium catalyst. Aryl bromides, iodides and triflates

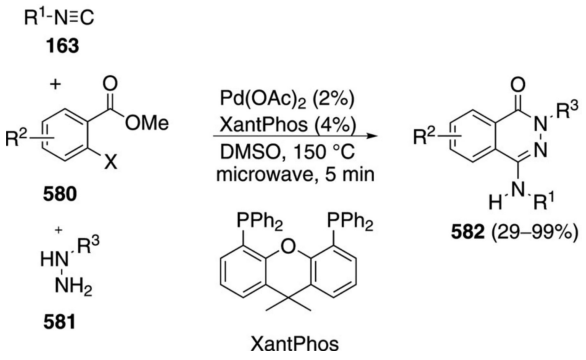


(125)

couple equally well but aryl chlorides are inefficient coupling partners.

Mechanistically, insertion of the palladium catalyst **165** into the aryl halide **580** affords the palladium(II) complex **583** which then inserts isonitrile **163** to yield **584** (Scheme 88). Coordination of hydrazine to the palladium complex **584** facilitates the subsequent deprotonation and halide displacement. Reductive elimination from **585** followed by cyclization and tautomerization provides the aminophthalazin-1(2*H*)-ones **582**.

*t*-BuNC (**1a**) is an efficient cyanating reagent for indoles and related heterocycles (Scheme 89).[175] The indole nitrogen substituent $R^2$ determines the regioselectivity of the cyanation. With aryl, alkyl, or benzyl substituents, the cyanation occurs at C-3 of the indole ring **586**→**587**. When the substituent $R^2$ contains a closely positioned heteroatom capable of coordination, the metallation is redirected to the C-2 position of the indole ring **586**→**588**.

The catalytic cycle is likely initiated by direct metallation of the indole ring (Scheme 90). For indoles without chelating groups, palladation occurs at the more electron-rich C-3 position whereas chelating groups bind to palladium and direct palladation to C-2, **586**→**589**. The resulting palladium complex **589** is stabilized by internal coordination with the adjacent heteroatom. Delivery of the isonitrile via the copper complex **590** provides **591** which is poised for isonitrile insertion into the palladium-carbon bond to afford **592**. Loss of isobutylene from **592** ejects the cyanoindole **588** and palladium(0) that is reoxidized through an air-mediated Cu(I) to Cu(II) cycle.

A virtually identical palladium acetate-catalyzed cyanation of substituted indoles **593** also employs *t*-BuNC [Eq. (126)].[176] In this case, $^{13}$C-labelling of *t*-BuNC

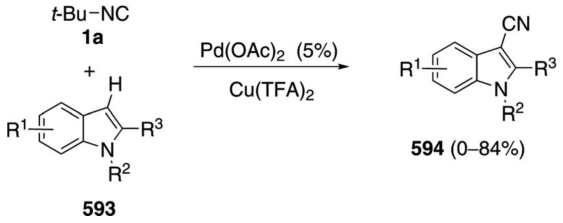


(126)

(**1a**) confirms that the nitrile carbon is derived from the isonitrile. $Cu(TFA)_2$ and air are employed to reoxidize the palladium catalyst. An electron-rich substituent is required on the indole nitrogen. Electron-deficient groups in the indole retard the reaction. Cyanations are also effective with 2-phenylpyridine and similar substrates bearing chelating groups. These substrates require TsOH and elevated temperatures, typically 120°C.

Electrophilic palladation of the indole **593**, or other aromatics, likely initiates the cyanation process by forming **595** (Scheme 91). Insertion of the isonitrile **1a** into the α-indolylpalladium(II) trifluoroacetate **595** leads to **596** that subsequently fragments through the loss of isobutylene and cyanoindole **594**. Palladium(0) is then reoxidized by $Cu(TFA)_2$ to complete the catalytic cycle. Overall, *t*-BuNC (**1a**) functions as a cyanide source through an insertion followed by scission of the *t*-Bu-nitrogen bond.

$Pd(OAc)_2$ catalyzes the sequential cyclization of 2-alkynylbenzaldimines **597** and reaction with isonitriles in an unusual cyanation route to cyanoisoquinolines **598** [Eq. (127)].[177] The reaction employs substituted

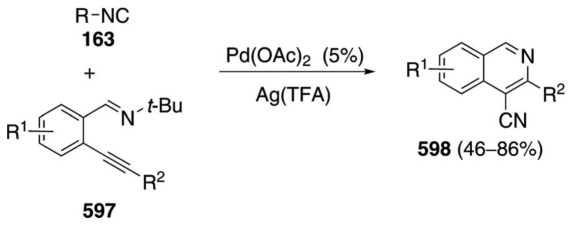


(127)

alkynes and proceeds with electron-rich or electron-deficient substituents in the aromatic ring. Although most cyanations employ *tert*-butyl isonitrile, the transformation is equally as effective with cyclohexyl isonitrile.

Aminopalladation of **597** generates the isoquinoline core of **599** (Scheme 92). Isonitrile binding to palladium, followed by insertion affords **600** which eliminates isobutylene to form the palladium complex **601**. A second isobutylene elimination from **601** affords **598** and zerovalent palladium species (**165**) that is subsequently oxidized to reenter the catalytic cycle.

Copper iodide catalyzes the synthesis of 2-substituted 1,3-benzoselenazoles **603** from 2-bromophenyl or 2-iodophenyl isonitriles **602**, selenium, and an amine, thiol or alcohol [Eq. (128)].[178] The amine nucleophile

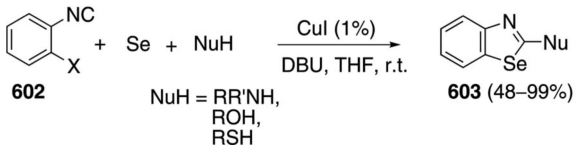


(128)

can be primary, secondary, or aromatic. *para*-Substituted phenols and thiophenols can replace the amines and may contain Me, OMe or Cl substituents. The yield with *p*-$MeO_2CC_6H_6OH$ was significantly lower.

Mechanistic studies demonstrate that the isonitrile **602** reacts with selenium and the nucleophile to give the selenium enolate **604** (Scheme 93). The subsequent progression to the benzoselenazole is unclear. Copper iodide may promote the cyclization through oxidative addition to the aryl halide bond to give **605** that cyclizes to **606**. Subsequent reductive elimination of **606** can form **603** and CuI. Alternatively an $S_NAr$ reaction may convert **604** to **607** that collapses to benzoselenazole **603**. Given the propensity of copper to coordinate isonitriles, an alternative cycle may operate in which copper first binds the isonitrile **602** leading to the copper-bound selenide **604** which could accelerate the C–X insertion en route to **605**.

$Co(acac)_2$ catalyzes the condensation of tertiary and secondary aliphatic isonitriles **163** with 2-arylani-lines **608** to afford 6-aminophenanthridines **609** [Eq. (129)].[179] The reaction requires oxygen for the radical process. Electronically diverse substituents are tolerated in both aromatic rings including, in one case, a nitro group.

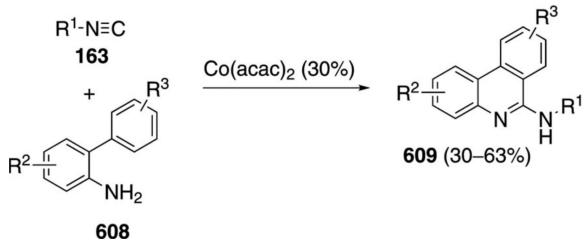


(129)

The cobalt-catalyzed reaction likely proceeds through complexation of a cobalt(II) catalyst **610** with the isonitrile **163** to form **611** (Scheme 94). Binding of the aniline **608** and isonitrile insertion leads to Co(II) complex **612**. The sequence of isonitrile then aniline complexation from **610** to **612** may be reversed, although given the strong binding of isonitriles the sequence shown appears more likely. Air oxidation of **612** forms Co(III) complex **613**. Homolysis of the cobalt-carbon bond releases the cobalt catalyst **610** and

generates the imidoyl radical **614** that adds to the aromatic ring to afford **615**. Oxidation of radical **615** to **616** and subsequent proton loss, affords **609**. The homolytic aromatic substitution process represents a C–H functionalization in generating phenanthri-dines **609**.

CuCl catalyzes a tandem Michael addition of TosMIC (**49a**) to enones **617** which is followed by an isonitrile insertion process leading to pyrroles **618** [Eq. (130)].[180] Catalytic copper chloride and stoichiometric

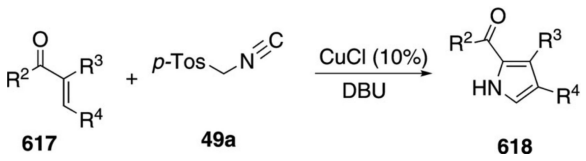


(130)

DBU provide the optimal combination, although CuBr and CuI also catalyze the reaction. Enones bearing electron-withdrawing substituents on the a-carbon are suitable substrates. Cyclic enediones require the use of $K_2CO_3$ rather than a copper catalyst, indicating that the metal is required in the deprotonation rather than being intimately required for the rearrangement.

Metal complexes readily activate isonitriles toward deprotonation by complexing to the carbon of the CN unit (Scheme 95). Formation of **17b** through copper-assisted deprotonation, provides a nucleophile suited for conjugate addition to the doubly activated olefin **617** resulting in **619**. Intramolecular attack of the enolate on the isonitrile affords **620**. Nucleophilic attack of the C–Cu bond of **620** onto the acetyl group forms the transient cyclopropane **621** which fragments to **622**. Protonation of **622**, sulfinate elimination, and tautomerization afford **618** and release the copper catalyst. The mechanism implies that DBU is required only in catalytic amounts.

## 10 Conclusion

Isonitrile insertions, additions and condensations are being increasingly developed because they provide a concise route to heterocycles, alkaloids, and carbon-yl derivatives. Isonitriles are unique in having a functional group capable of bond formation through three very different modes: nucleophilic attack, electrophilic attack, and insertion into carbon-metal bonds. Pendant heteroatoms often intercept these intermediates to afford heterocycles.

The carbene character of the isonitrile carbon causes the reaction of an isonitrile to often generate a charged intermediate for further alkylation. Isonitriles feature as carbon monoxide surrogates in several reactions. Although the substitution for CO is not atom economical, the non-gaseous isonitriles are easier to handle and do not require the use of special equipment.

Several catalytic reactions require hindered isonitriles. Sterically demanding isonitriles generally exhibit higher thermal stability than their less-substituted counterparts and may

facilitate catalysis by preventing the binding of isonitrile to the catalyst. One catalytic cycle uses an arylborane to preferentially bind the isonitrile, allowing slow release of the isonitrile. The strategy seems underdeveloped and provides a potentially valuable reservoir of isonitrile to prevent catalyst deactivation.

A variety of organocatalysts and metals catalyse the reactions of isonitriles but palladium-based catalysts are by far the most common. Many of the catalytic cycles involve isonitrile insertion into metal-carbon bonds. In some cases intermediate steps intervene between an initial oxidative addition by the metal and the isonitrile insertion. The exceptional propensity of isonitriles to coordinate to metals suggests that a more likely mechanism is prior coordination of the isonitrile to the metal with insertion occurring immediately after oxidative addition. This sequence explains why many reactions require bulky ligands and why isonitrile insertion occurs faster in many substrates than alternative intramolecular pathways.

Many catalytic cycles propose a sequence in which a metal catalyst engages in an oxidative addition or C–H insertion to generate a high-valent metal bound to a carbon center. In a subsequent step the metal is proposed to bind to an isonitrile which rapidly inserts into the metal-carbon bond (see, for example, Scheme 76). The sequence is likely naive given the excellent propensity of isonitriles to form very strong bonds to transition metals. A more likely sequence is for the active metal catalyst to already contain a bound isonitrile ligand (**623**, Scheme 96). Consistent with this catalytic cycle is the reduction of several high-valent metal precatalysts to active catalysts by sacrificial oxidation of the isonitrile, and the slow addition of the isonitrile that is sometimes required.

The metal-ligand optimization performed for many reactions may serve to tune the isonitrile coordination to the catalyst allowing catalytic turnover without further addition of isonitrile as a ligand. Oxidative addition of the catalytic species to form 624 ideally positions the bound isonitrile for a subsequent insertion **624**→**625**. The fate of **625** depends on the transformation but is illustrated with nucleophilic attack to give **626**. Reductive elimination **626**→**627** opens a coordination site for isonitrile ligation to reform the catalyst **623**.

The unique reactivity of isonitriles as 1,1-bis-electrophiles allows the facile entry into a diverse array of nitrogen-containing scaffolds. The prevalence of nitrogen in pharmaceuticals, particularly heterocycles, is likely to facilitate the continued development of catalysts for isonitrile insertions, condensations, and addition reactions. The increasing ability to control metal-ligand complexes bodes well for the future development of catalytically controlled processing of isonitriles in efficient and novel processes.

## Acknowledgments

Support from the National Institutes of Health (NIH, 2R15AI051352-04) and the National Science Foundation (IRD) is gratefully acknowledged. The views expressed in the manuscript do not necessarily reflect those of NIH or NSF.

## Biography

*Arpit Doshi* was born in Gujarat, India and received his B.Pharm from the Principal K. M. Kundnani College of Pharmacy, Mumbai, India. In the fall of 2011 he joined the research group of Dr. Aleem Gangjee. He is an integrated Masters and Ph.D. candidate at Duquesne University. His research focuses on the synthesis of single agents as mul tiple receptor tyrosine kinases and thymidylate synthase inibitors as anticancer agents.

*Dhruv Shah* was born in New Delhi, India and received his B.Pharm. from the Delhi Institute of Pharmaceutical Sciences and Research, India. In the fall of 2009 Dhruv joined the research group of Dr. Patrick T. Flaherty at Duquesne University as a Ph.D. candidate. His research focuses on the synthesis of ami nothiazole derivatives as cyclin-dependent kinase 5 inhibitors.

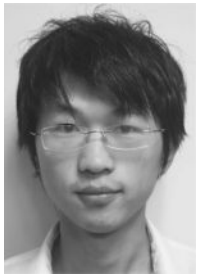

*Fa-Qiang Liu* was born in Qingdao, China and received his B.S. from Fudan University, Shanghai, China. In 2010 he joined the research group of Dr. Aleem Gangjee at Duquesne University as a Ph.D. candidate. His research focuses on the synthesis of indole derivatives with anti-cancer potential.

*Manasa P. Ravindra* was born in Andhra Pradesh, India and received her B.Pharm. from Jawaharlal Nehru Technological University, India. In 2011 she joined the research group of Dr. Aleem Gangjee at Duquesne University as an integrated Masters and Ph.D. candidate. Her research focuses on the synthesis of folate derivatives with anticancer potential.

*Rishabh Mohan* was born in New Delhi, India and received his B.Pharm (Hons.) from Panjab University, Chandigarh, India. In 2010 Rishabh joined the research group of Dr. Aleem Gangjee at Duquesne University as a Ph.D. candidate. His research focuses on the synthesis of pyrimidine derivatives with anticancer potential.

*Shruti Choudhary* was born in New Delhi, India and received her B.Pharm. from the Delhi Institute of Pharmaceutical Sciences and Research, India. In 2010 she joined the research group of Dr. Aleem Gangjee at Duquesne University as a Ph.D. candidate. Her research focuses on the synthesis of pyri midine based compounds with anticancer and anti-infective potential.

*Suravi Chakrabarty* was born in Kolkata, India and received her B.Pharm from the Delhi Institute of Pharmaceutical Sciences and Research, India. In the fall of 2010 Suravi joined the research group of Dr. Patrick T. Flaherty at Duquesne University as an M.S. candidate. Her research focuses on the synthesis of diphenylamine derivatives as mitogen activated kinase 5 inhibitors.

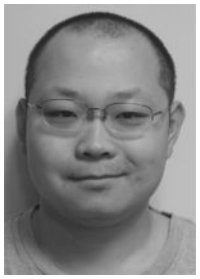

*Xun Yang* completed his undergraduate B.E. degree at Dalian University of Technology, China, in 2010. In 2010 he moved to the University of Pittsburgh and after a year transferred to Duquesne University where he is working with Dr. Fraser Fleming on the chemistry of metallated nitriles.

*Fraser Fleming* completed his B.Sc. (Hons.) at Massey University, New Zealand, in 1986 and then pursued a Ph.D. under the direction of Edward Piers at the University of British Columbia, Canada. After postdoctoral research with James D. White at Oregon State University he joined the faculty at Duquesne University, Pitts burgh, in 1992. He is currently on leave from Duquesne University and serving as a rotating Program Officer at the National Science Foundation. His research interests focus on stereoselectivity, particularly as applied to reactions of metallated nitriles.

## References


1. a Dömling A. Chem. Rev. 2006; 106:17–89. [PubMed: 16402771] b Zhu J. Eur. J. Org. Chem. 2003:1133–1144.
2. For an excellent review see: Nenajdenko VG. Isocyanide Chemistry. Applications in Synthesis and Material Science. 2012John Wiley & SonsWeinheim
3. a Vlaar T, Ruijter E, Maes BUW, Orru RVA. Angew. Chem. 2013; 125:7222–7236.Angew. Chem. Int. Ed. 2013; 52:7084–7097.b Qiu G, Ding Q, Wu J. Chem. Soc. Rev. 2013; 42:5257–5269. [PubMed: 23456037] c Gulevich AV, Zhdanko AG, Orru RVA, Nenajdenko VG. Chem. Rev. 2010; 110:5235–5331. [PubMed: 20608735] d Tobisu M, Chatani N. Chem. Lett. 2011; 40:330–340.
4. a Lygin AV, de Meijere A. Angew. Chem. 2010; 122:9280–9311.Angew. Chem. Int. Ed. 2010; 49:9094–9124.b Nakamura I, Yamamoto Y. Chem. Rev. 2004; 104:2127–2198. [PubMed: 15137788]
5. De Moliner F, Banfi L, Riva R, Basso A. Com. Chem. High T. Scr. 2011; 14:782–810.
6. a Garson MJ, Simpson JS. Nat. Prod. Rep. 2004; 21:164–179. [PubMed: 15039841] b Edenborough MS, Herbert RB. Nat. Prod. Rep. 1988; 5:229–245. [PubMed: 3067133]
7. a van Berkel SS, Bögels BGM, Wijdeven MA, Westermann B, Rutjes FPJT. Eur. J. Org. Chem. 2012:3543–3559.b de Graaff C, Ruijter E, Orru RVA. Chem. Soc. Rev. 2012; 41:3969–4009. [PubMed: 22546840] c Heravi MM, Moghimi S, Iran J. Chem. Soc. 2011; 8:306–373.
8. Lazar, M.; Angelici, RJ. Modern Surface Organometallic Chemistry. Wiley-VCH; Weinham: 2009. Isocyanide Binding Modes on Metal Surfaces and in Metal Complexes. Chap. 13
9. Nesper R, Pregosin P, Püntener K, Wörle M, Albinati A. J. Organomet. Chem. 1996; 507:85–101.
10. Mehendale NC, Sietsma JRA, de Jong KP, van Walree CA, Klein Gebink RJM, van Koten G. Adv. Synth. Catal. 2007; 349:2619–2630.
11. Sharma V, Piwnica-Worms D. Chem. Rev. 1999; 99:2545–2560. [PubMed: 11749491]
12. Galan BR, Kalbarczyk KP, Szczepankiewicz S, Keister JB, Diver ST. Org. Lett. 2007; 9:1203–1206. [PubMed: 17326645]
13. a de Frémont P, Marion N, Nolan SP. Coord. Chem. Rev. 2009; 253:862–892.b McGlinchey, MJ.; Ortin, Y.; Steward, CM. Comprehensive Organometallic Chemiistry III. Elsevier; Oxford: 2007. Chromium Compounds with CO or Isocyanides; p. 271-278.c Michelin RA, Pombeiro AJL, Guedes da Silva MFC. Coord. Chem. Rev. 2001; 218:75–112.d Pombeiro AJL, Guedes da Silva MFC, Michelin RA. Coord. Chem. Rev. 2001; 218:43–74.e Tamm M, Hahn FE. Coord. Chem. Rev. 1999; 182:175–209.f Vogler, A. Coordinated Isonitriles. In: Ugi, I., editor. Isonitrile Chemisty. Academic Press; New York: 1971. Chap. 10
14. Comprehensive Organometallic Chemistry III. Elsevier; Oxford: 2007. Palladium Complexes with Carbonyl, Isocyanide, and Carbene Ligands; p. 246-260.
15. Fehlhammer WP, Bartel K, Pteri W. J. Organomet. Chem. 1975; 87:C34.
16. Elders N, Ruijter E, de Kanter FJJ, Groen MB, Orru RVA. Chem. Eur. J. 2008; 14:4961–4973. [PubMed: 18431735]
17. Grigg R, Landsell MI, Thornton-Pett M. Tetrahedron. 1999; 55:2025–2044.
18. Snegasa T, Ito Y, Kinoshita H, Tomita S. J. Org. Chem. 1971; 36:3316–3323.
19. Bon RS, van Vliet B, Sprenkels NE, Schmitz RF, de Kanter FJJ, Stevens CV, Swart M, Bickelhaupt FM, Groen MB, Orru RVA. J. Org. Chem. 2005; 70:3542–3553. [PubMed: 15844989]
20. Elders N, Schmitz RF, de Kanter FJJ, Ruijter E, Groen MB, Orru RVA. J. Org. Chem. 2007; 72:6135–6142. [PubMed: 17628108]
21. a Soloshonok VA, Kacharov AD, Avilov DV, Ishikawa K, Nagashima N, Hayashi T. J. Org. Chem. 1997; 62:3470–3479.b Soloshonok VA, Kacharov DA, Avilov VD, Hayashi T. Tetrahedron Lett. 1996; 37:7845–7848.
22. Panella L, Aleixandre AM, Kruidhof GJ, Robertus J, Feringa BL, de Vries JG, Minnaard AJ. J. Org. Chem. 2006; 71:2026–2036. [PubMed: 16496990]
23. Mori K, Hara T, Mizugaki T, Ebitani K, Kaneda K. J. Am. Chem. Soc. 2003; 125:11460–11461. [PubMed: 13129324]

24. Meng T, Zou Y, Khorev O, Jin Y, Zhou H, Zhang Y, Hu D, Ma L, Wang X, Shen J. Adv. Synth. Catal. 2011; 353:918–924.
25. Shinada T, Ikebe E, Oe K, Namba K, Kawasaki M, Ohfune Y. Org. Lett. 2007; 9:1765–1767. [PubMed: 17411060]
26. Li S, Wu J. Chem. Commun. 2012; 48:8973–8975.
27. Benito-Garagorri D, Bocokić V, Kirchner K. Tetrahedron Lett. 2006; 47:8641–8644.
28. Zhou XT, Lin YR, Dai LX, Sun J. Tetrahedron. 1998; 54:12445–12456.
29. Lin Y-R, Zhou X-T, Dai L-X, Sun J. J. Org. Chem. 1997; 62:1799–1803.
30. Shinada T, Oe K, Ohfune Y. Tetrahedron Lett. 2012; 53:3250–3253.
31. Yugandar S, Acharya A, Ila H. J. Org. Chem. 2013; 78:3948–3960. [PubMed: 23496176]
32. Aydin J, Kumar KS, Eriksson L, Szabo KJ. Adv. Synth. Catal. 2007; 349:2585–2594.
33. Togni A, Pastor SD. J. Org. Chem. 1990; 55:1649–1664.
34. Gosiewska S, in't Veld MH, de Pater JJM, Bruijnincx PCA, Lutz M, Spek AL, van Koten G, Klein Gebbink RJM. Tetrahedron: Asymmetry. 2006; 17:674–686.
35. a Soro B, Stoccoro S, Minghetti G, Zucca A, Cinellu MA, Manassero M, Galdiali S. Inorg. Chim. Acta. 2006; 359:1879–1888.b Yoon MS, Ramesh R, Kim J, Ryu D, Ahn KH. J. Organomet. Chem. 2006; 691:5927–5934.
36. Motoyama Y, Kawakami H, Shimozono K, Aoki K, Nishiyama H. Organometallics. 2002; 21:3408–3416.
37. Guillena G, Rodriguez G, van Koten G. Tetrahedron Lett. 2002; 43:3895–3898.
38. Gosiewska S, Martinez SH, Lutz M, Spek AL, van Koten G, Klein Gebbink RJM. Eur. J. Inorg. Chem. 2006:4600–4607.
39. Williams BS, Dani P, Lutz M, Spek AL, van Koten G. Helv. Chim. Acta. 2001; 84:3519–3530.
40. Gagliardo M, Selander N, Mehendale NC, van Koten G, Klein Gebbink RJM, Szab KJ. Chem. Eur. J. 2008; 14:4800–4809. [PubMed: 18432627]
41. Longmire JM, Zhang X, Shang M. Organometallics. 1998; 17:4374–4379.
42. Gorla F, Togni A, Venanzi LM, Albinati A, Lianza F. Organometallics. 1994; 13:1607–1616.
43. Aydin J, Rydén A, Szabó KJ. Tetrahedron: Asymmetry. 2008; 19:1867–1870.
44. Gimenez R, Swager TM. J. Mol. Catal. A: Chem. 2001; 166:265–273.
45. Slagt MQ, Jastrzebski JTBH, Gebbink RJMK, van Ramesdonk HJ, Verhoeven JW, Ellis DD, Spek AL, van Koten G. Eur. J. Org. Chem. 2003:1692–1703.
46. Schlenk C, Kleij AW, Frey H, Van Koten G. Angew. Chem. 2000; 112:3587–3589.Angew. Chem. Int. Ed. 2000; 39:3445–3447.
47. van de Coevering R, Alfers AP, Meeldijk JD, Mart nez-Viviente E, Pregosin PS, Klein Gebbink RJM, van Koten G. J. Am. Chem. Soc. 2006; 128:12700–12713. [PubMed: 17002364]
48. For a related dendrimer-pincer complex, see: Suijkerbuijk BMJM, Shu L, Klein Gebbink RJM, Schlüter AD, van Koten G. Organometallics. 2003; 22:4175–4177.
49. Meijer MD, Ronde N, Vogt D, van Klink GPM, van Koten G. Organometallics. 2001; 20:3993–4000.
50. Kim HY, Oh K. Org. Lett. 2011; 13:1306–1309. [PubMed: 21314170]
51. Nakamura S, Maeno Y, Ohara M, Yamamura A, Funahashi Y, Shibata N. Org. Lett. 2012; 14:2960–2963. [PubMed: 22656050]
52. von R. Schleyer P, Allerhand A. J. Am. Chem. Soc. 1962; 84:1322–1323.
53. Wang L-L, Bai J-F, Peng L, Qi L-W, Jia L-N, Guo Y-L, Luo X-Y, Xu X-Y, Wang L-X. Chem. Commun. 2012; 48:5175–5177.
54. Sladojevich F, Trabocchi A, Guarna A, Dixon DJ. J. Am. Chem. Soc. 2011; 133:1710–1713. [PubMed: 21247165]
55. Ito Y, Sawamura M, Hayashi T. J. Am. Chem. Soc. 1986; 108:6405–6406.
56. a Hayashi T, Sawamura M, Ito Y. Tetrahedron. 1992; 48:1999–2012.b Pastor SD, Togni A. Tetrahedron Lett. 1990; 31:839–840.c Pastor SD, Togni A. Helv. Chim. Acta. 1991; 74:905–933.
57. Togni A, Pastor SD. J. Org. Chem. 1990; 55:1649–1664.

58. Togni A, Pastor SD. J. Organomet. Chem. 1990; 381:C21–C25.
59. Togni A, Häusel R. Synlett. 1990:633–635.
60. a Lianza F, Macchioni A, Pregosin P, Ruegger H. Inorg. Chem. 1994; 33:4999–5002.b Hayashi T, Uozumi Y, Yamazaki A, Sawamura M, Hamashima H, Ito Y. Tetrahedron Lett. 1991; 32:2799–2802.
61. Sawamura M, Hamashima H, Ito Y. J. Org. Chem. 1990; 55:5935–5936.
62. a Zhou X-T, Lin Y-R, Dai L-X, Sun J, Xia L-J, Tang M-H. J. Org. Chem. 1999; 64:1331–1334.b Zhou XT, Lin YR, Dai LX. Tetrahedron: Asymmetry. 1999; 10:855–862.c Hayashi T, Kishi E, Soloshonok VA, Uozumi Y. Tetrahedron Lett. 1996; 37:4969–4972.
63. a Soloshonok VA, Kacharov AD, Hayashi T. Tetrahedron. 1996; 52:245–254.b Soloshonok VA, Hayashi T. Tetrahedron Lett. 1994; 35:2713–2716.
64. a Sawamura M, Nakayama Y, Kato T, Ito Y. J. Org. Chem. 1995; 60:1727–1732.b Soloshonok VA, Hayashi T. Tetrahedron: Asymmetry. 1994; 5:1091–1094.
65. a Ono, N.; Okujima, T. Synthesis of Pyrroles and Their Derivatives from Isocyanides in Isocyanide Chemistry. Applications in Synthesis and Material Science. Nenajdenko, V., editor. Wiley-VCH; Weinheim: 2012. b Estévez V, Villacampa M, Menéndez JC. Chem. Soc. Rev. 2010; 39:4402–4421. [PubMed: 20601998] c Campo J, García-Valverde M, Marcaccini S, Rojoa MJ, Torroba T. Org. Biomol. Chem. 2006; 4:757–765. [PubMed: 16493455]
66. a Chatani N, Murai S, Hanafusa T. Chem. Express. 1991; 6:339–342.b Chatani N, Hanafusa T. J. Org. Chem. 1991; 56:2166–2170.
67. Grigg R, Lansdell MI, Thornton-Pett M. Tetrahedron. 1999; 55:2025–2044.
68. Arróniz C, Gil-González A, Semak V, Escolano C, Bosch J, Amat M. Eur. J. Org. Chem. 2011:3755–3760.
69. Guo C, Xue MX, Zhu MK, Gong LZ. Angew. Chem. 2008; 120:3462–3465.Angew. Chem. Int. Ed. 2008; 47:3414–3417.
70. Wang LL, Bai JF, Peng L, Qi LW, Jia LN, Guo YL, Luo XY, Xu XY, Wang LX. Chem. Commun. 2012; 48:5175–5177.
71. Melchiorre P. Angew. Chem. 2012; 124:9886–9909.Angew. Chem. Int. Ed. 2012; 51:9748–9770.
72. Song J, Guo C, Chen PH, Yu J, Luo SW, Guo LZ. Chem. Eur. J. 2011; 17:7786–7790. [PubMed: 21618634]
73. Takaya H, Kojima S, Murahashi SI. Org. Lett. 2001; 3:421–424. [PubMed: 11428029]
74. a Lygin AV, Larionov OV, Korotkov VS, de Meijere A. Chem. Eur. J. 2009; 15:227–236. [PubMed: 19025729] b Kamijo S, Kanazawa C, Yamamoto Y. J. Am. Chem. Soc. 2005; 127:9260–9266. [PubMed: 15969607] c Larionov OV, de Meijere A. Angew. Chem. 2005; 117:5809–5813.Angew. Chem. Int. Ed. 2005; 44:5664–5667.
75. Gao M, He C, Chen H, Bai R, Cheng B, Lei A. Angew. Chem. 2013; 125:7096–7099.Angew. Chem. Int. Ed. 2013; 52:6958–6961.
76. Barnea E, Majumder S, Staples RJ, Odom AL. Organometallics. 2009; 28:3876–3881.
77. Li Y, Zhao J, Chen H, Liu B, Jiang H. Chem. Commun. 2012; 48:3545–3547.
78. Cai Q, Zhou F, Xu T, Fu L, Ding K. Org. Lett. 2011; 13:340–343. [PubMed: 21162591]
79. Zhou F, Fu L, Wie J, Ding K, Cai Q. Synthesis. 2011:3037–3044.
80. Zhou F, Liu J, Ding K, Liu J, Cai Q. J. Org. Chem. 2011; 76:5346–5353. [PubMed: 21591728]
81. Hsu GC, Kosar WP, Jones WD. Organometallics. 1994; 13:385–396.
82. Nanjo T, Tsukano C, Takemoto Y. Org. Lett. 2012; 14:4270–4273. [PubMed: 22849720]
83. Curran DP, Du W. Org. Lett. 2002; 4:3215–3218. [PubMed: 12227752]
84. Ji F, Lv M.-f. Yi W.-b. Cai C. Adv. Synth. Catal. 2013; 355:3401–3406.
85. Qiu G, Chen C, Yao L, Wu J. Adv. Synth. Catal. 2013; 355:1579–1584.
86. Qiu G, Qiu X, Liu J, Wu J. Adv. Synth. Catal. 2013; 355:2441–2446.
87. Hu Z, Wang J, Liang D, Zhu Q. Adv. Synth. Catal. 2013; 355:3290–3294.
88. Nanjo T, Yamamoto S, Tsukano C, Takemoto Y. Org. Lett. 2013; 15:3754–3757. [PubMed: 23822877]
89. Tobisu M, Imoto S, Ito S, Chatani N. J. Org. Chem. 2010; 75:4835–4840. [PubMed: 20550203]

90. Tobisu M, Fujihara H, Koh K, Chatani N. J. Org. Chem. 2010; 75:4841–4847. [PubMed: 20557065]
91. Cai Q, Li Z, Wei J, Ha C, Pei D, Ding K. Chem. Commun. 2009; 45:7581–7583.
92. Onitsuka K, Suzuki S, Takahashi S. Tetrahedron Lett. 2002; 43:6197–6199.
93. Qiu G, Wu J. Chem. Commun. 2012; 48:6046–6048.
94. Ley SV, Thomas AW. Angew. Chem. 2003; 115:5558–5607.Angew. Chem. Int. Ed. 2003; 42:5400–5449.
95. Kanazawa C, Kamijo S, Yamamoto Y. J. Am. Chem. Soc. 2006; 128:10662–10663. [PubMed: 16910644]
96. Bonin M-A, Giguére D, Roy R. Tetrahedron. 2007; 63:4912–4917.
97. a Bochatay VN, Boissarie PJ, Murphy JA, Suckling CJ, Lang S. J. Org. Chem. 2013; 78:1471–1477. [PubMed: 23316812] b Boissarie PJ, Hamilton ZE, Lang S, Murphy JA, Suckling CJ. Org. Lett. 2011; 13:6256–6259. [PubMed: 22047037]
98. Geden JV, Pancholi AK, Shipman M. J. Org. Chem. 2013; 78:4158–4164. [PubMed: 23472583]
99. Vlaar T, Cioc RC, Mampuys P, Maes BUW, Orru RVA, Ruitjer E. Angew. Chem. 2012; 124:13235–13238.Angew. Chem. Int. Ed. 2012; 51:13058–13061.
100. Liu B, Yin M, Gao H, Wu W, Jiang H. J. Org. Chem. 2013; 78:3009–3020. [PubMed: 23477617]
101. Vlaar T, Orru RVA, Maes BUW, Ruijter E. J. Org. Chem. 2013; 78:10469–10475. [PubMed: 24063265]
102. Tanaka M, Hayashi T. J. Mol. Catal. 1990; 60:L5–L7.
103. Ishiyama T, Oh-e T, Miyaura N, Suzuki A. Tetrahedron Lett. 1992; 33:4465–4468.
104. Jones WD, Hessell ET. Organometallics. 1990; 9:718–727.
105. Wicker BF, Scott J, Fout AR, Pink M, Mindiola DJ. Organometallics. 2011; 30:2453–2456.
106. Takayoshi H, Li-Biao H. J. Am. Chem. Soc. 2006; 128:7422–7423. [PubMed: 16756279]
107. Yoshihiko I, Michinori S, Takaharu M, Masahiri M. J. Am. Chem. Soc. 1991; 113:8899–8908.
108. Otsuka S, Yoshida T, Tatsuno Y. J. Am. Chem. Soc. 1971; 93:6462–6469.
109. Lygin AV, de Meijere A. J. Org. Chem. 2009; 74:4554–4559. [PubMed: 19449864]
110. Ito Y, Kobayosli K, Saegusa T. Tetrahedron Lett. 1978; 19:2087–2090.
111. Jiang H, Yin M, Li Y, Liu B, Zhao J, Wu W. Chem. Commun. 2014; 50:2037–2039.
112. Fei X-D, Ge Z-Y, Tang T, Zhu Y-M, Ji S-J. J. Org. Chem. 2012; 77:10321–10328. [PubMed: 23101723]
113. Fei X-D, Tang T, Ge Z-Y, Zhu Y-M. Synth. Commun. 2013; 43:3262–3271.
114. a Zhu C, Xie W, Falck JR. Chem. Eur. J. 2011; 17:12591–12595. [PubMed: 21972033] b Park S, Shintani R, Hayashi T. Chem. Lett. 2009; 38:204–205.
115. Tyagi V, Khan S, Chauhan PMS. Synlett. 2013; 24:645–651.
116. Ohe K, Matauda H, Ishihara T, Ogoshi S, Chatani N, Murai S. J. Org. Chem. 1993; 58:1173–1177.
117. Miura T, Nishida Y, Morimoto M, Yamauchi M, Murakami M. Org. Lett. 2011; 13:1429–1431. [PubMed: 21319832]
118. Park S, Shintani R, Hayashi T. Chem. Lett. 2009; 38:204–205.
119. Tamao K, Kobayashi K, Ilo Y. Synlett. 1992:539–546.
120. a Berk SC, Grossman RB, Buchwald SL. J. Am. Chem. Soc. 1994; 116:8593–8601.b Grossman RB, Buchwald SL. J. Am. Chem. Soc. 1993; 115:4912–4913.
121. K 0.01 for the trialkylsilyl isonitrile: Rasmussen JK, Heilmann SM, Krepski LR. Larson GL. Advances in Silicon Chemistry. 1991; 1:67.JAI PressGreenwich
122. Zhang M, Buchwald SL. J. Org. Chem. 1996; 61:4498–4499. [PubMed: 11667365]
123. Shibata T, Yamashita K, Katayama E, Takagi K. Tetrahedron. 2002; 58:8661–8667.
124. Barnea E, Eisen MS. Coord. Chem. Rev. 2006; 250:855–899.
125. Fukumoto Y, Hagihara M, Kinashi F, Chatani N. J. Am. Chem. Soc. 2011; 133:10014–10017. [PubMed: 21644512]
126. Cao C, Shi Y, Odom AL. J. Am. Chem. Soc. 2003; 125:2880–2881. [PubMed: 12617647]

127. Banerjee S, Shi Y, Cao C, Odom AL. J. Organomet. Chem. 2005; 690:5066–5077.
128. Yan X, Liao J, Lu Y, Liu J, Zeng Y, Cai Q. Org. Lett. 2013; 15:2478–2481. [PubMed: 23642149]
129. Zhang W-X, Nishiura M, Hou Z. Angew. Chem. 2008; 120:9846–9849.Angew. Chem. Int. Ed. 2008; 47:9700–9703.
130. Barnea E, Eisen MS. Coord. Chem. Rev. 2006; 250:855–899.
131. a Barnea E, Andrea T, Berthet J-C, Ephritikhine M, Eisen MS. Organometallics. 2008; 27:3103–3112.b Barnea E, Andrea T, Kapon M, Berthet J-C, Ephritikhine M, Eisen MS. J. Am. Chem. Soc. 2004; 126:10860–10861. [PubMed: 15339168]
132. Komeyama K, Sasayama D, Kawabata T, Take-hira K, Takaki K. Chem. Commun. 2005:634–636.
133. Komeyama K, Sasayama D, Kawabata T, Take-hira K, Takaki K. J. Org. Chem. 2005; 70:10679–10687. [PubMed: 16355985]
134. Tang T, Fei X-D, Ge Z-Y, Chen Z, Zhu Y-M, Ji S-J. J. Org. Chem. 2013; 78:3170–3175. [PubMed: 23438012]
135. Tyagi V, Khan S, Giri A, Gauniyal HM, Sridhar B, Chauhan PMS. Org. Lett. 2012; 14:3126–3129. [PubMed: 22625424]
136. Baelen GV, Kuijer S, Rýček L, Sergeyev S, Janssen E, de Kanter FJJ, Maes BUW, Ruijter E, Orru RVA. Chem. Eur. J. 2011; 17:15039–15044. [PubMed: 22125085]
137. Wong Y, Wang H, Peng J, Zhu Q. Org. Lett. 2011; 13:4604–4607. [PubMed: 21819077]
138. Qiu G, He Y, Wu J. Chem. Commun. 2012; 48:3836–3838.
139. Qiu G, Liu G, Pu S, Wu J. Chem. Commun. 2012; 48:2903–2905.
140. Qiu G, Lu Y, Wu J. Org. Biomol. Chem. 2013; 11:798–802. [PubMed: 23229113]
141. Liu B, Gao H, Yu Y, Wu W, Jiang H. J. Org. Chem. 2013; 78:10319–10328. [PubMed: 24060188]
142. Ji F, Lv M.-f. Yi W.-b. Cai C. Synthesis. 2013; 45:1965–1974.
143. Schmidbaur, H.; Schier, A. Comprehensive Organometallic Chemistry III. Elsevier; Oxford: 2007. Gold Organometallics; p. 279-285.
144. Lazar M, Zhu B, Angelici RJ. J. Phys. Chem. C. 2007; 111:4074–4076.
145. Angelici RJ. J. Organomet. Chem. 2008; 693:847–856.
146. Lazar M, Angelici RJ. J. Am. Chem. Soc. 2006; 128:10613–10620. [PubMed: 16895429]
147. Klobukowski ER, Angelici RJ, Woo LK. Organometallics. 2012; 31:2785–2792.
148. de Lange PPMD, Fruhauf H-W, Kraakman MJ, van Wijnkoop M, Krauenburg M, Groot AHJP, Vrieze K, Fraanje J, Wang Y, Numan M. Organometallics. 1993; 12:417.
149. Zhu T-H, Xu X-P, Cao JJ, Wei TQ, Wang S-Y, Ji S-J. Adv. Synth. Catal. 2014; 356:509–518.
150. Zhu T-H, Wang S-Y, Wang G-N, Ji S-J. Chem. Eur. J. 2013; 19:5850–5853. [PubMed: 23526676]
151. Pri-Bar I, Schwartz J. Chem. Commun. 1997:347–348.
152. Kiyoi T, Seko N, Yoshino K, Ito Y. J. Org. Chem. 1993; 58:5118–5120.
153. Peng J, Liu L, Hu Z, Huang J, Zhu Q. Chem. Commun. 2012; 48:3772–3774.
154. Hu Z, Liang D, Zhao J, Huang J, Zhu Q. Chem. Commun. 2012; 48:7371–7373.
155. Jiang H, Liu B, Li Y, Wang A, Huang H. Org. Lett. 2011; 13:1028–1031. [PubMed: 21294563]
156. Huang L, Guo H, Pan L, Xie C. Eur. J. Org. Chem. 2013:6027–6031.
157. Saluste CG, Whitby RJ, Furber M. Angew. Chem. 2000; 112:4326–4328.Angew. Chem. Int. Ed. 2000; 39:4156–4158.
158. Kishore K, Tetala R, Whitby RJ, Light ME, Hurtshouse MB. Tetrahedron Lett. 2004; 45:6991–6994.
159. Saluste CG, Crumpler S, Furber M, Whitby RJ. Tetrahedron Lett. 2004; 45:6995–6996.
160. Saluste CG, Whitby RJ, Furber M. Tetrahedron Lett. 2001; 42:6191–6194.
161. Whitby RJ, Saluste CG, Furber M. Org. Biomol. Chem. 2004; 2:1974–1976. [PubMed: 15254622]
162. Zhou F, Ding K, Cai Q. Chem. Eur. J. 2011; 17:12268–12271. [PubMed: 21938752]

163. Wang Y, Zhu Q. Adv. Synth. Catal. 2012; 354:1902–1908.
164. Padilla S, Adrio J, Carretero JC. J. Org. Chem. 2012; 77:4161–4166. [PubMed: 22458516]
165. a Dissanayake AA, Odom AL. Tetrahedron. 2012; 68:807–812.b Majumder S, Gipson KR, Staples RJ, Odom AL. Adv. Synth. Catal. 2009; 351:2013–2023.c Dissanayake AA, Odom AL. Chem. Commun. 2012; 48:440–442.
166. Majumder S, Gipson KR, Odom AL. Org. Lett. 2009; 11:4720–4723. [PubMed: 19754043]
167. Tsunenishi Y, Ishida H, Itoh K, Ohno M. Synlett. 2000:1318–1320.
168. Arisawa M, Ashikawa M, Suwa A, Yamaguchi M. Tetrahedron Lett. 2005; 46:1727–1729.
169. Adam W, Bargon RM, Bosio SG, Schenk WA, Stalke D. J. Org. Chem. 2002; 67:7037–7041. [PubMed: 12353997]
170. Kamijo S, Jin T, Yamamoto Y. Angew. Chem. 2002; 114:1858–1860.Angew. Chem. Int. Ed. 2002; 41:1780.
171. Kamijo S, Jin T, Yamamoto Y. J. Am. Chem. Soc. 2001; 123:9453–9454. [PubMed: 11562233]
172. Kamijo S, Yamamoto Y. J. Am. Chem. Soc. 2002; 124:11940–11945. [PubMed: 12358538]
173. Kazmaier U, Ackermann S. Synlett. 2004:2576–2578.
174. a Vlaar T, Mampuys P, Helliwell M, Maes BUW, Orru RVA, Ruijter E. J. Org. Chem. 2013; 78:6735–6745. [PubMed: 23768066] b Vlaar T, Ruijter E, Znabet A, Janssen E, de Kanter FJJ, Maes BUW, Orru RVA. Org. Lett. 2011; 13:6496–6499. [PubMed: 22085248]
175. Xu S, Huang X, Hong X, Xu B. Org. Lett. 2012; 14:4614–4617. [PubMed: 22905784]
176. Peng J, Zhao J, Hu Z, Liang D, Huang J, Zhu Q. Org. Lett. 2012; 14:4966–4969. [PubMed: 22937807]
177. Qiu G, Qiu X, Wu J. Adv. Synth. Catal. 2013; 355:3205–3209.
178. Fujiwara S-I, Asanuma Y, Yoshiaki S-I, Shin-Ike T, Kambe N. J. Org. Chem. 2007; 72:8087–8090. [PubMed: 17867702]
179. Zhu T-H, Wang S-Y, Tao Y-Q, Wei T-Q, Ji S-J. Org. Lett. 2014; 16:1260–1263. [PubMed: 24506323]
180. Zhang L, Xu X, Shao Q.-r. Pana L, Liu Q. Org. Biomol. Chem. 2013; 11:7393–7399. [PubMed: 24065185]

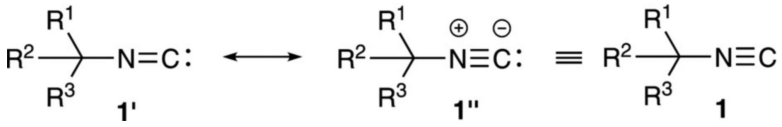


**Figure 1.**
Isonitrile representations.

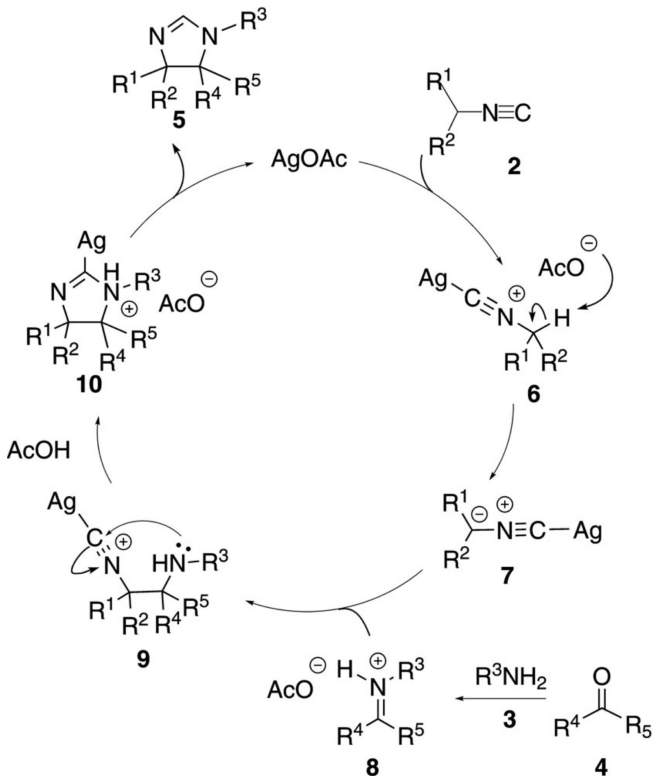


**Scheme 1.**
Silver-catalyzed imidazoline synthesis.

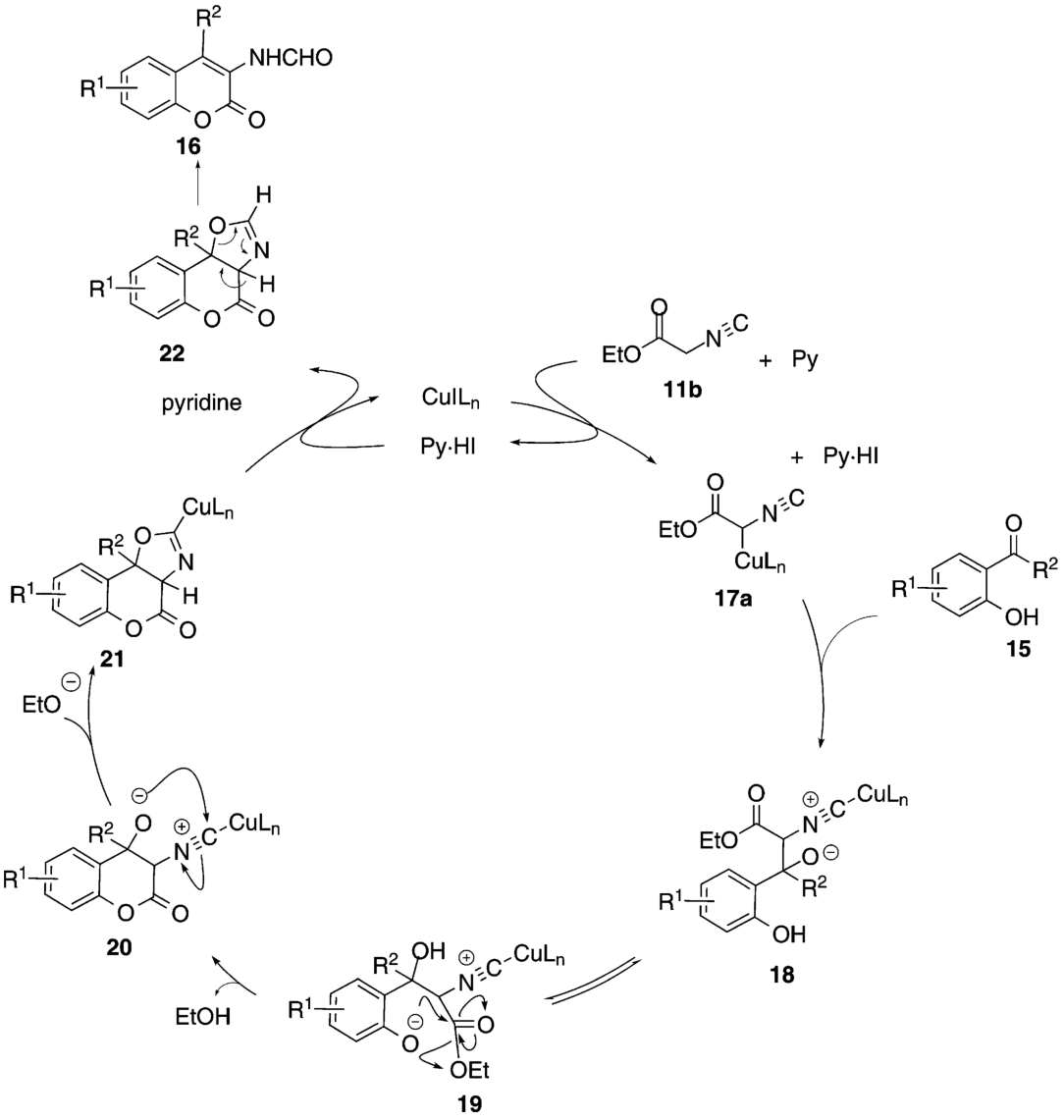


**Scheme 2.**

Copper-catalyzed aminocoumarin synthesis.

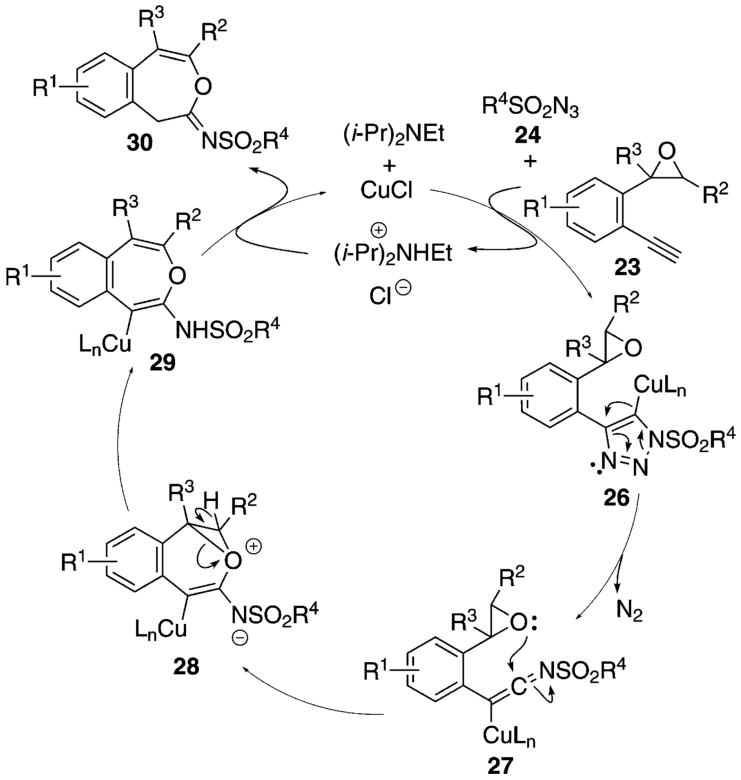


**Scheme 3.**
Copper-catalyzed epoxide–alkyne cyclization.

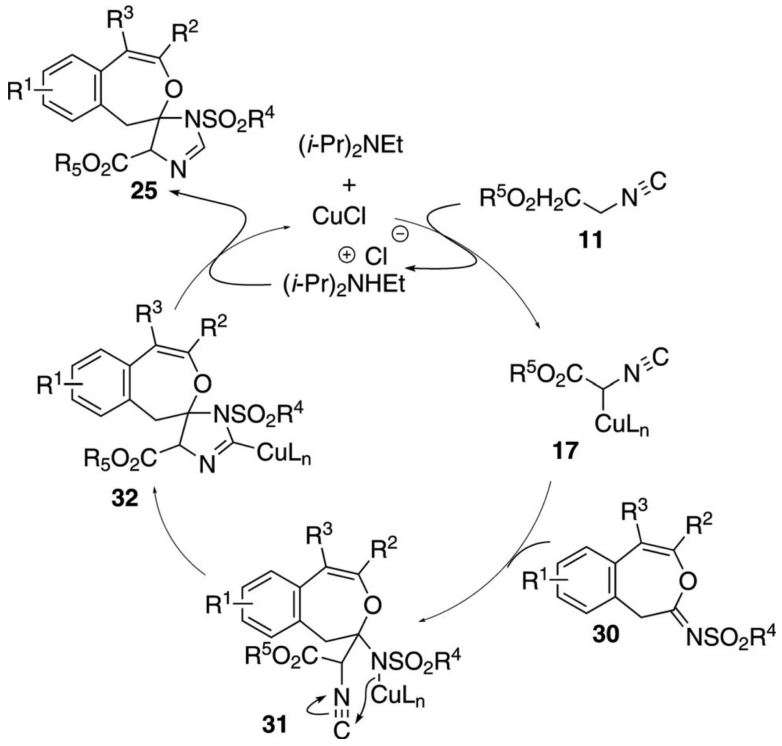


**Scheme 4.**
Formal [3+2]isonitrile route to spiro imidazolines.

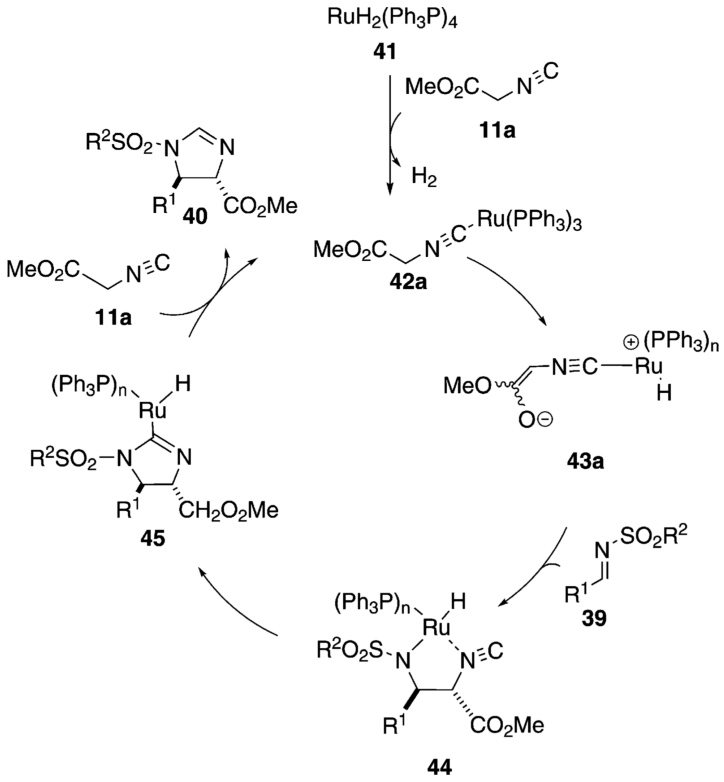


**Scheme 5.**
Ruthenium-catalyzed isocyanoacetate condensation with imines.

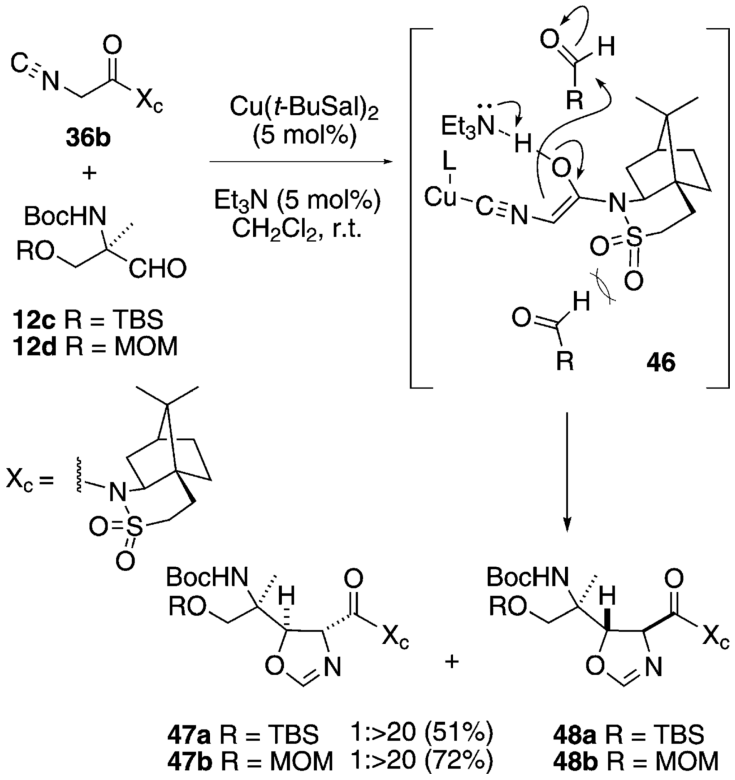


**Scheme 6.**
Double stereodifferentiation in an isonitrile aldol-type condensation.

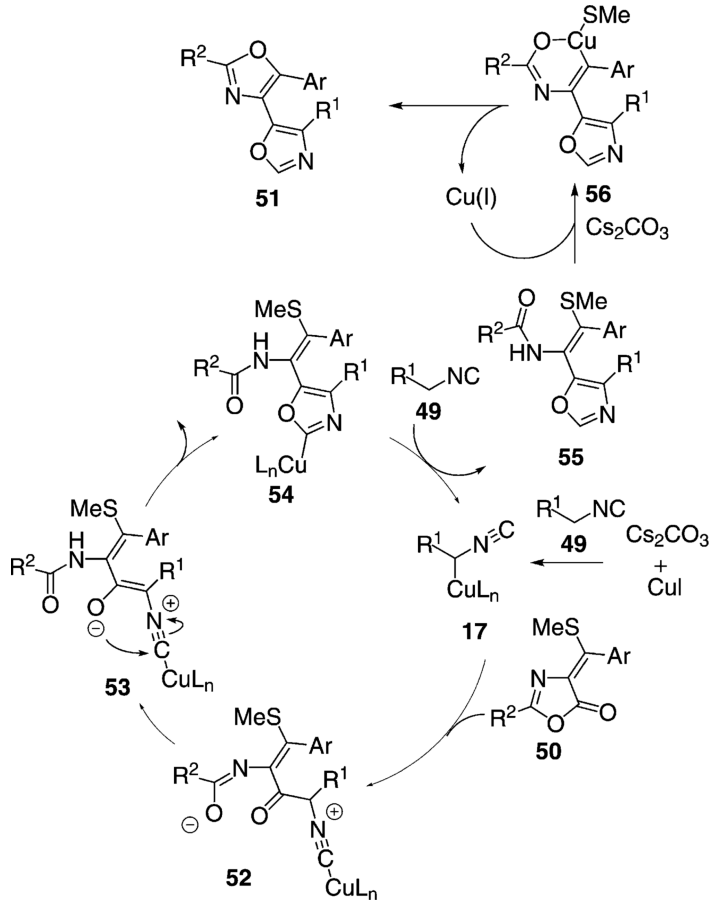


**Scheme 7.**
Copper-catalyzed bisoxazole formation.

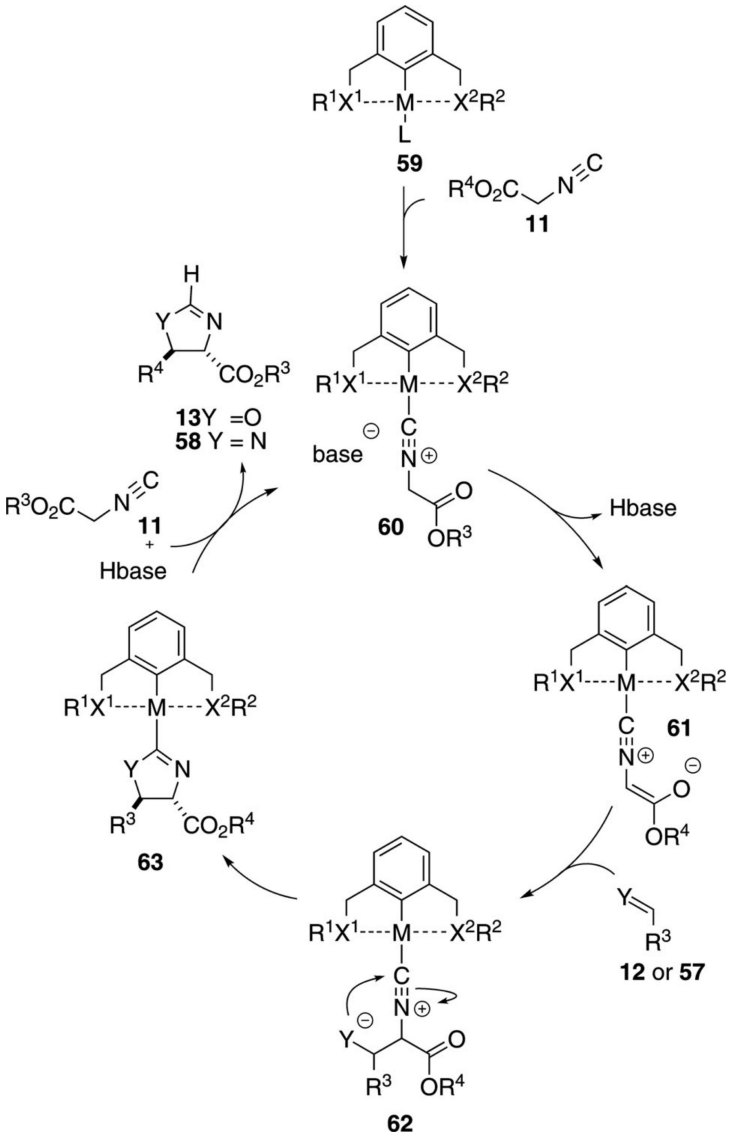


**Scheme 8.**
Pincer-catalyzed aldol cyclization.

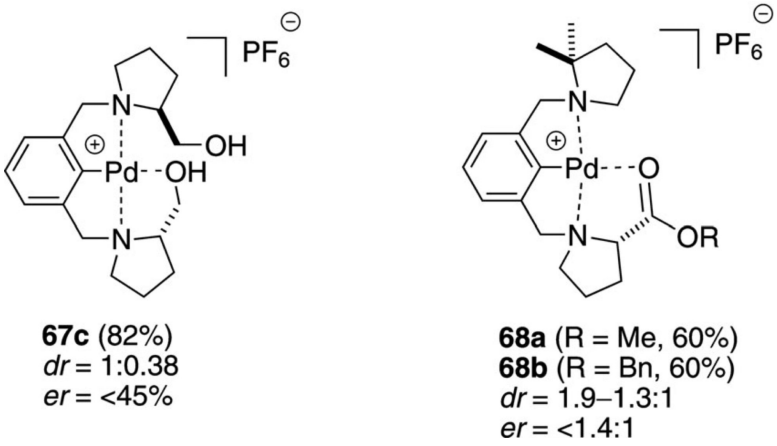


**Figure 2.**
Cationic pincer complexes.

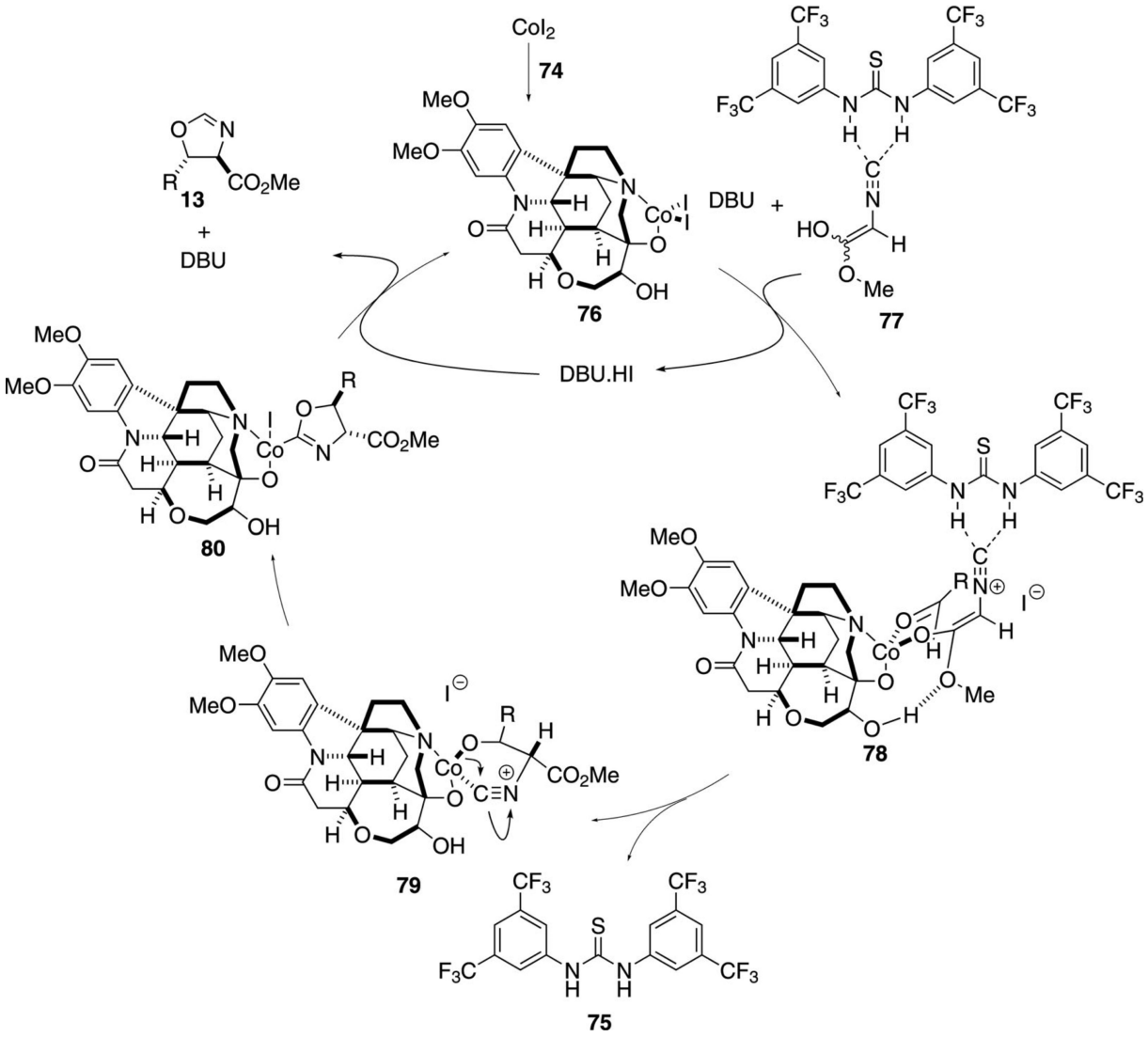


**Scheme 9.**
Cooperative $CoI_2$–organocatalysis.

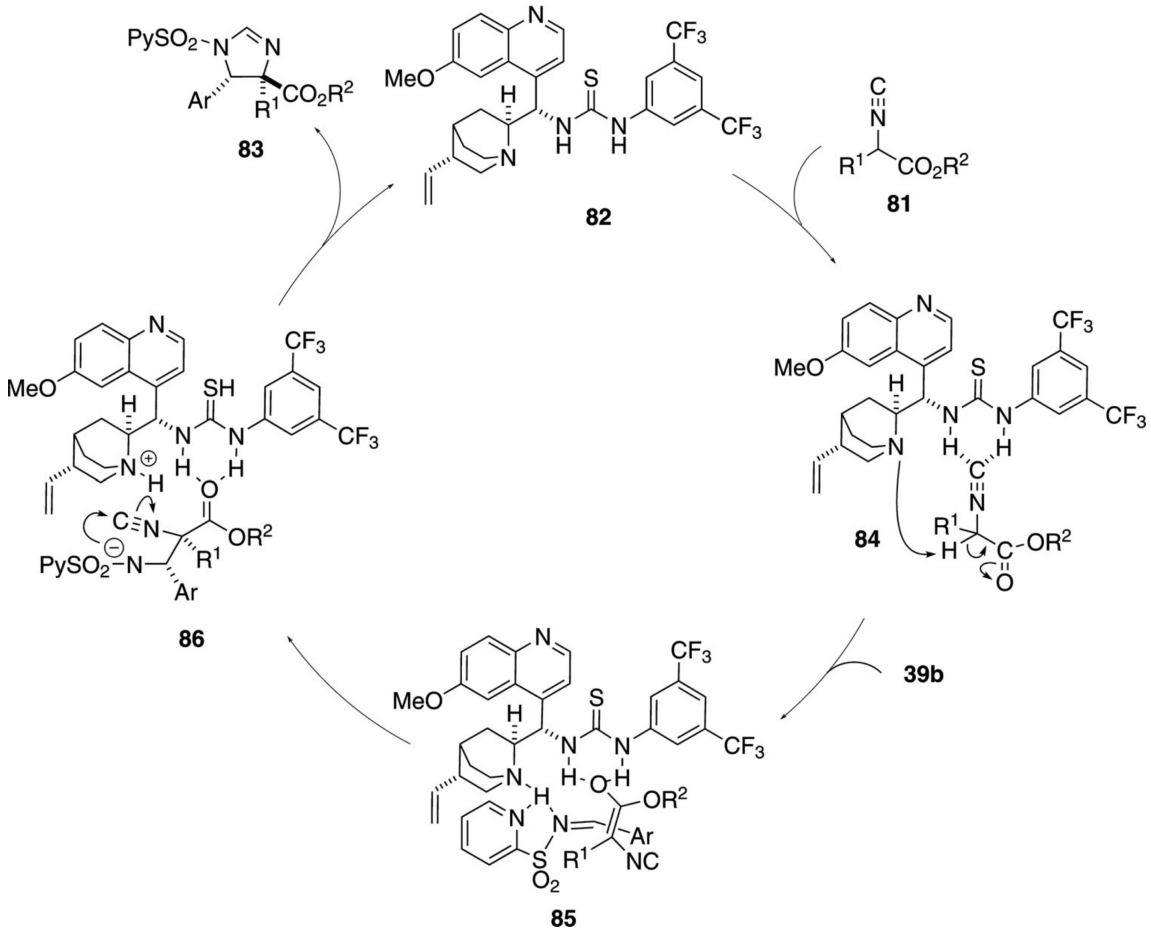


**Scheme 10.**
Organocatalyzed imidazoline synthesis.

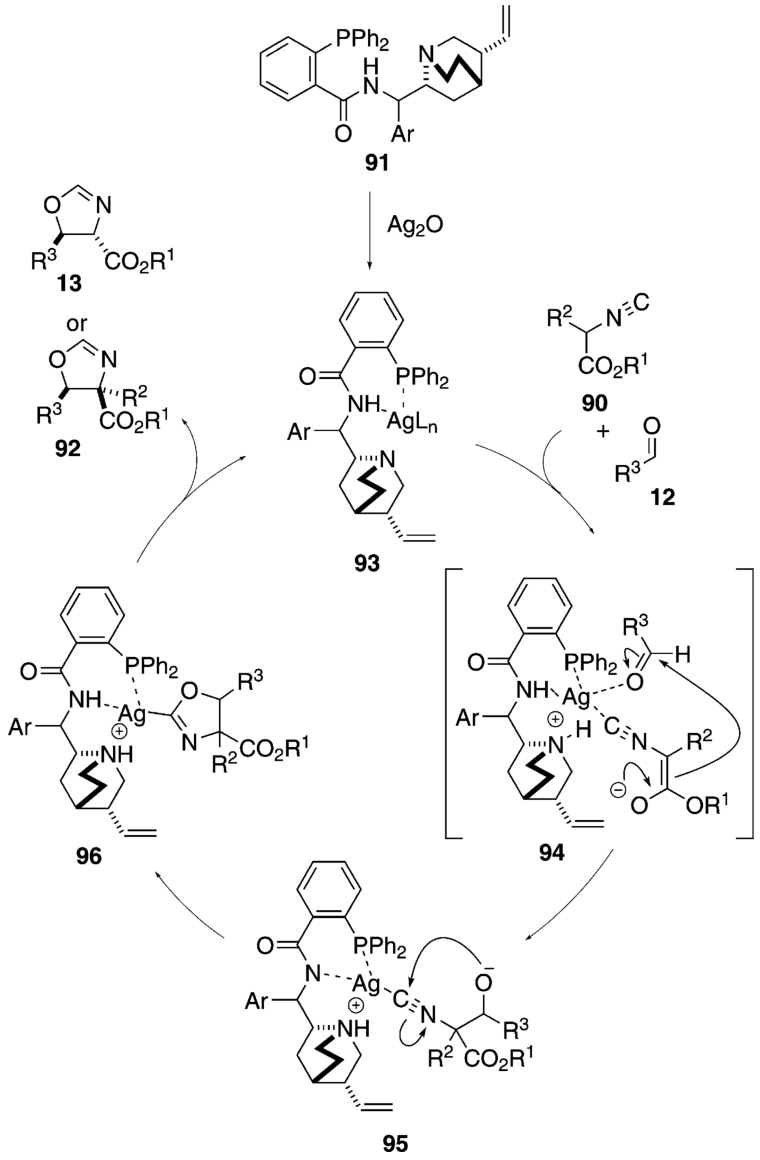


**Scheme 11.**

Cooperative catalysis with $Ag_2O$ and aminophosphine **91**.

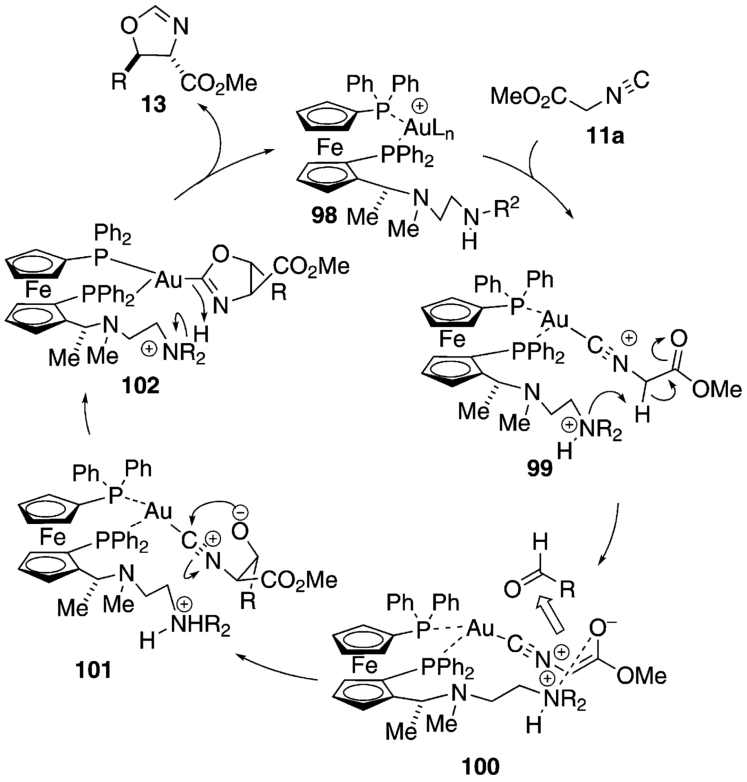


**Scheme 12.**
Gold-catalyzed isonitrile aldol.

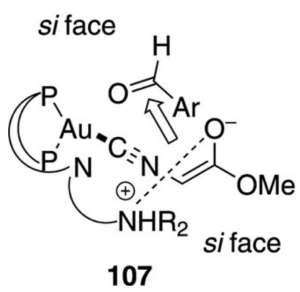


107

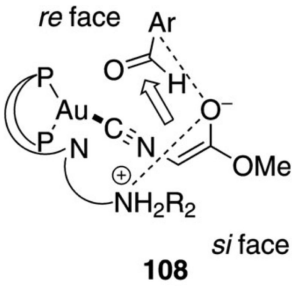


108

**Figure 3.**
Stereocontrol in gold-catalyzed reactions.

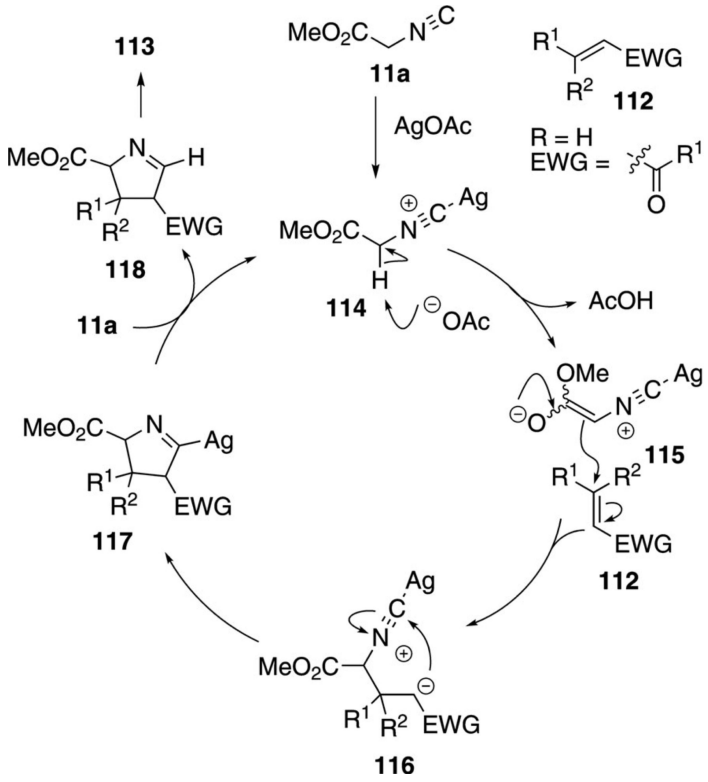


**Scheme 13.**
Silver-catalyzed pyrrole synthesis.

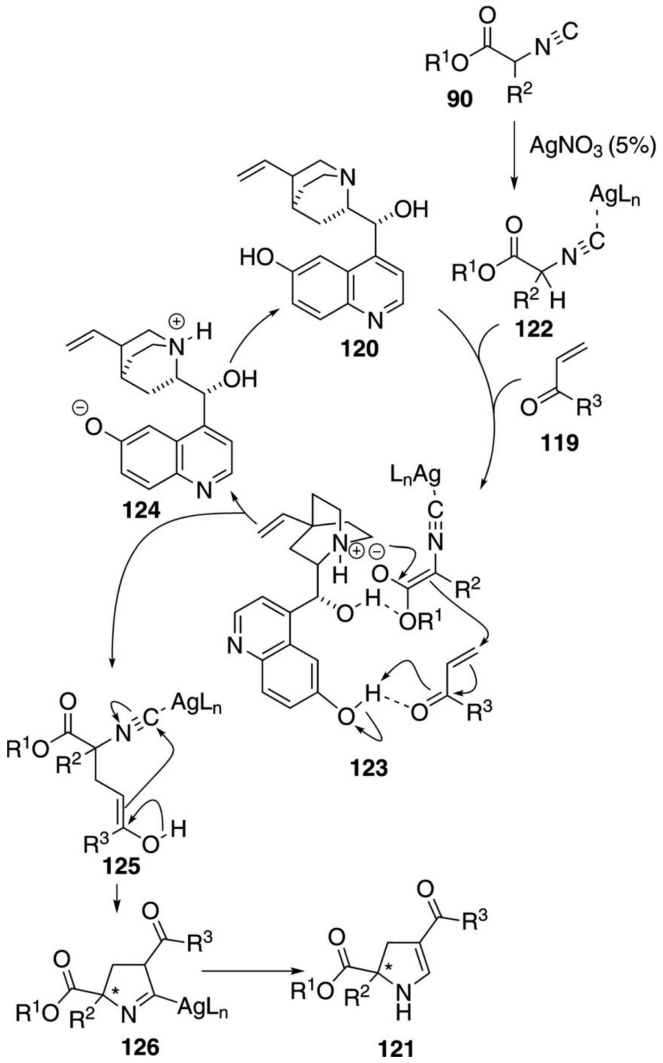


**Scheme 14.**
Silver-catalyzed enantioselective isonitrile condensation.

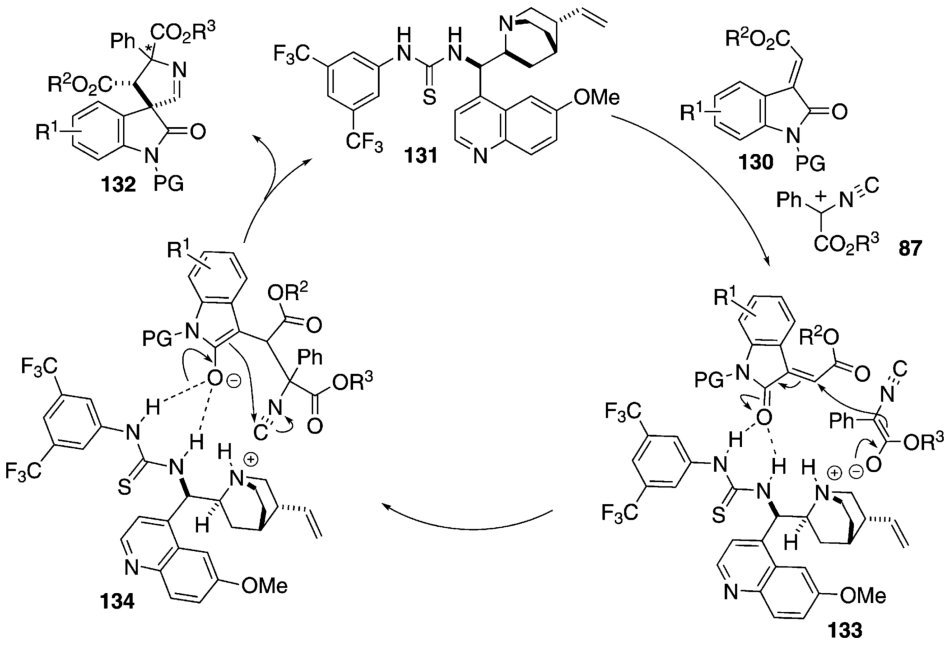


**Scheme 15.**
Organocatalyzed spirooxindole synthesis.

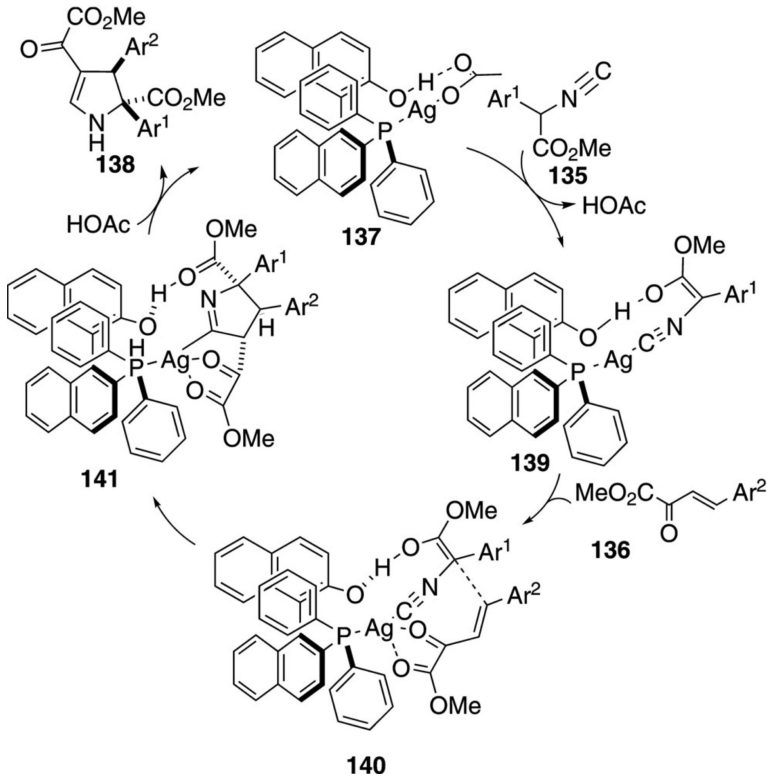


**Scheme 16.**

Silver-catalyzed formal [3+2]isonitrile addition to oxobutenoates.

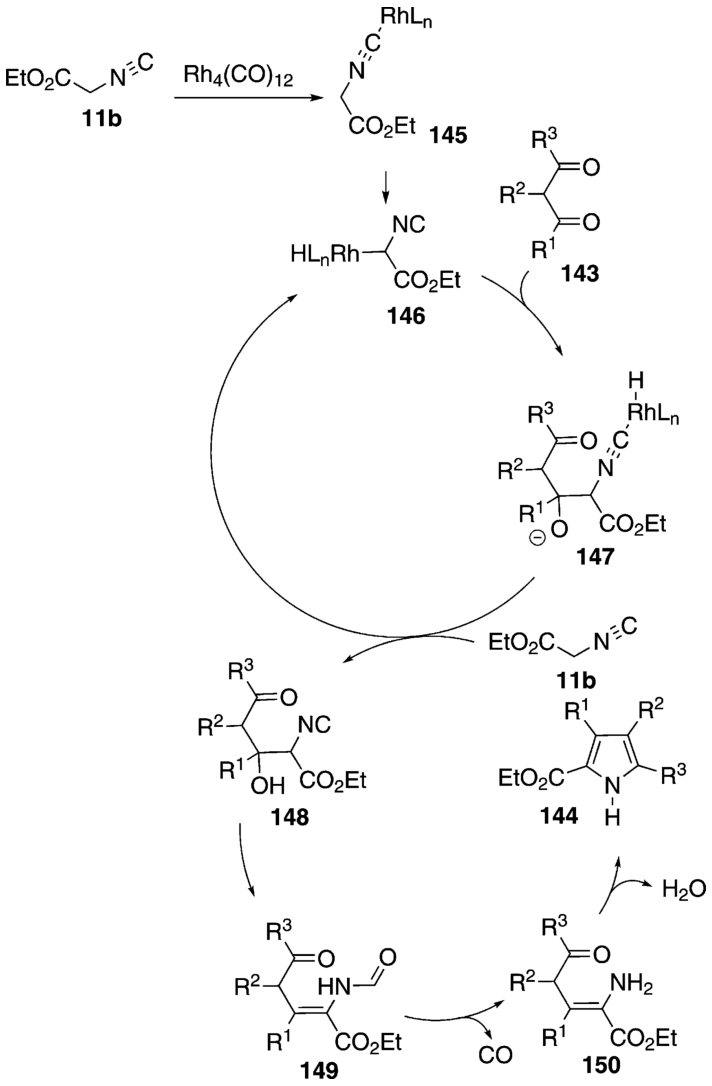


**Scheme 17.**
Rhodium-catalyzed pyrrole synthesis.

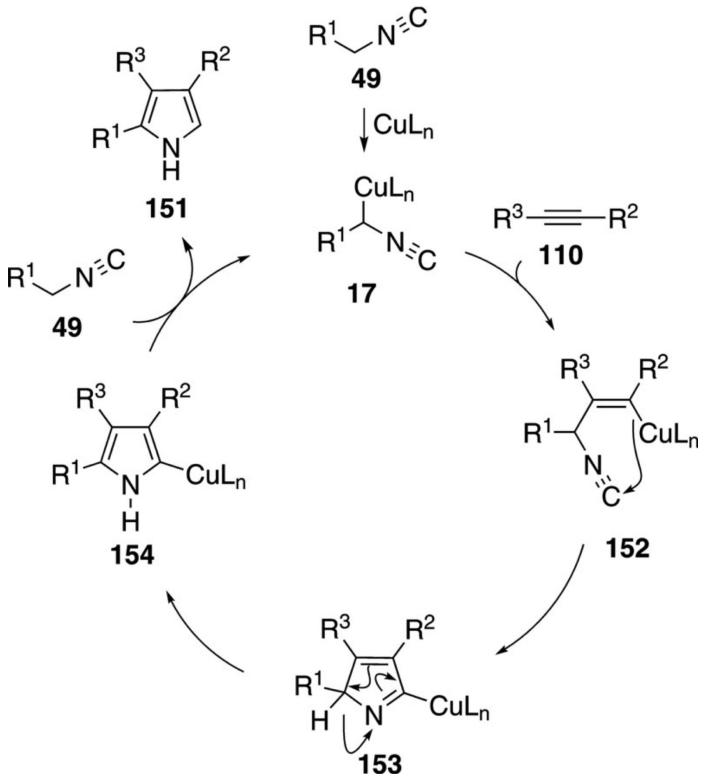


**Scheme 18.**
Copper-catalyzed pyrrole synthesis.

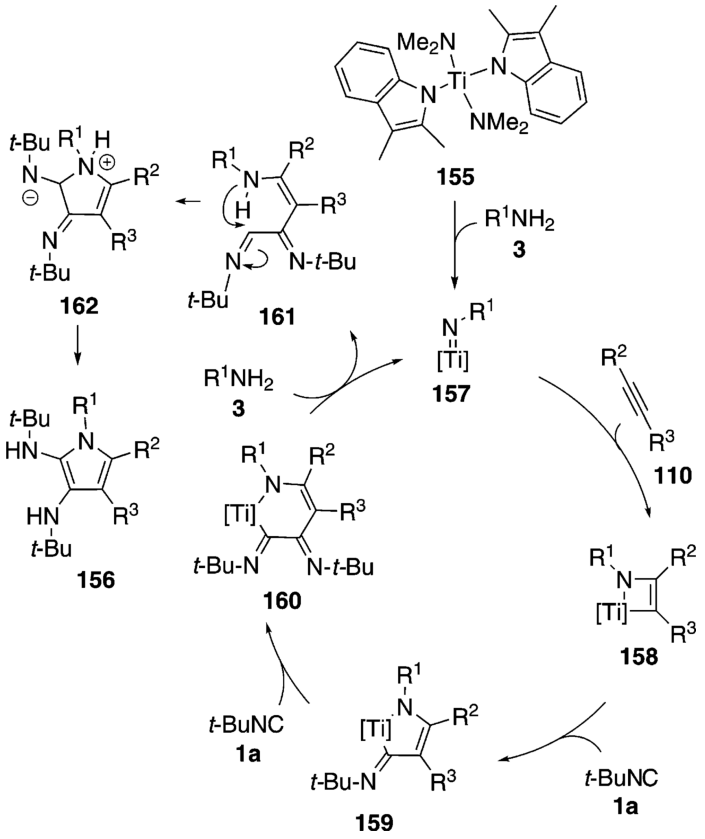


**Scheme 19.**

Titanium-catalyzed pyrrole synthesis.

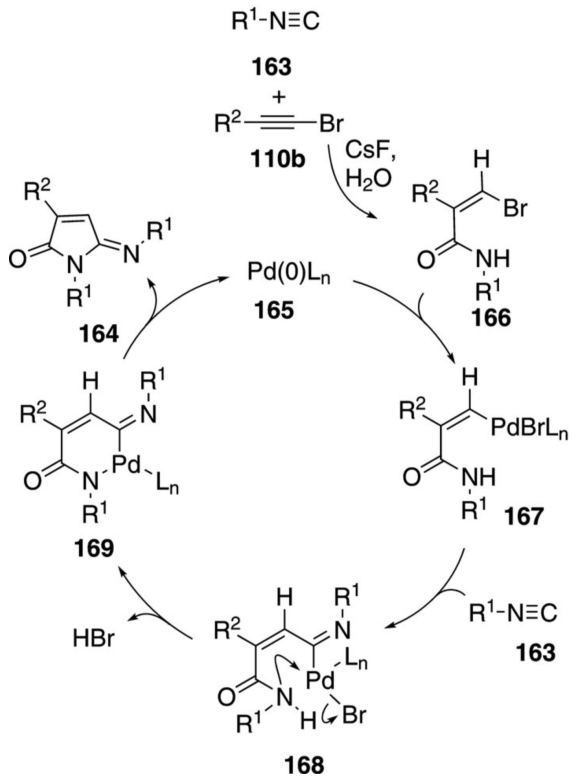


**Scheme 20.**
Palladium-catalyzed synthesis of 5-iminopyrrolones.

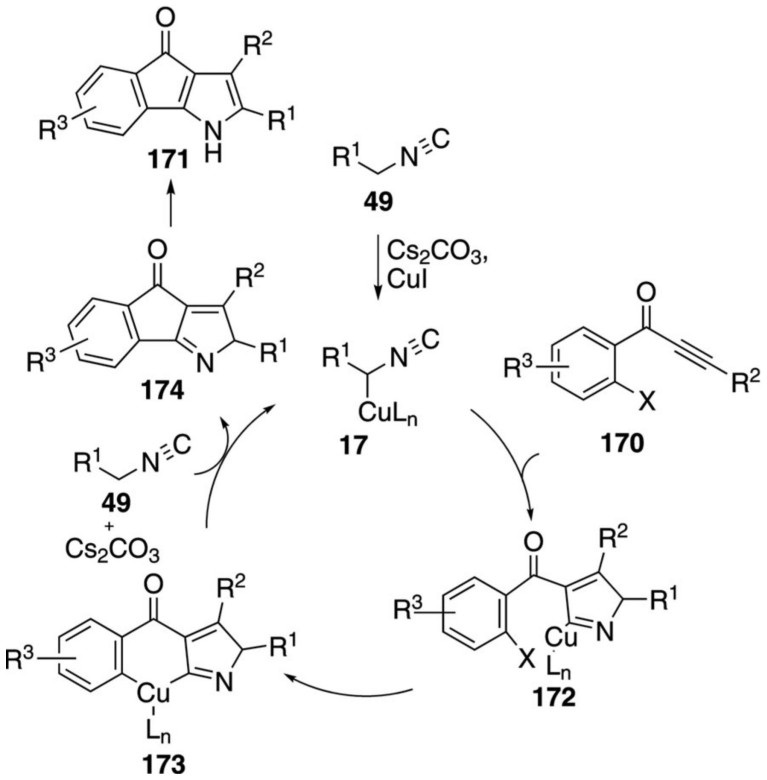


**Scheme 21.**
Copper-catalyzed 4-oxoindeno[1,2-*b*]pyrrole synthesis.

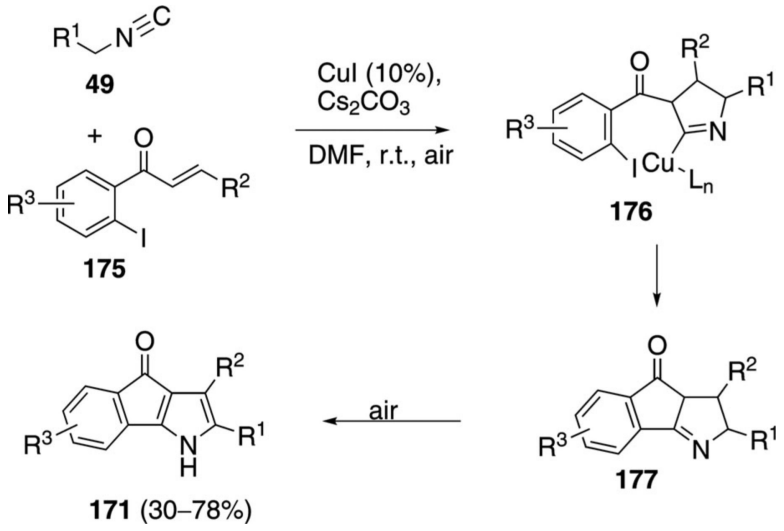


**Scheme 22.**
Copper-catalyzed isonitrile addition–cyclization–oxidation.

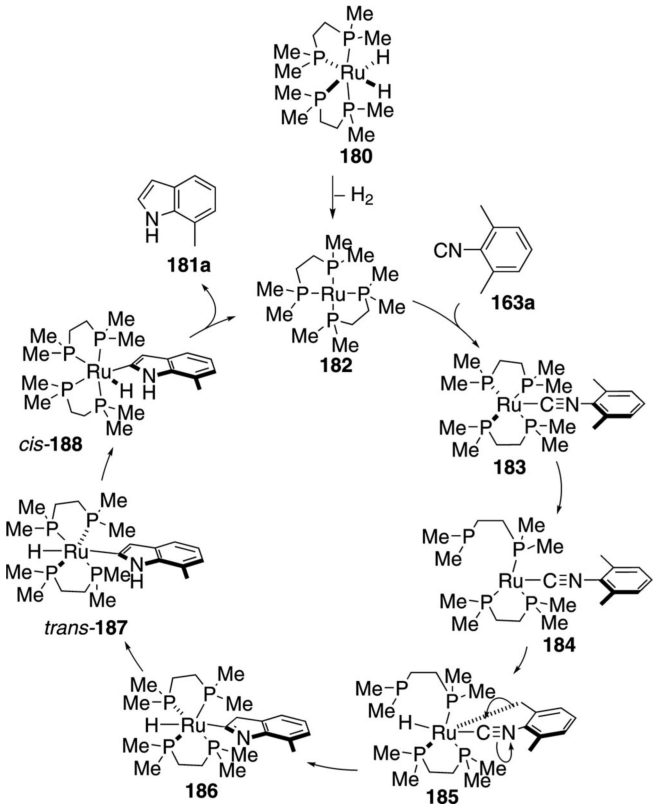


**Scheme 23.**
C–H insertion–cyclization with $RuH_2(dmpe)_2$.

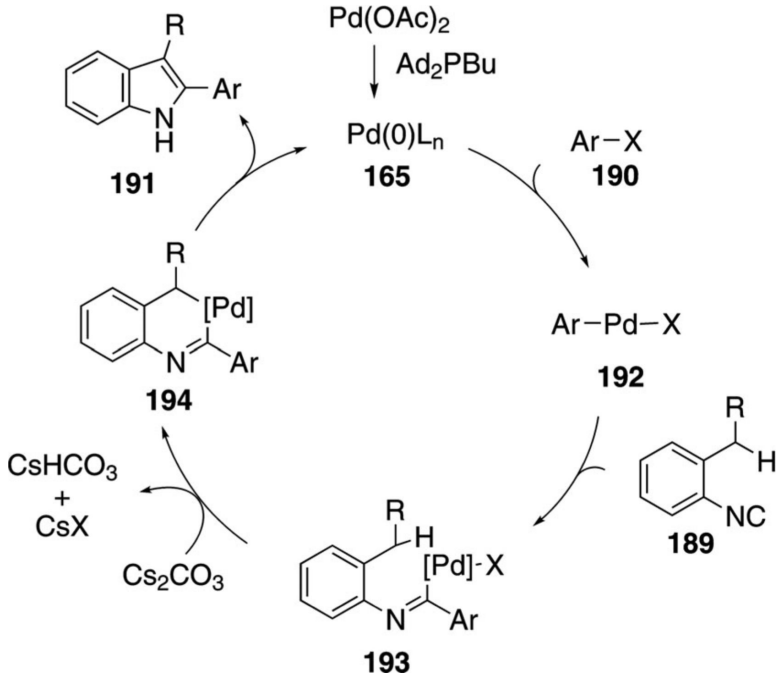


**Scheme 24.**
Palladium-catalyzed C–H insertion isonitrile coupling.

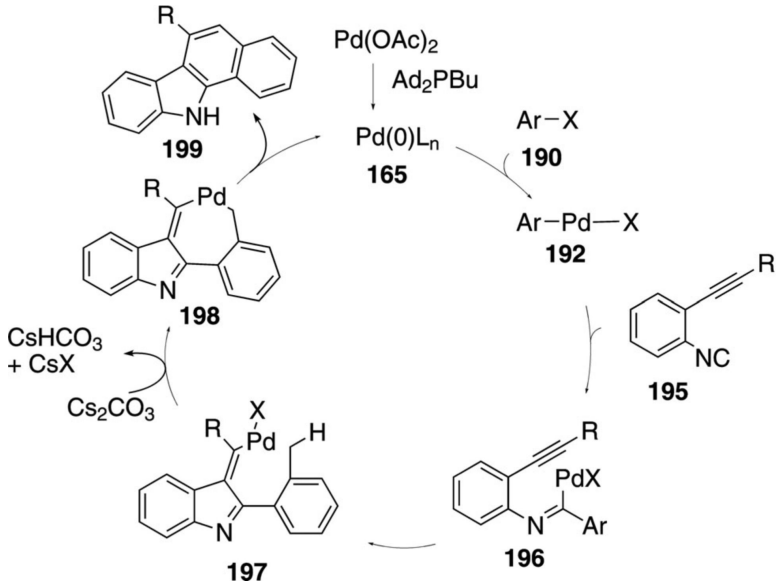


**Scheme 25.**

Palladium-catalyzed isonitrile addition, carbopalladation, C–H insertion.

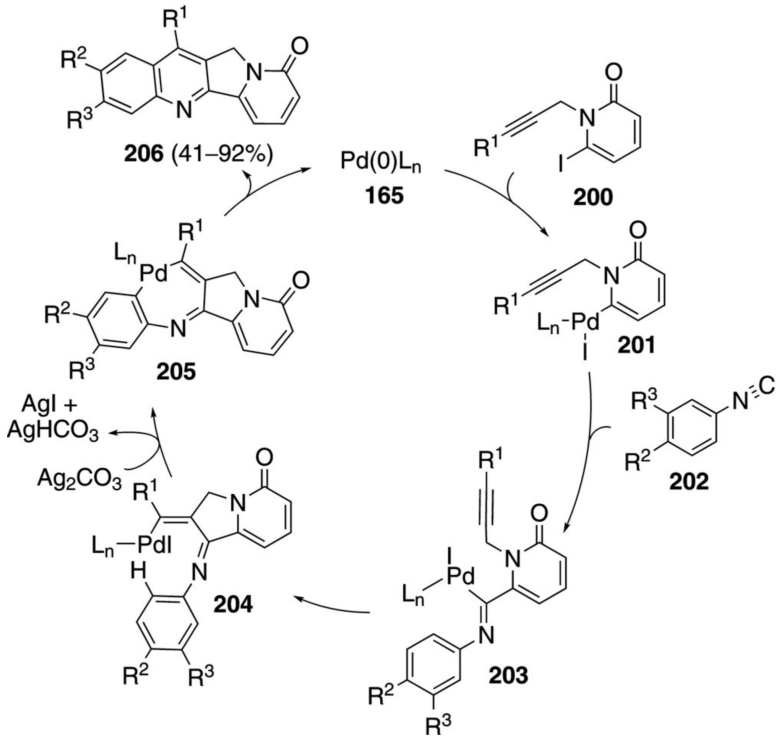


**Scheme 26.**
Palladium-catalyzed isonitrile–insertion–C–H activation route to camptothecins.

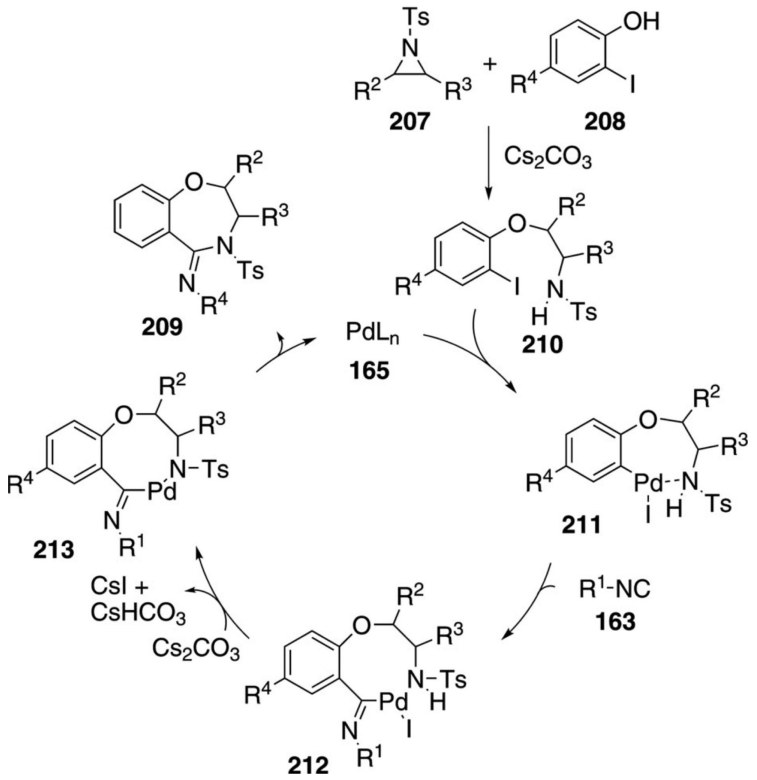


**Scheme 27.**
Palladium-catalyzed cyanation of 2-alkylindoles.

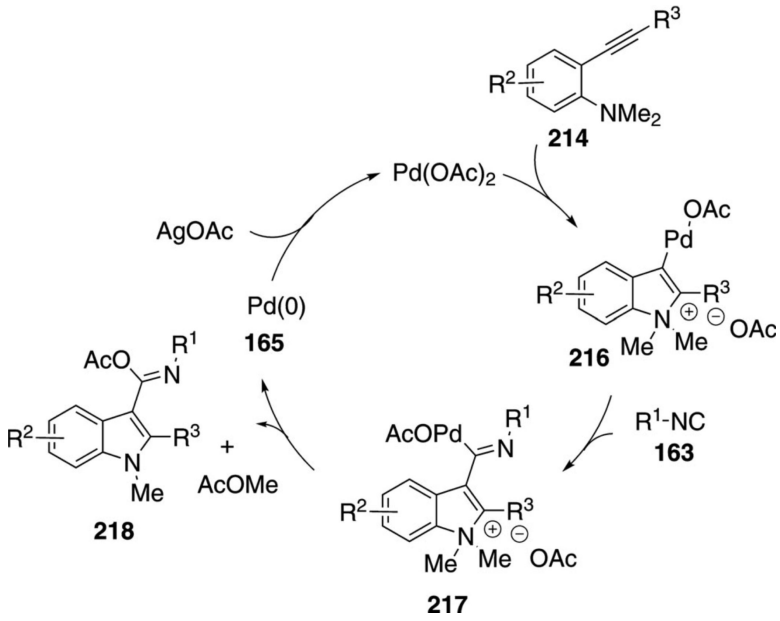


**Scheme 28.**

Palladium-catalyzed isonitrile condensation affording indoles.

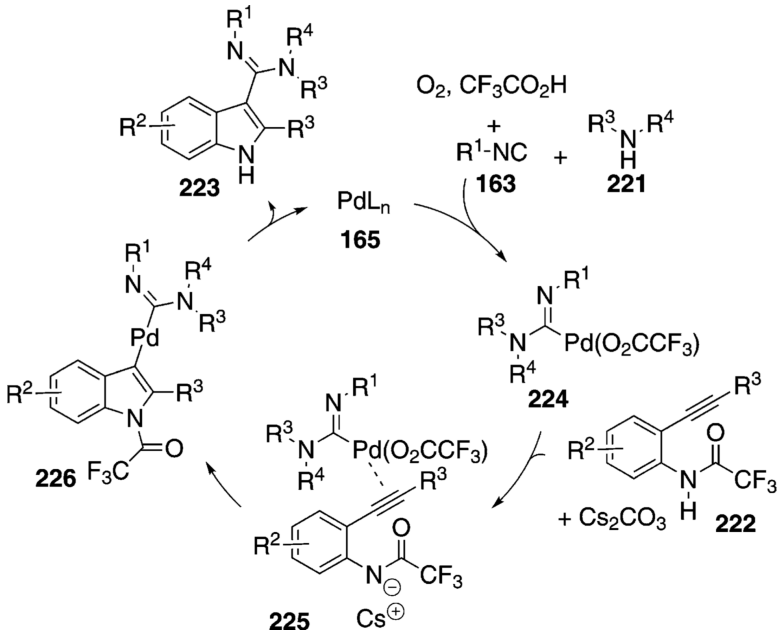


**Scheme 29.**
Palladium-catalyzed indole formation.

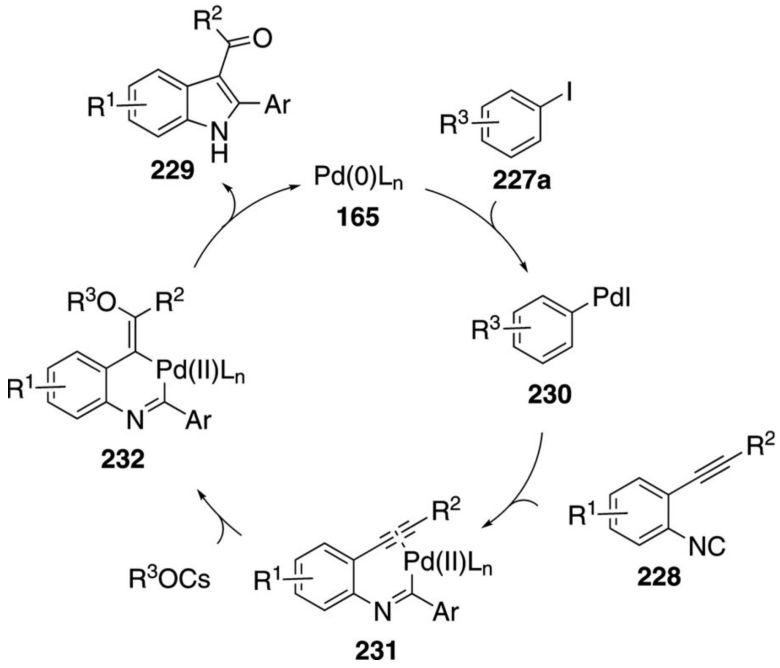


**Scheme 30.**
Palladium-catalyzed synthesis of indoles.

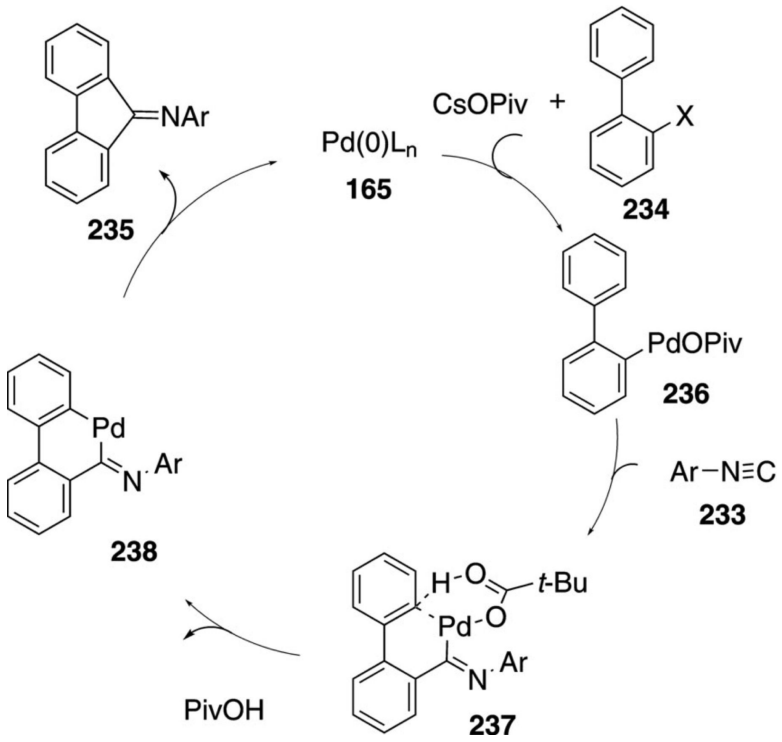


**Scheme 31.**
Palladium-catalyzed isonitrile–insertion–C–H activation route to iminofulvenes.

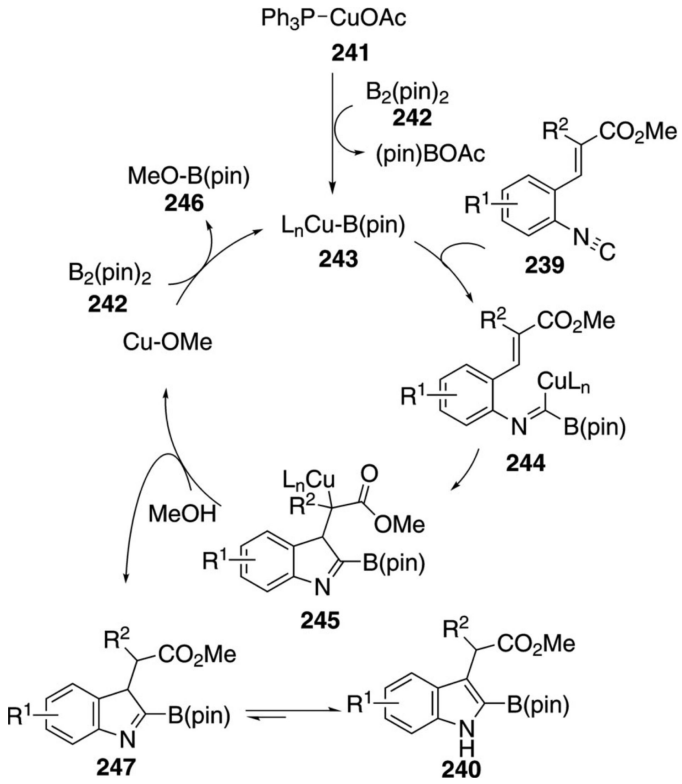


**Scheme 32.**
Copper-catalyzed borylation affording borylindoles.

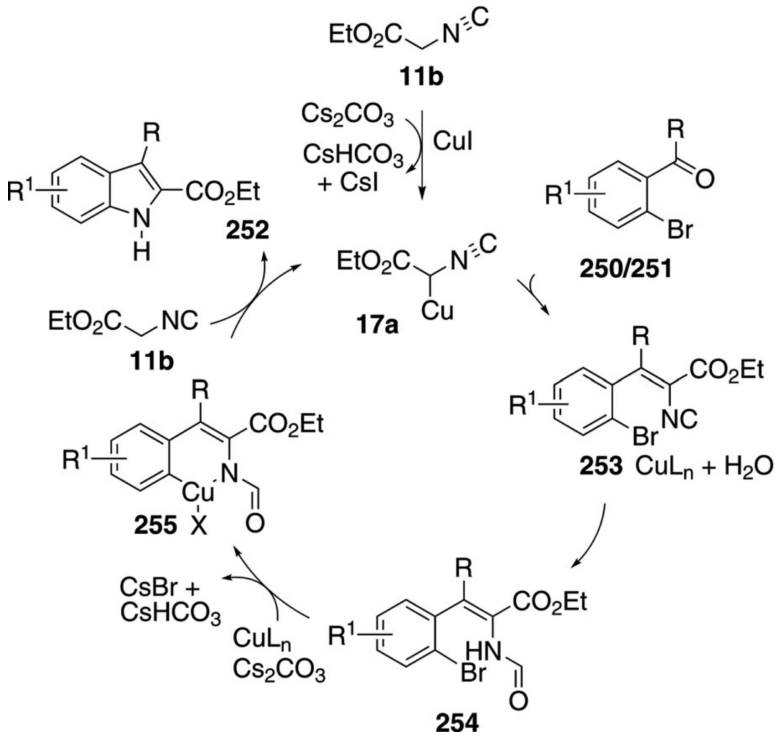


**Scheme 33.**
Copper-catalyzed indole formation.

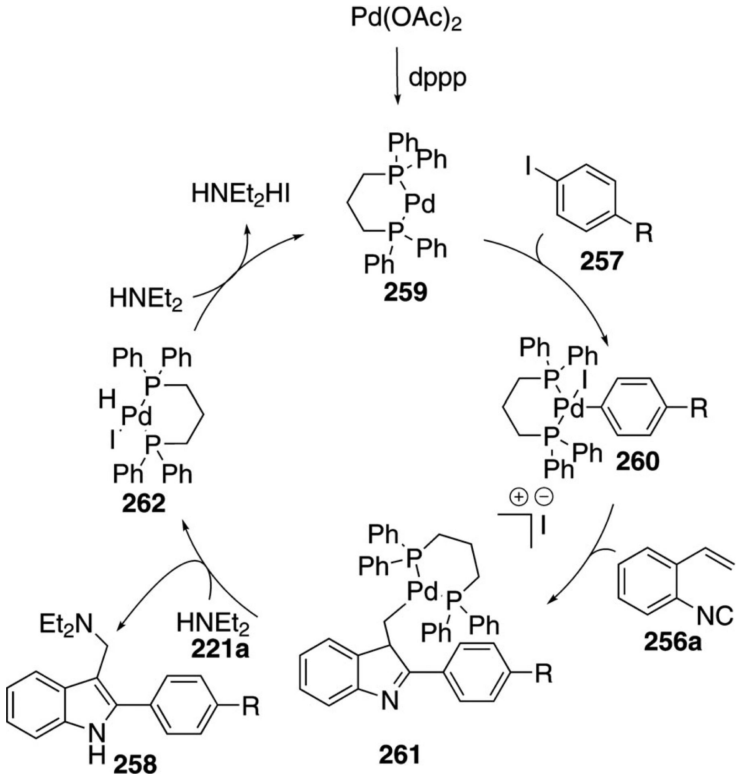


**Scheme 34.**
Palladium-catalyzed synthesis of indoles.

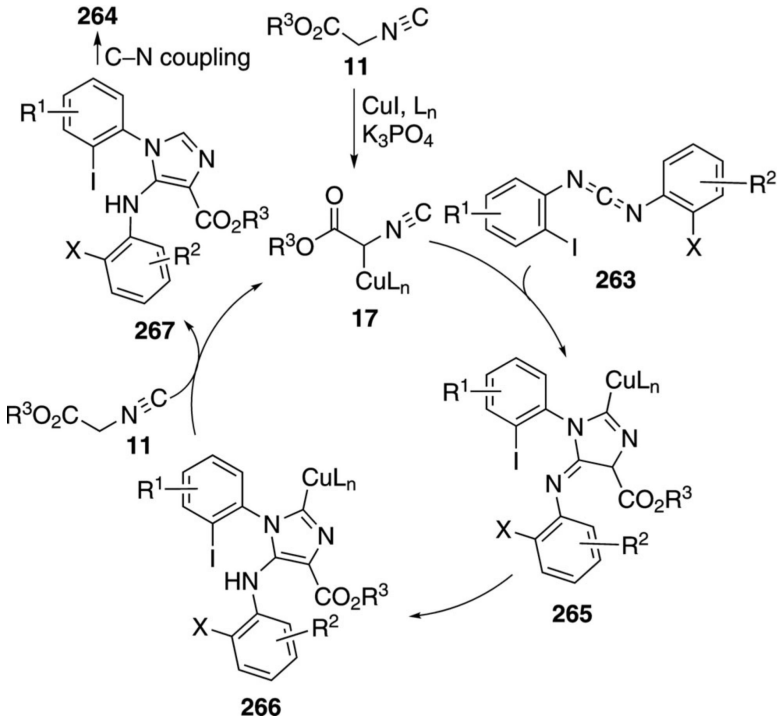


**Scheme 35.**
Copper-catalyzed bis-cyclization of carbodiimides.

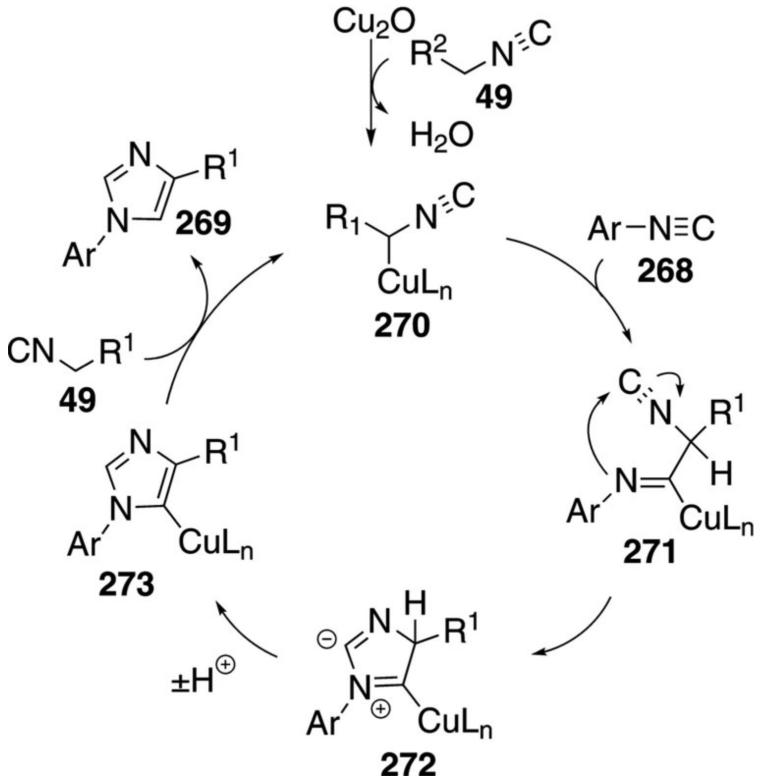


**Scheme 36.**
Copper-catalyzed synthesis of arylimidazoles.

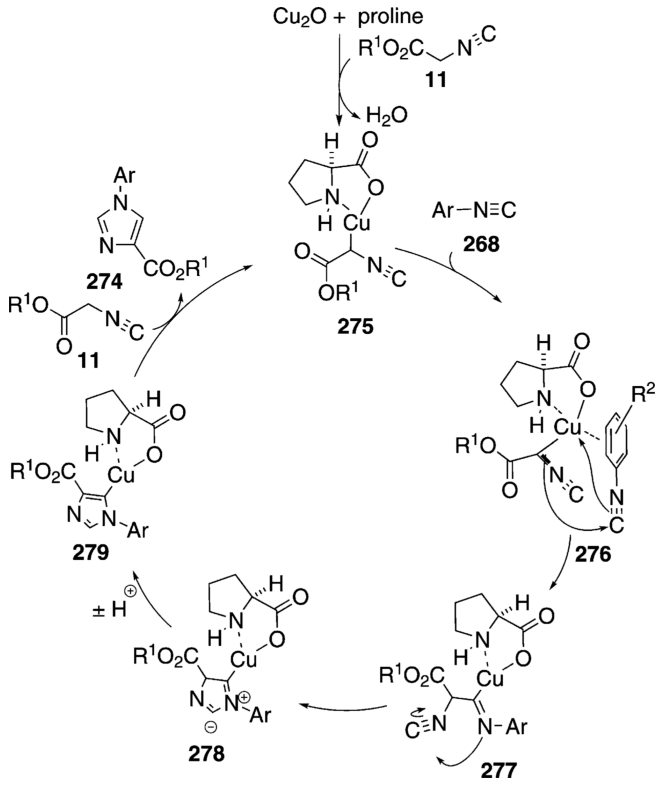


**Scheme 37.**
Copper–proline-catalyzed imidazole formation.

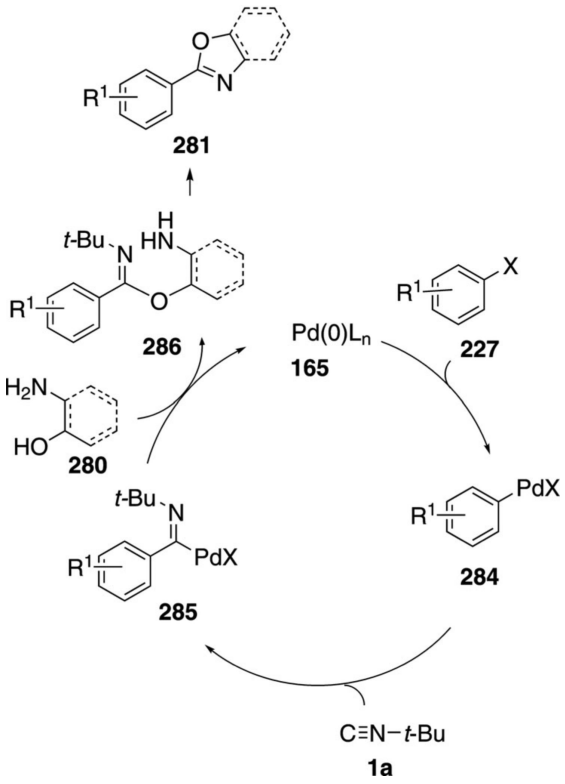


**Scheme 38.**
Isonitrile insertion route to oxazolines.

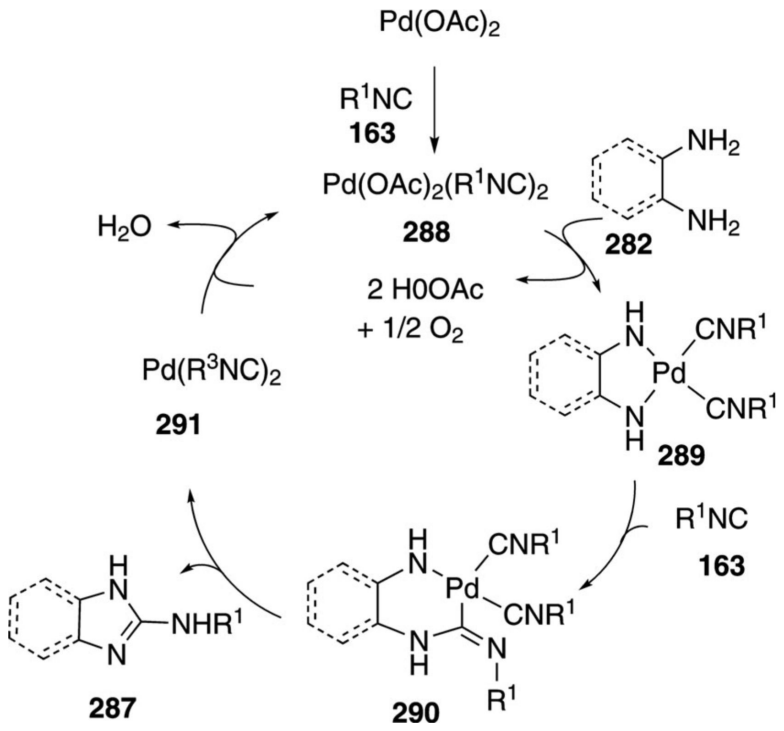


**Scheme 39.**
Palladium-catalyzed synthesis of 2-aminobenzimidazoles.

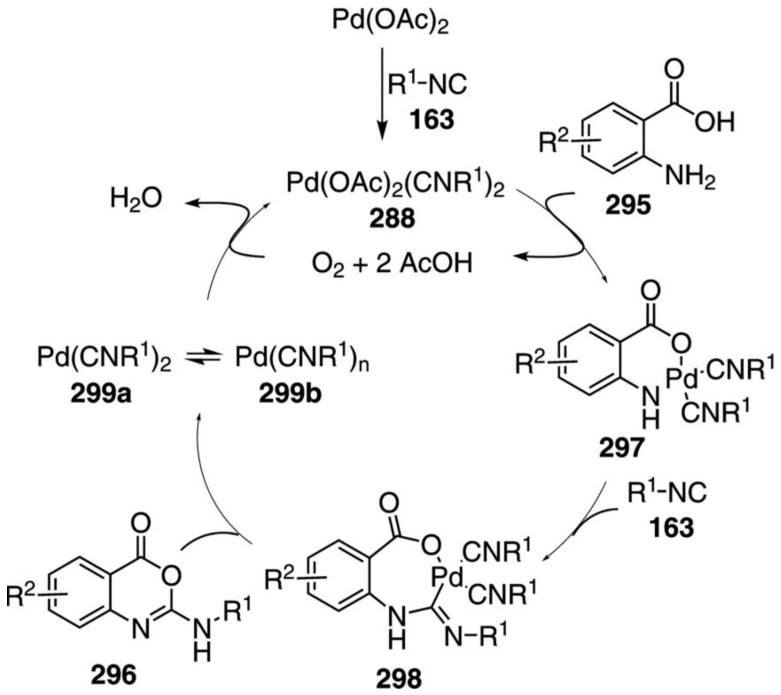


**Scheme 40.**
Palladium-catalyzed synthesis of 2-aminobenzoxazinones.

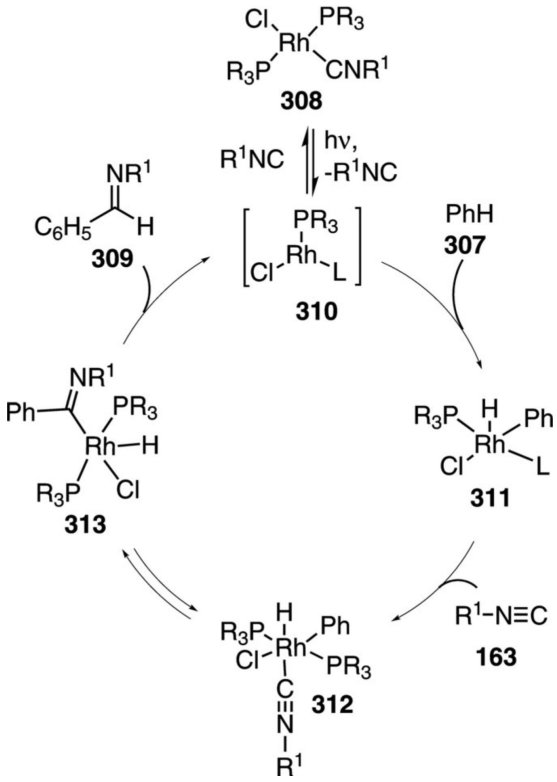


**Scheme 41.**
Palladium-catalyzed iminocarbonylative cross-coupling.

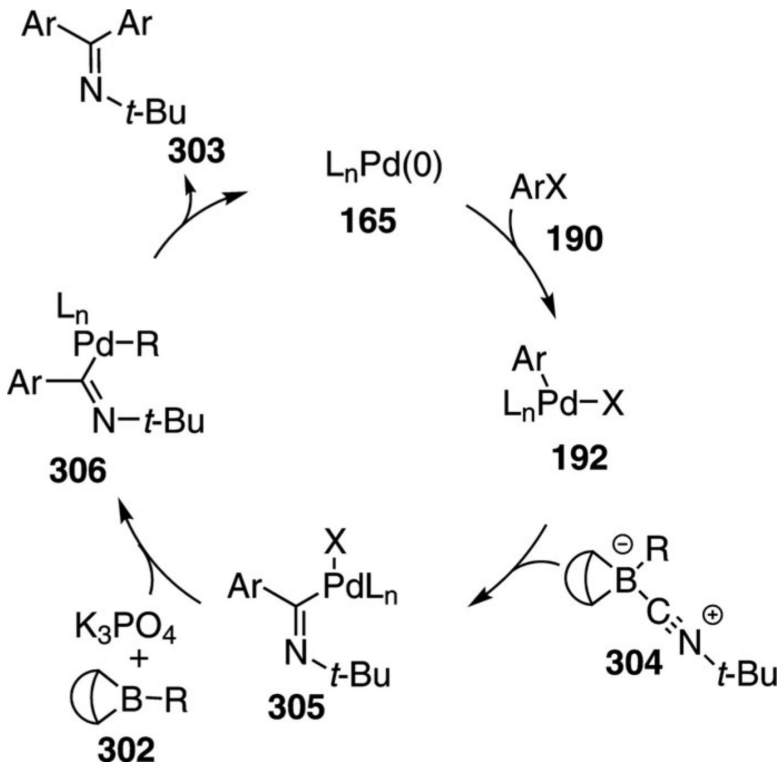


**Scheme 42.**
Rhodium-catalyzed C–H isonitrile insertion.

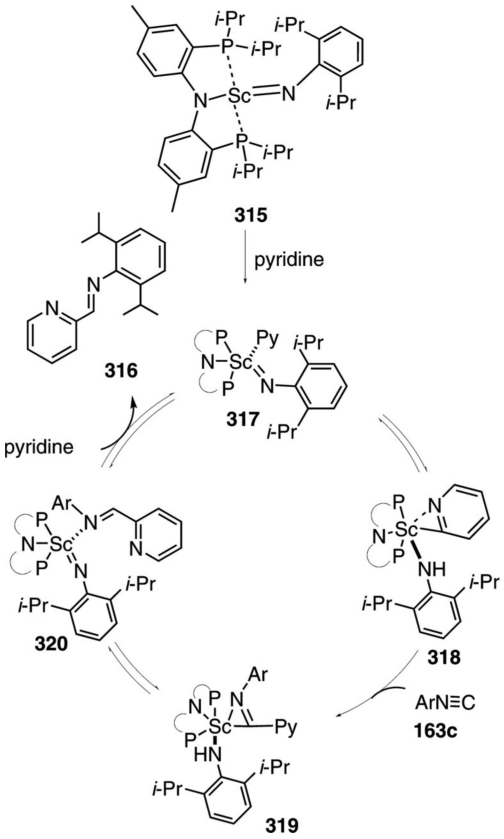


**Scheme 43.**
Scandium-catalyzed C–H and isonitrile insertion.

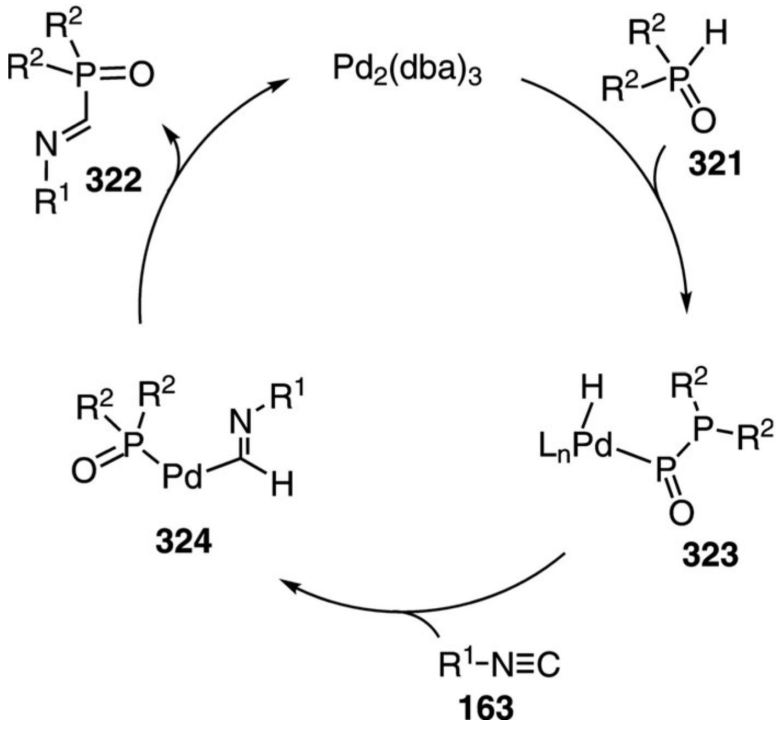


**Scheme 44.**
Palladium-catalyzed iminophosphine oxide formation.

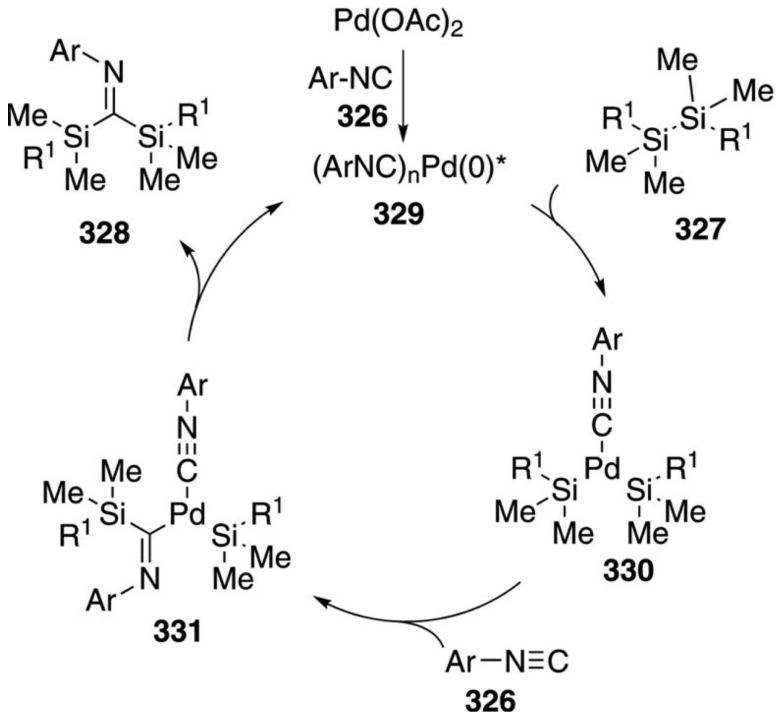


**Scheme 45.**
Palladium-catalyzed isonitrile insertion into Si–Si bonds.

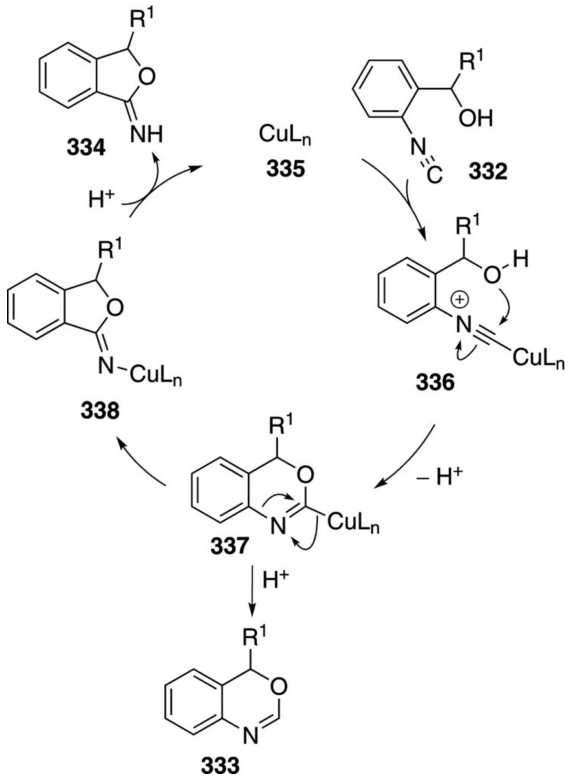


**Scheme 46.**
Copper(I) oxide-catalyzed cyclization of isocyanobenzyl alcohols.

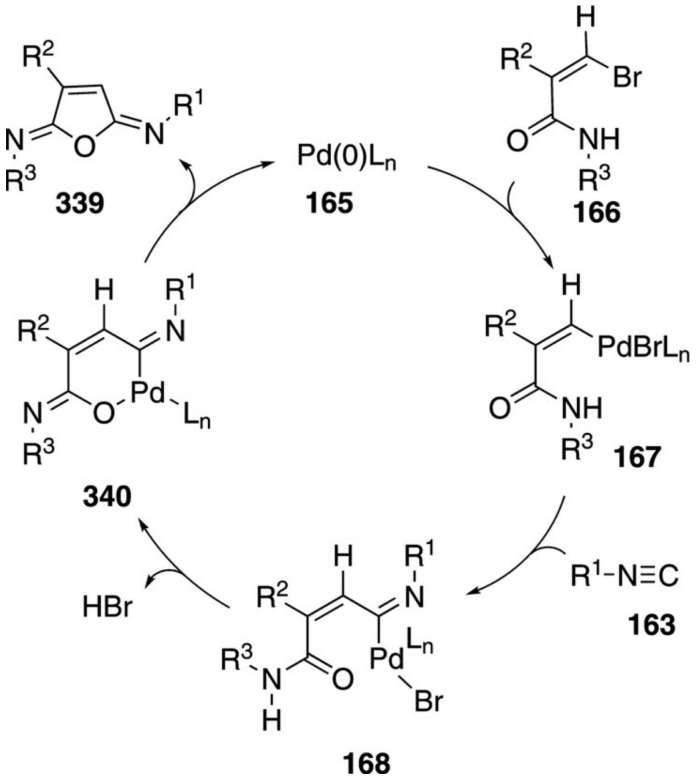


**Scheme 47.**
Palladium-catalyzed synthesis of diiminofurans.

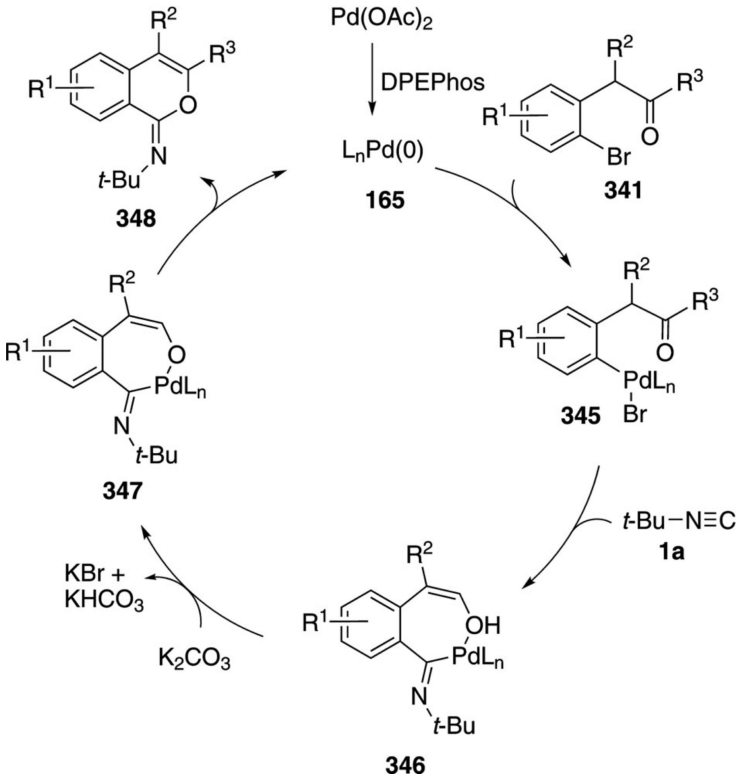


**Scheme 48.**
Palladium-catalyzed isocoumarin synthesis.

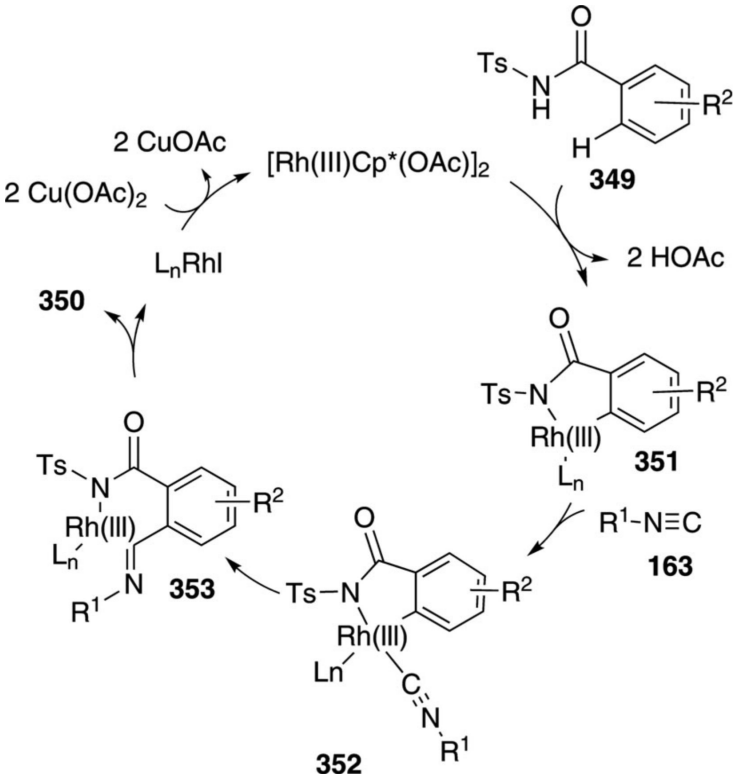


**Scheme 49.**
Rhodium-catalyzed (imino)-isonitrile synthesis.

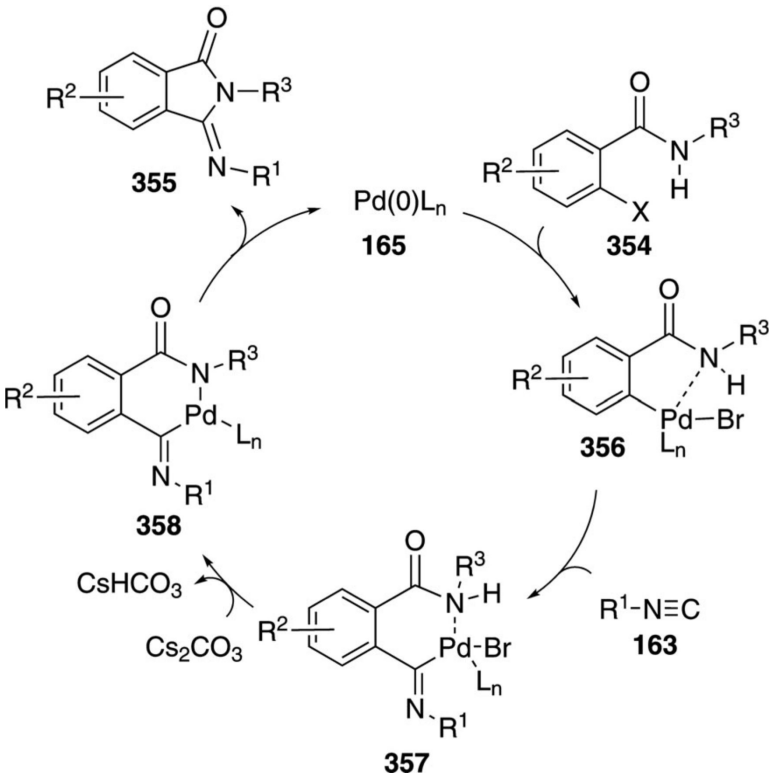


**Scheme 50.**
Palladium-catalyzed (imino)-indolinone synthesis.

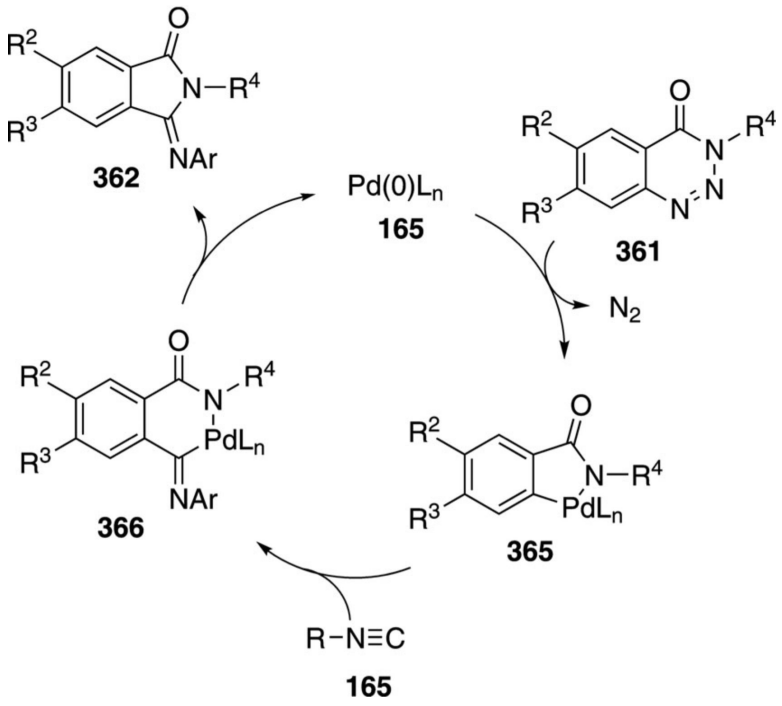


**Scheme 51.**
Palladium-catalyzed $N_2$ extrusion–isonitrile insertion.

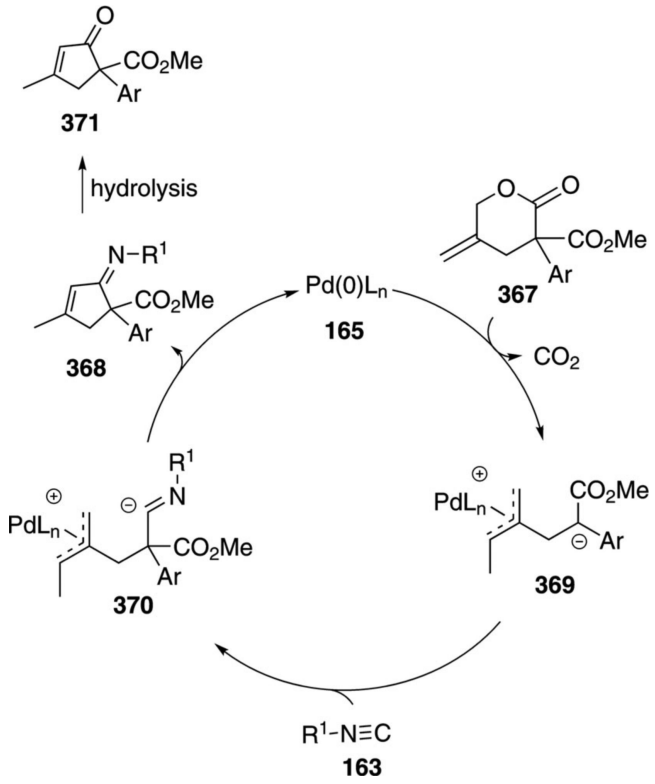


**Scheme 52.**
Palladium-catalyzed decarboxylative [4+1] isonitrile cyclization.

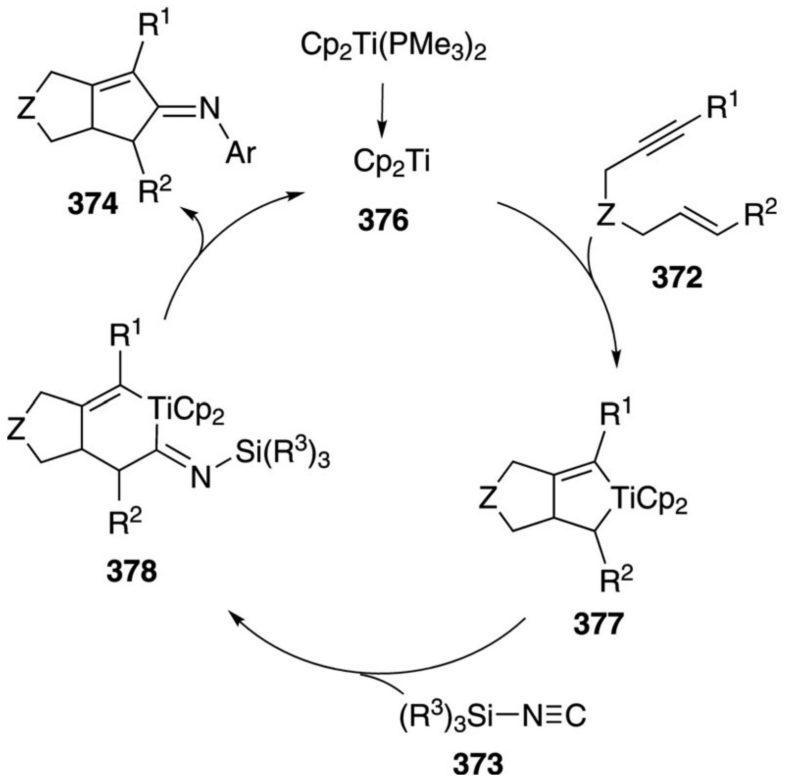


**Scheme 53.**
Titanium-catalyzed cyclopentene synthesis.

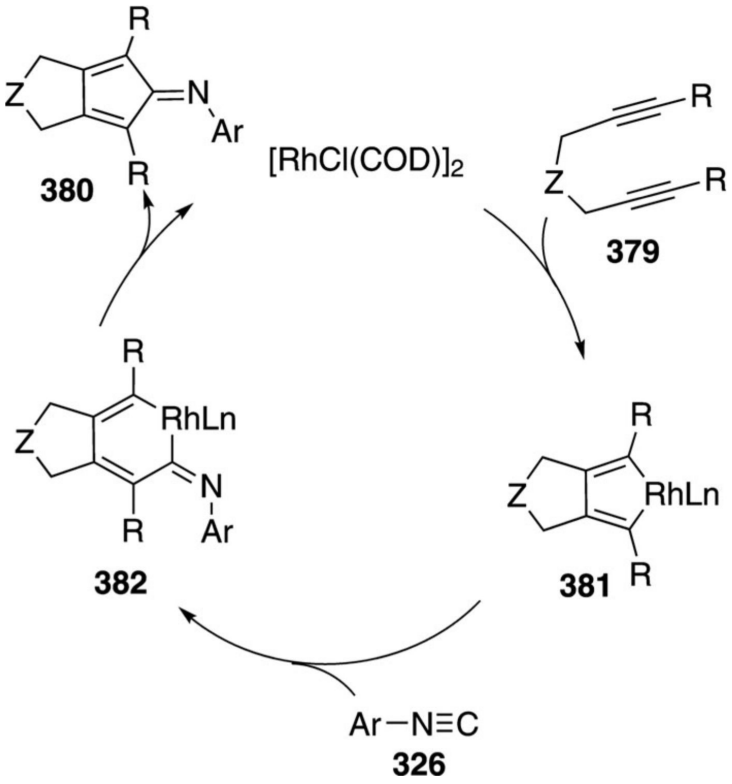


**Scheme 54.**
Rhodium-catalyzed diyne–isonitrile condensation.

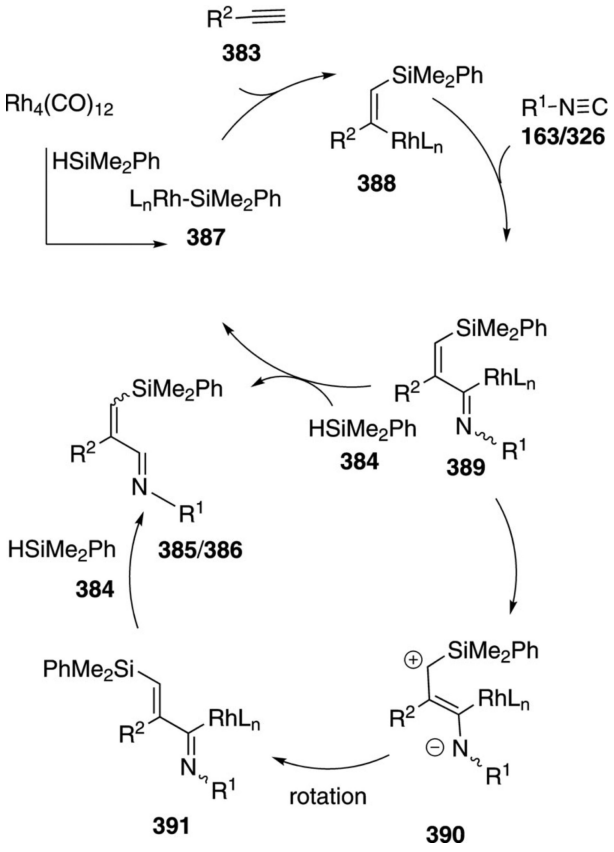


**Scheme 55.**
Rhodium-catalyzed silylimination of alkynes.

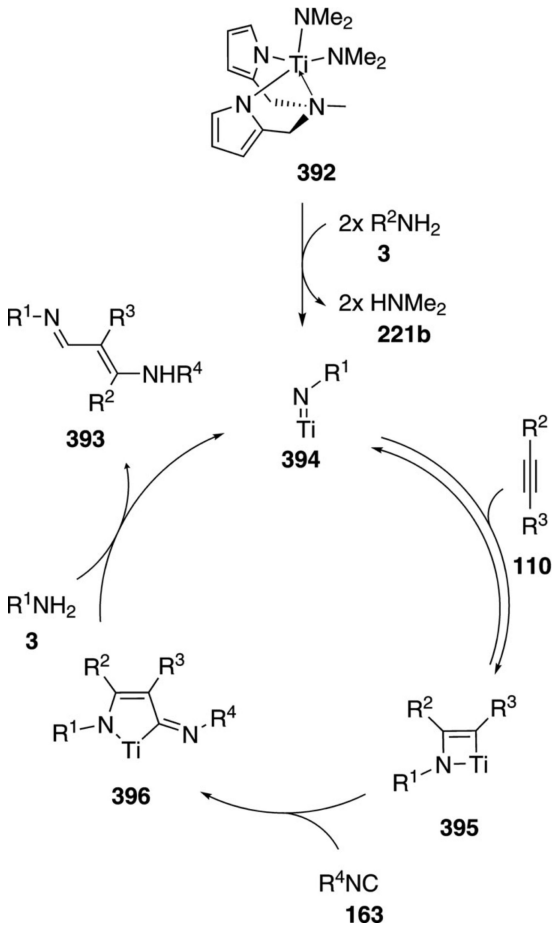


**Scheme 56.**
Titanium-catalyzed iminoenamine synthesis.

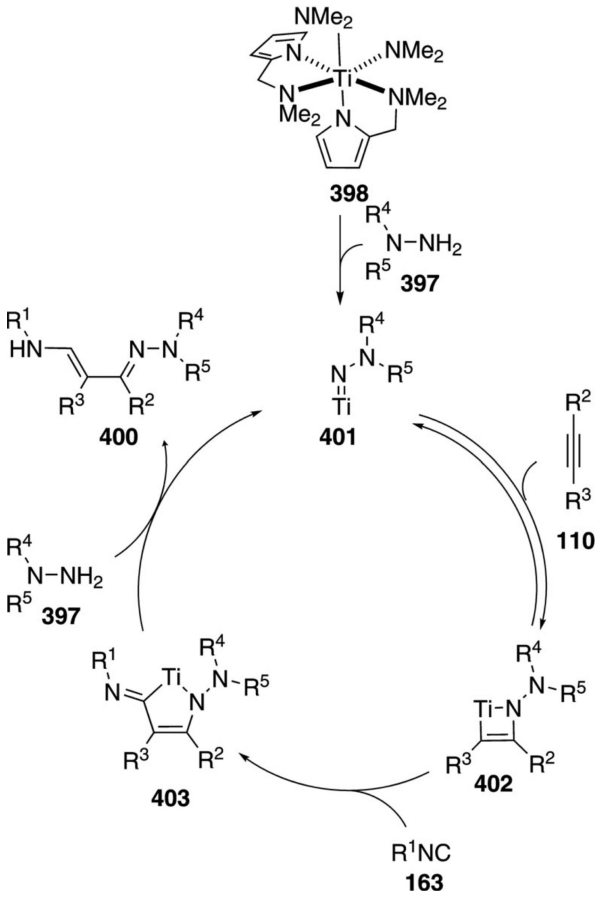


**Scheme 57.**
Titanium-catalyzed isonitrile–alkyne–amine coupling.

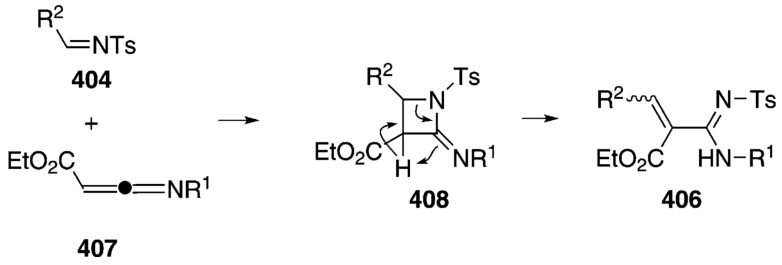


**Scheme 58.**
Palladium-catalyzed isonitrile–carbene coupling

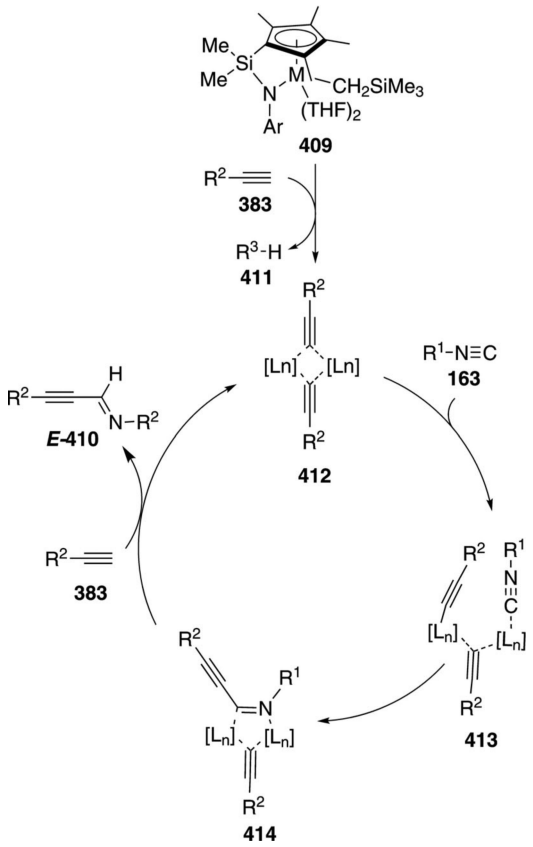


**Scheme 59.**
Lathanum-catalyzed isonitrile–acetylene coupling.

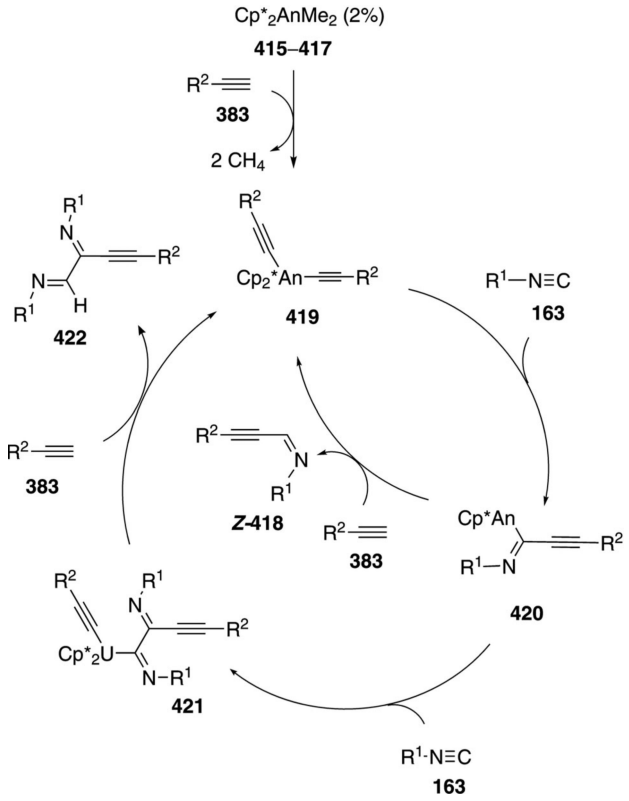


**Scheme 60.**
Organoactinide-catalyzed isonitrile–acetylene condensation.

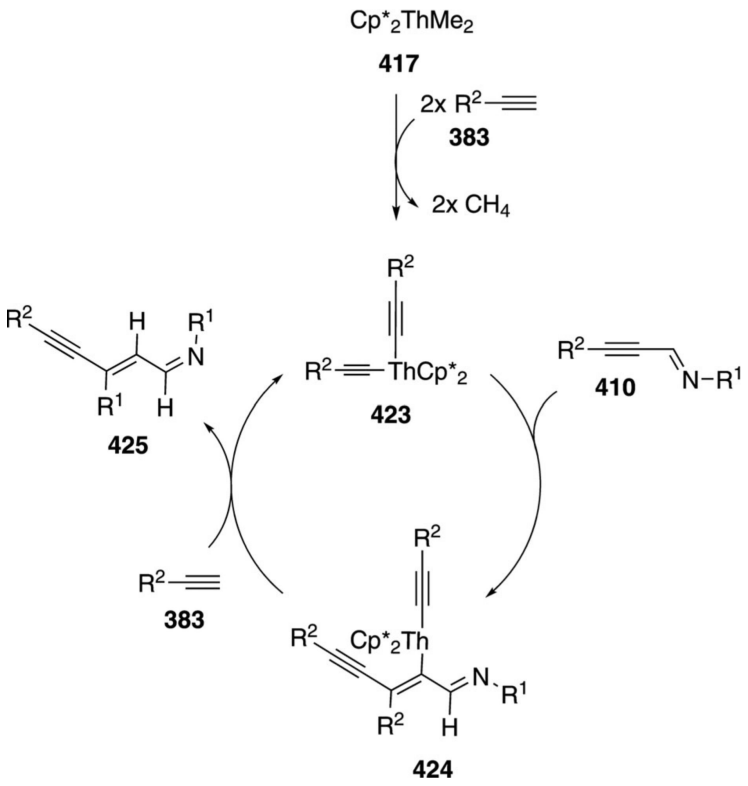


**Scheme 61.**
Organothorium conjugate addition.

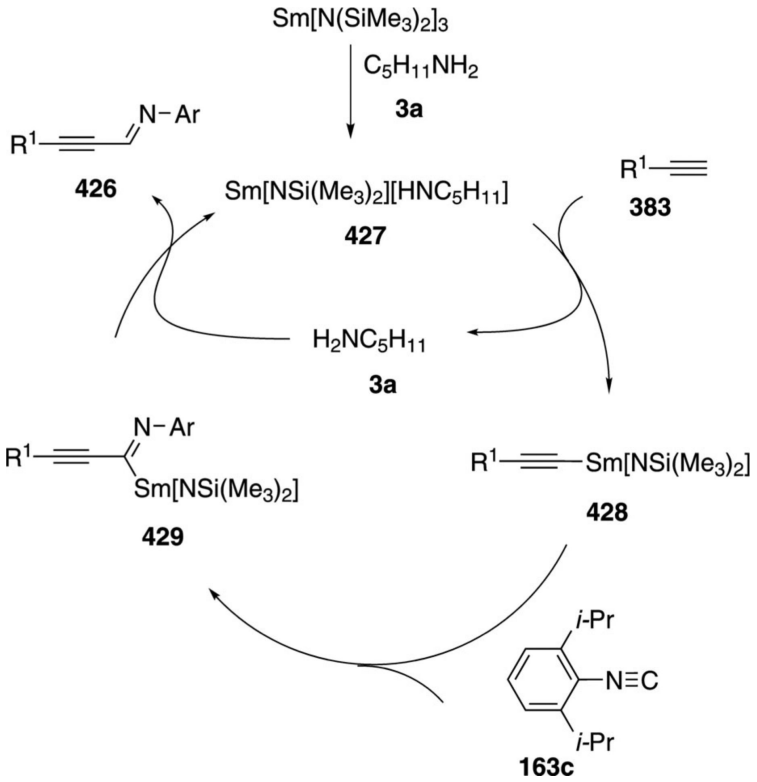


**Scheme 62.**
Samarium-catalyzed acetylenic imine synthesis.

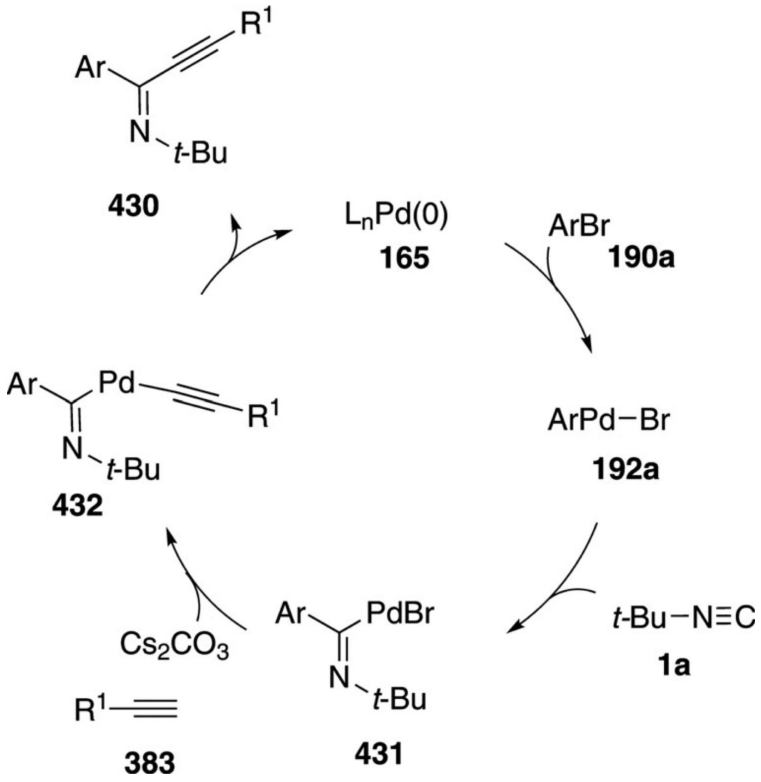


**Scheme 63.**
Palladium-catalyzed yneimine synthesis.

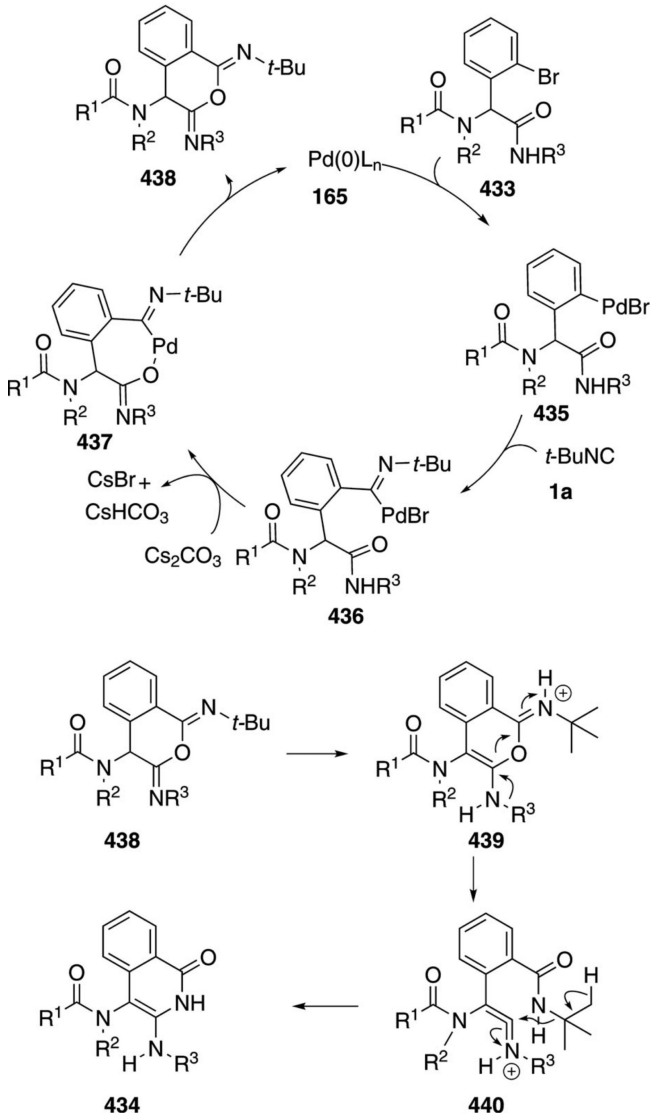


**Scheme 64.**
Palladium-catalyzed bromo amide condensation with isonitriles.

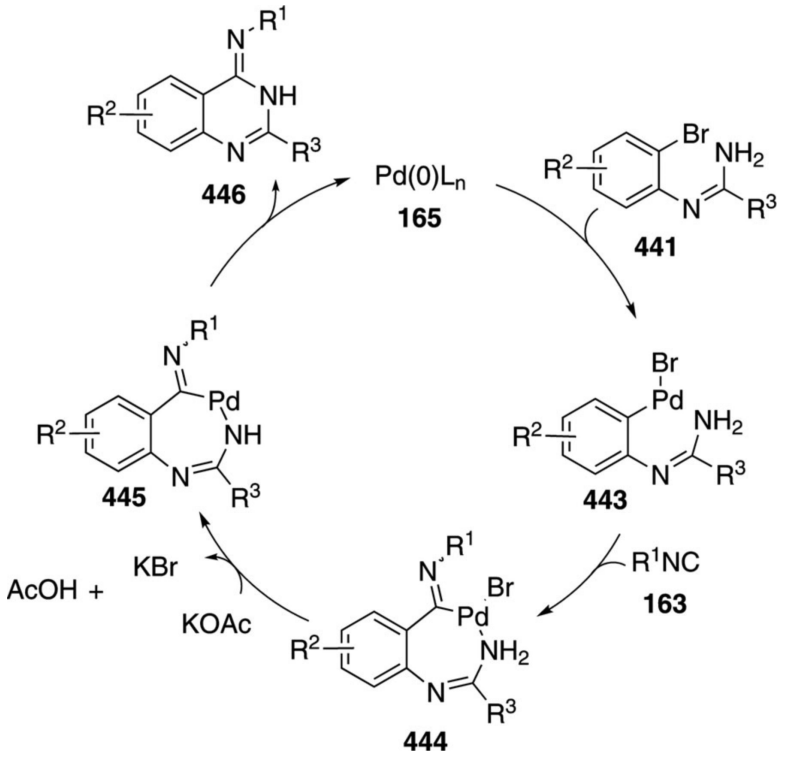


**Scheme 65.**
Palladium-catalyzed aminoquionline formation.

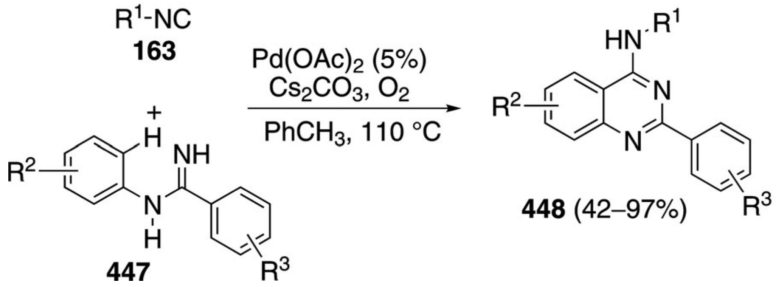


**Scheme 66.**
Palladium-catalyzed direct C–H insertion–isonitrile condensation.

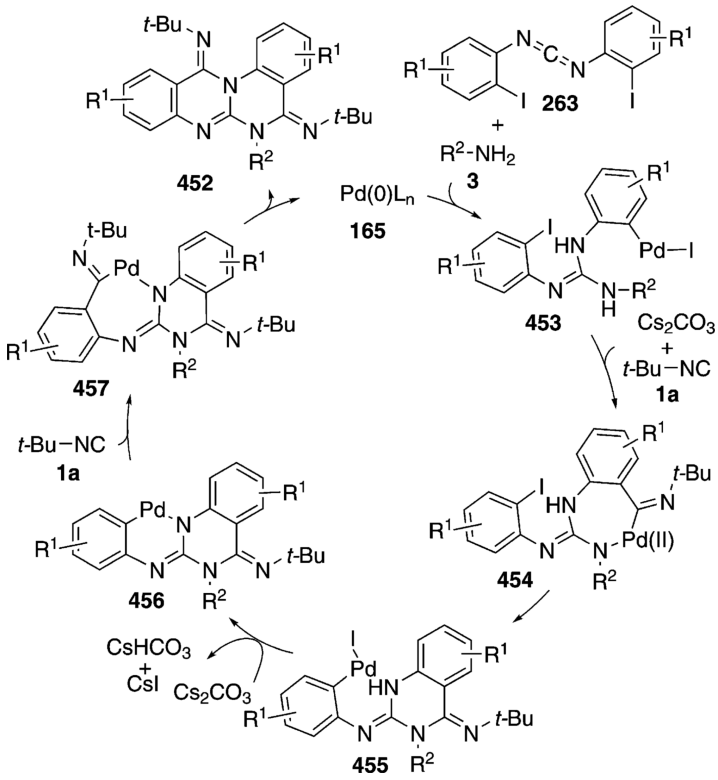


**Scheme 67.**
Cascade assembly of carbodiimides.

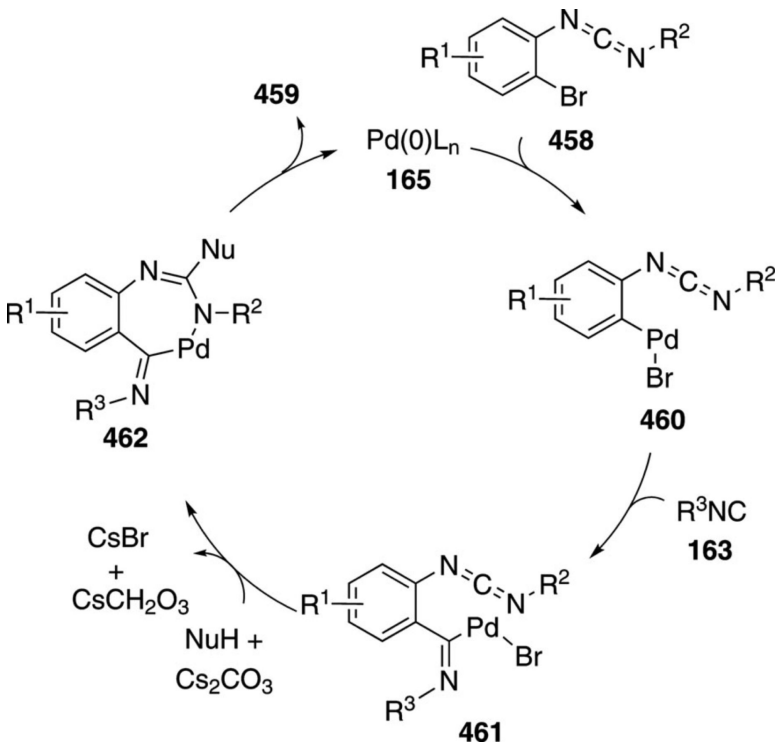


**Scheme 68.**
Palladium-catalyzed carbodiimide cyclization.

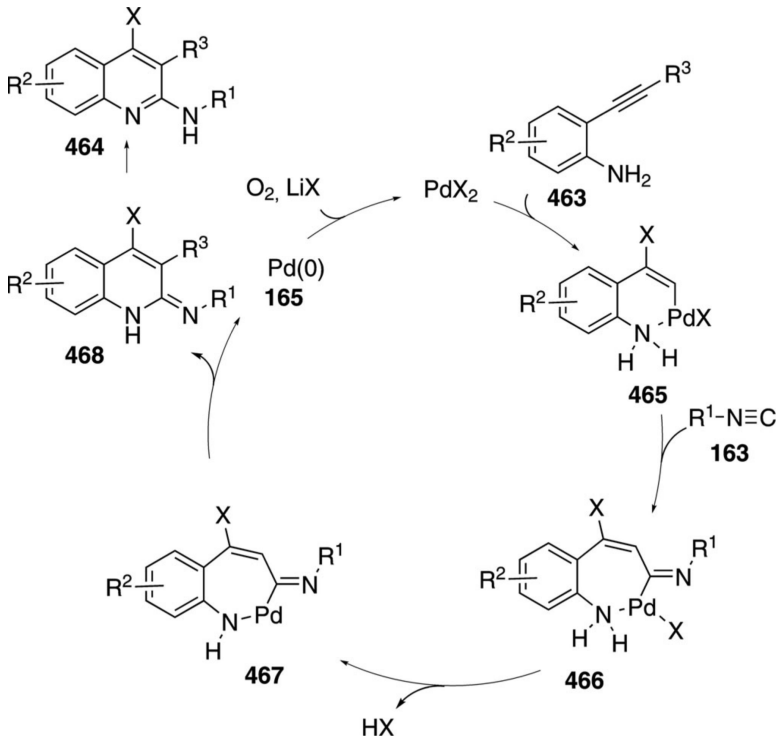


**Scheme 69.**
Palladium-catalyzed haloquinoline synthesis.

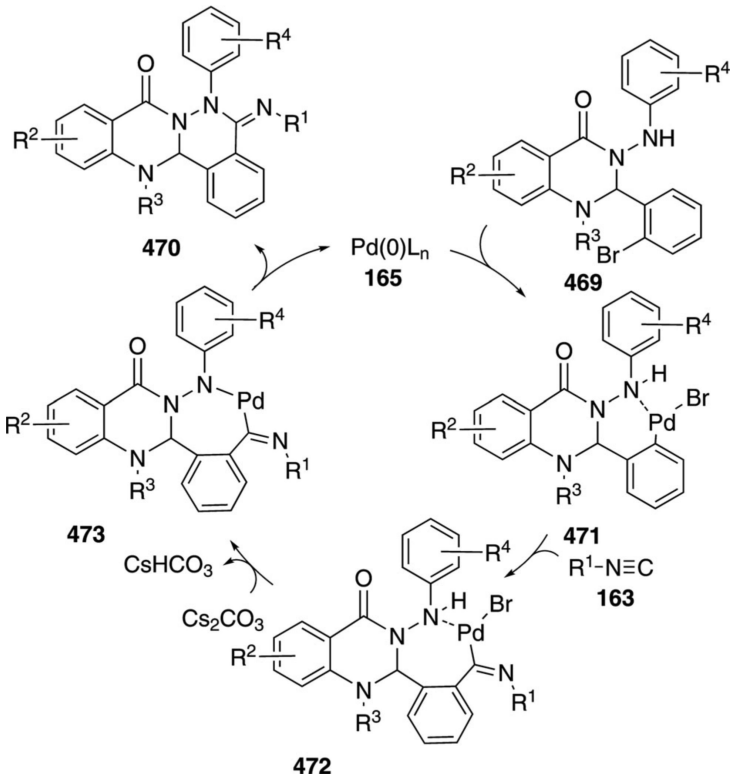


**Scheme 70.**
Palladium-catalyzed phthalazino[1,2-*b*]quinazoli-none synthesis.

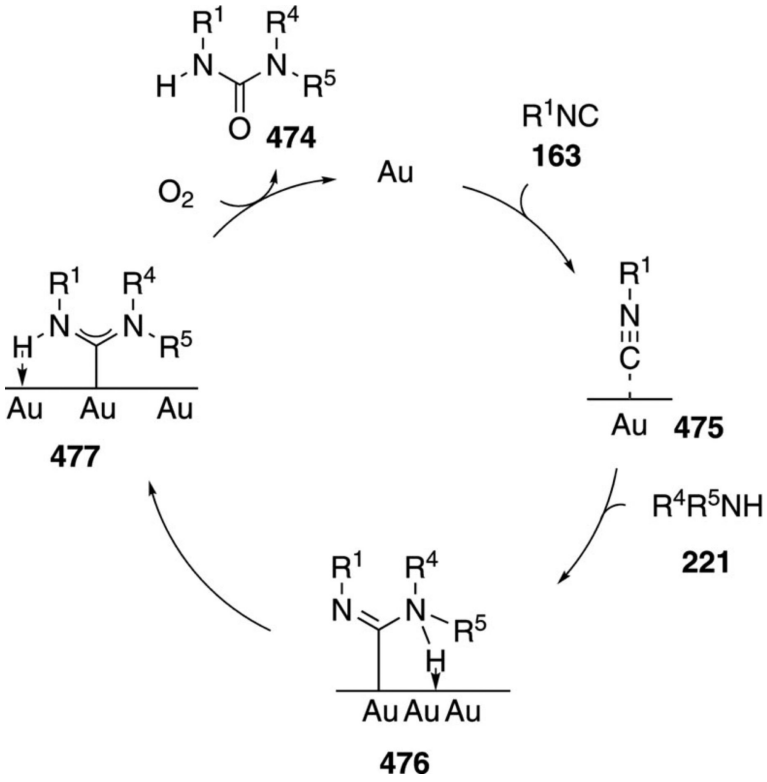


**Scheme 71.**
Gold-catalyzed isonitrile–amine coupling.

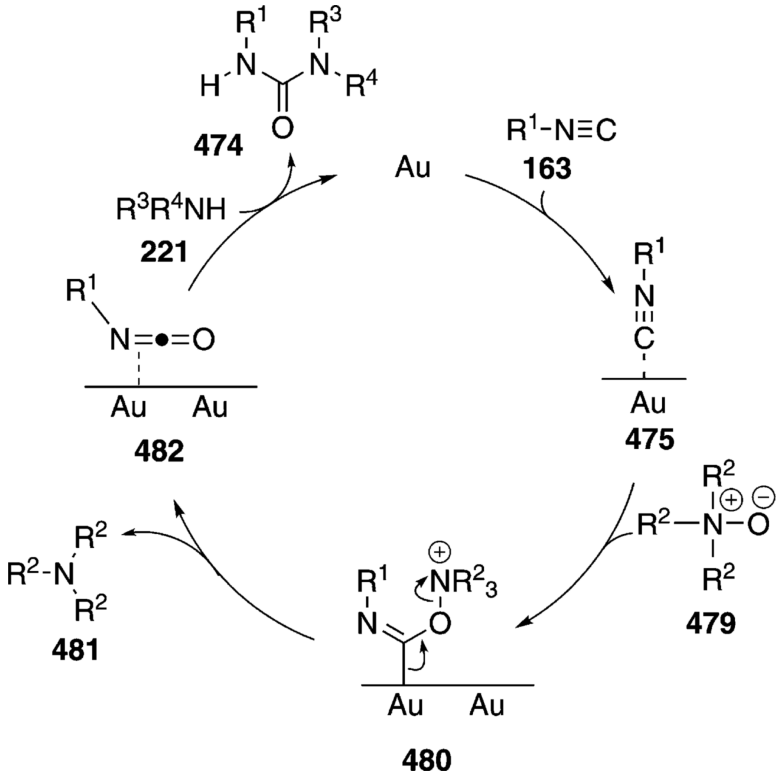


**Scheme 72.**
Gold-catalyzed isonitrile–amine coupling.

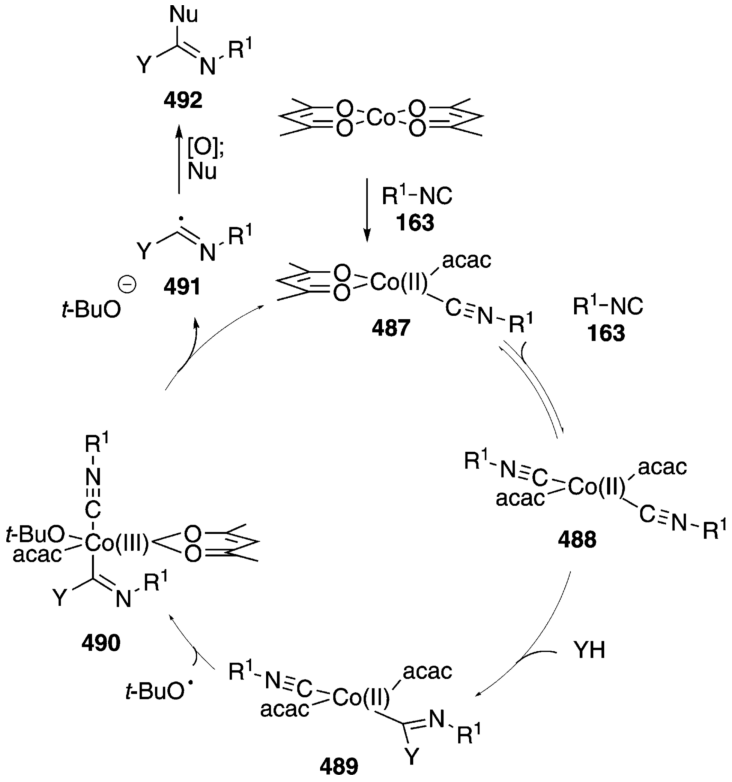


**Scheme 73.**
Cobalt-catalyzed urea synthesis.

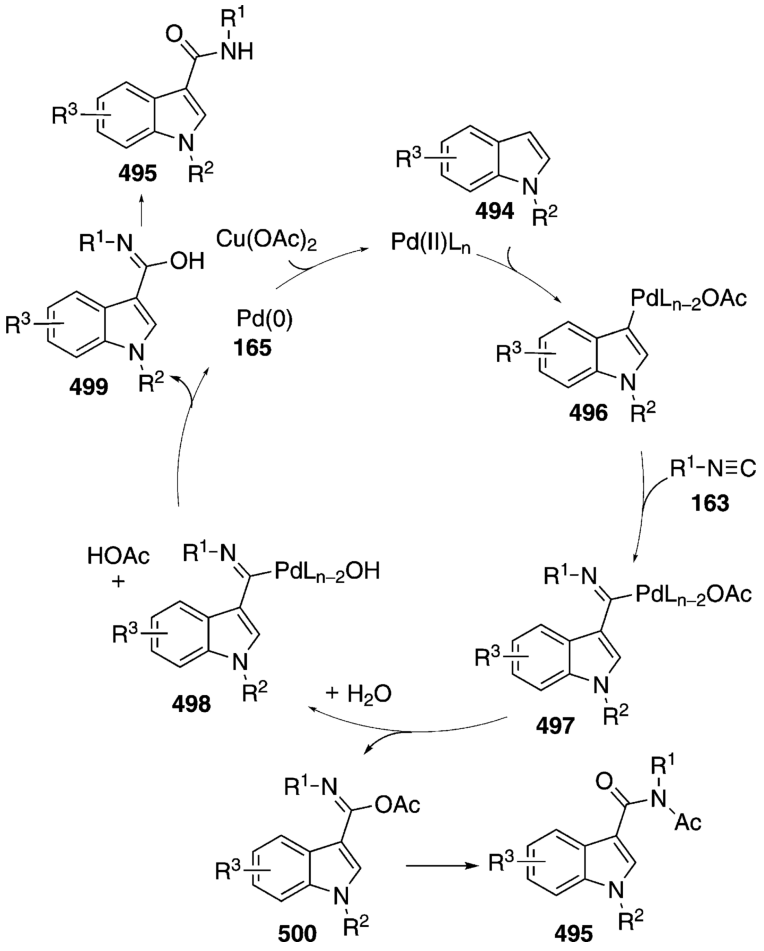


**Scheme 74.**
Palladium-catalyzed indole–isonitrile carboxamidation.

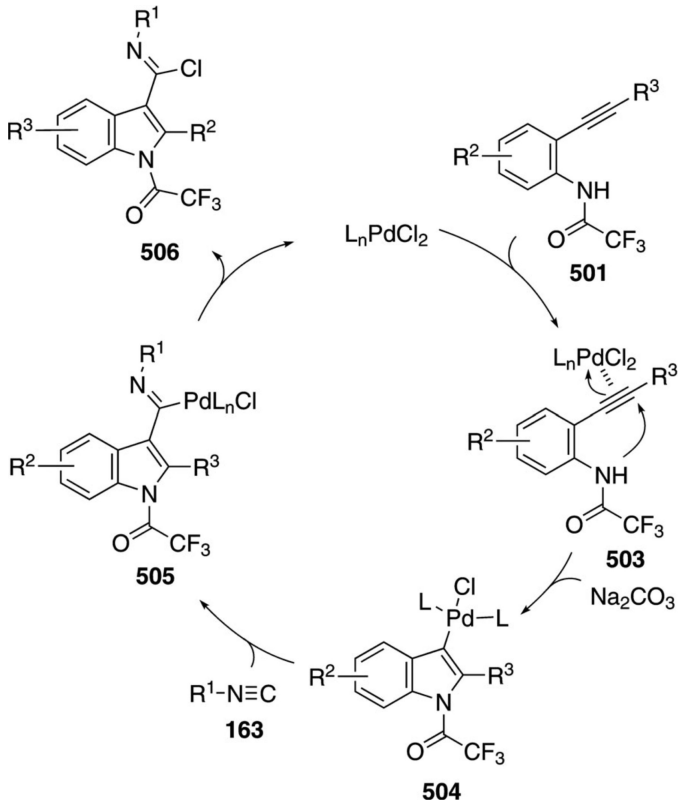


**Scheme 75.**
Palladium-catalyzed isonitrile–*ortho*-anilide coupling.

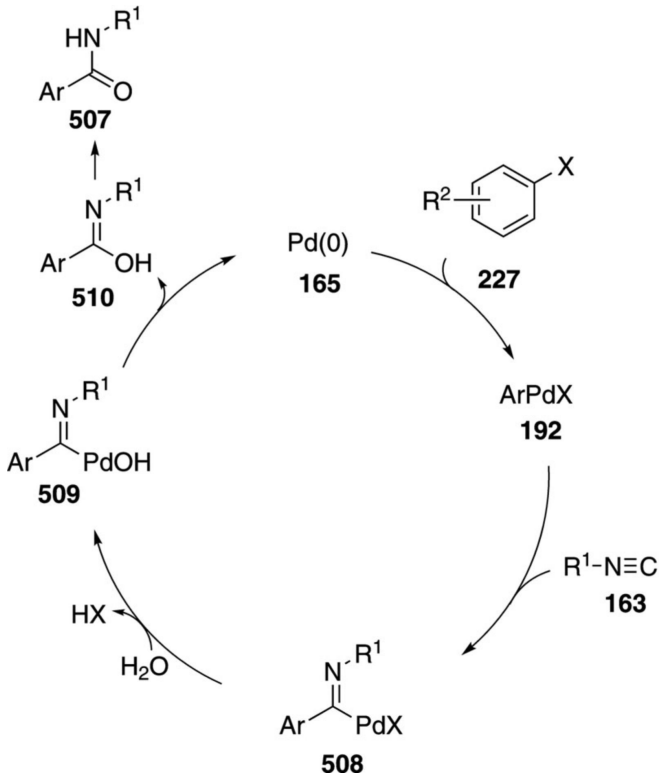


**Scheme 76.**
Palladium-catalyzed isonitrile–aryl halide coupling to amides.

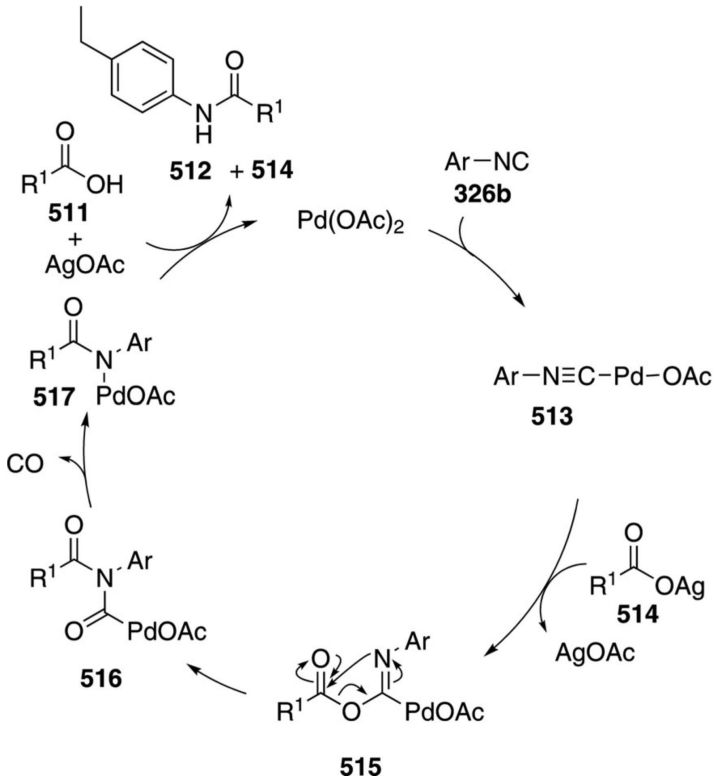


**Scheme 77.**
Palladium-catalyzed amide formation.

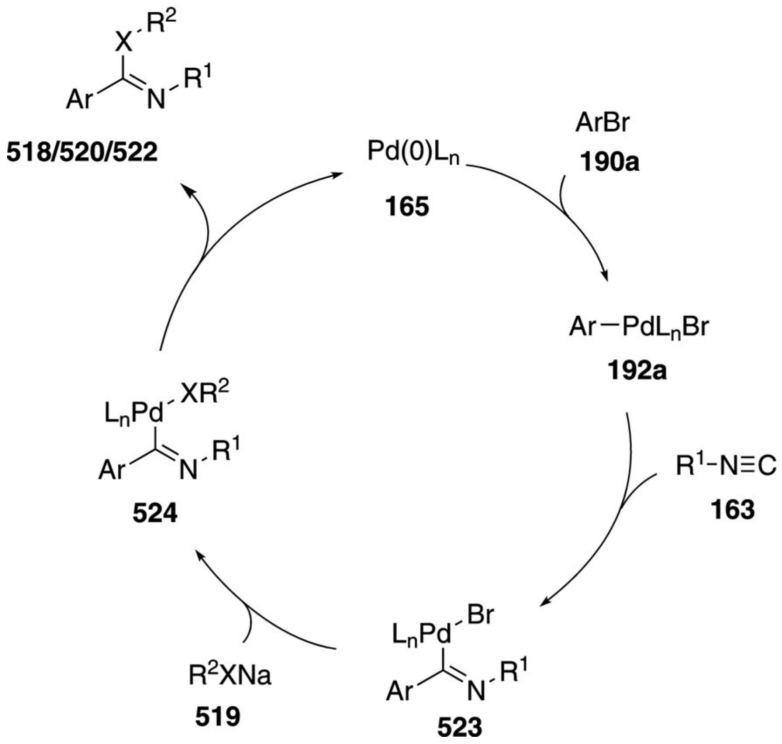


**Scheme 78.**
Palladium-catalyzed coupling of isonitriles to generate amidines and imidates.

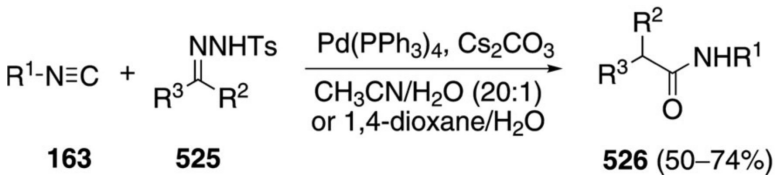


**Scheme 79.**
Palladium-catalyzed isonitrile–carbene coupling.

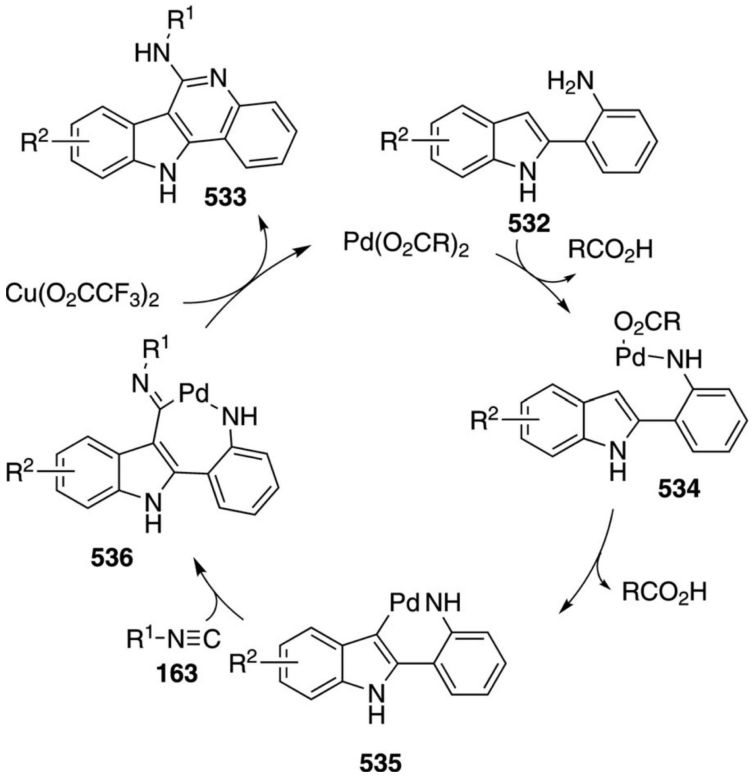


**Scheme 80.**
Palladium-catalyzed sequential C–H, isonitrile insertion.

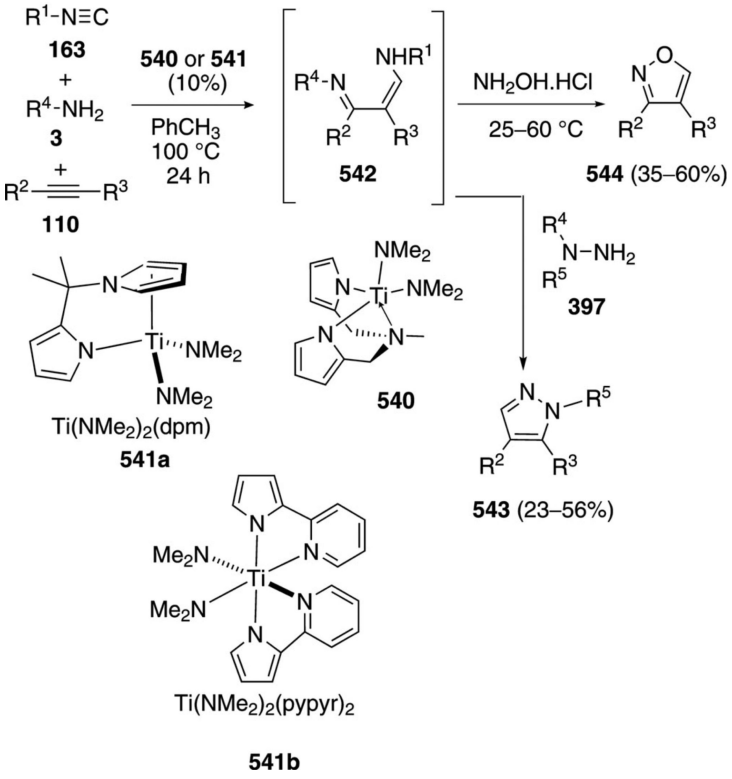


**Scheme 81.**
Titanium-catalyzed isoxazole synthesis.

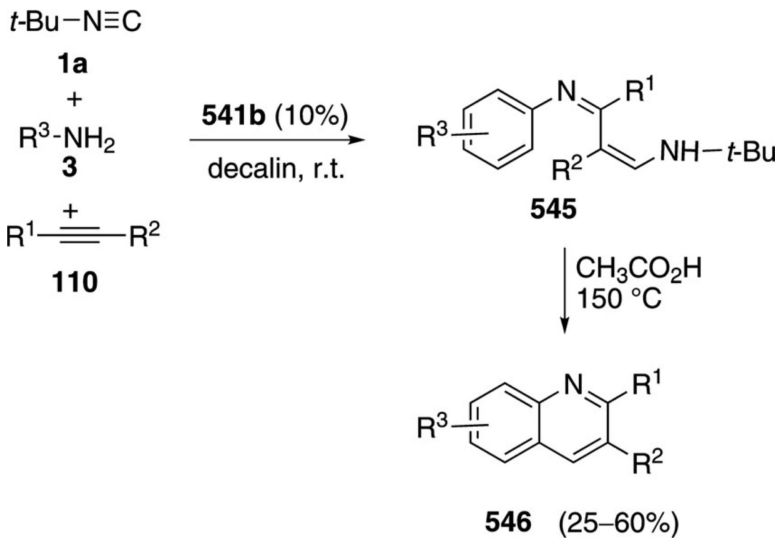


**Scheme 82.**
Titanium-catalyzed cyclization to quinolones.

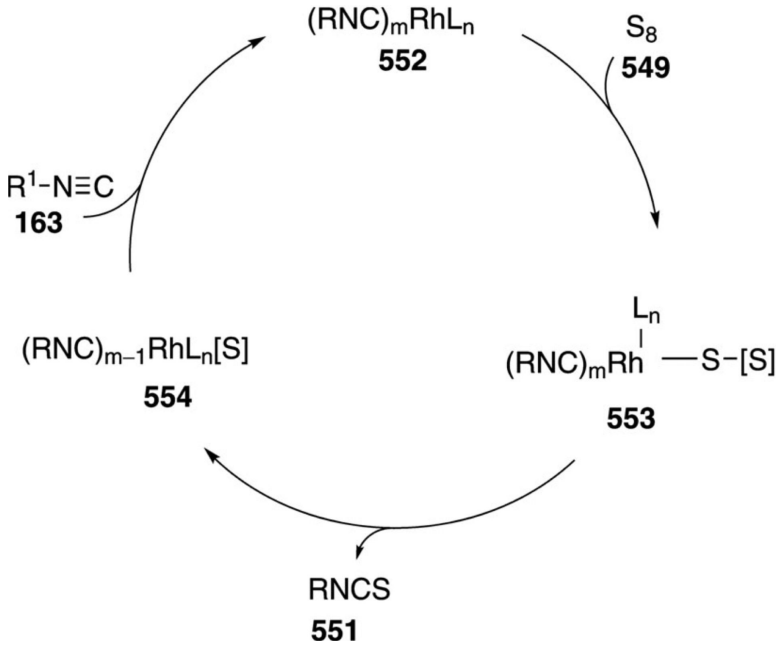


**Scheme 83.**
Rhodium-catalyzed isothiocyante synthesis.

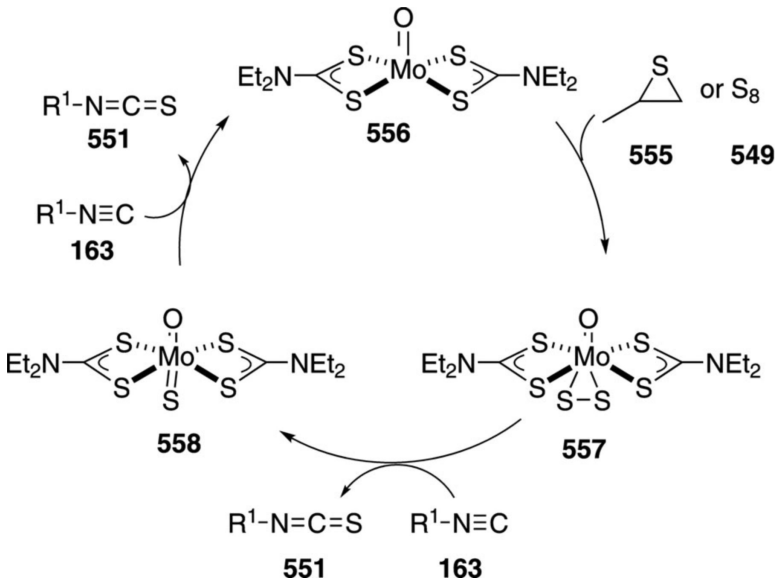


**Scheme 84.**
Molybdenum-catalyzed isothiocyanate synthesis.

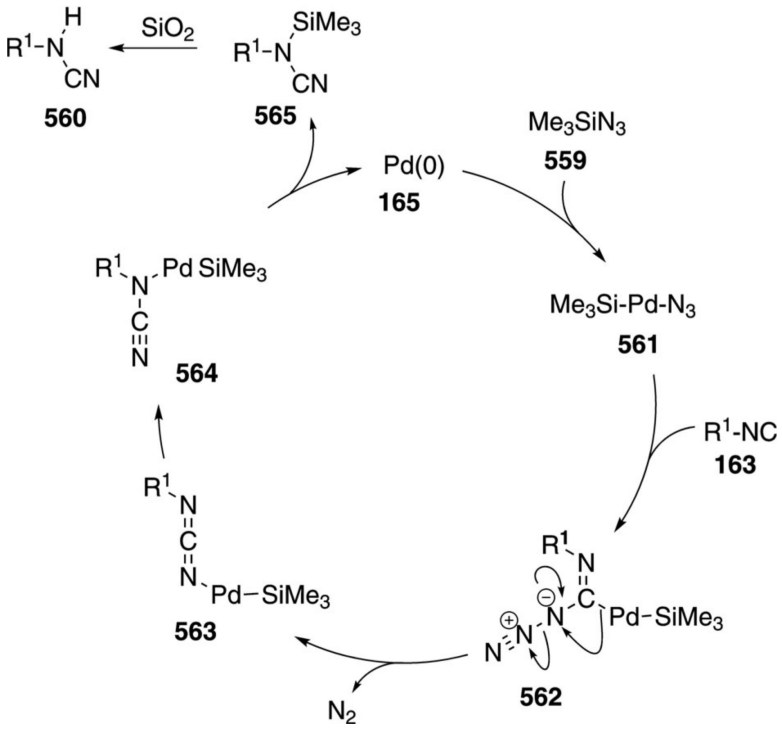


**Scheme 85.**
Palladium-catalyzed cyanamide synthesis.

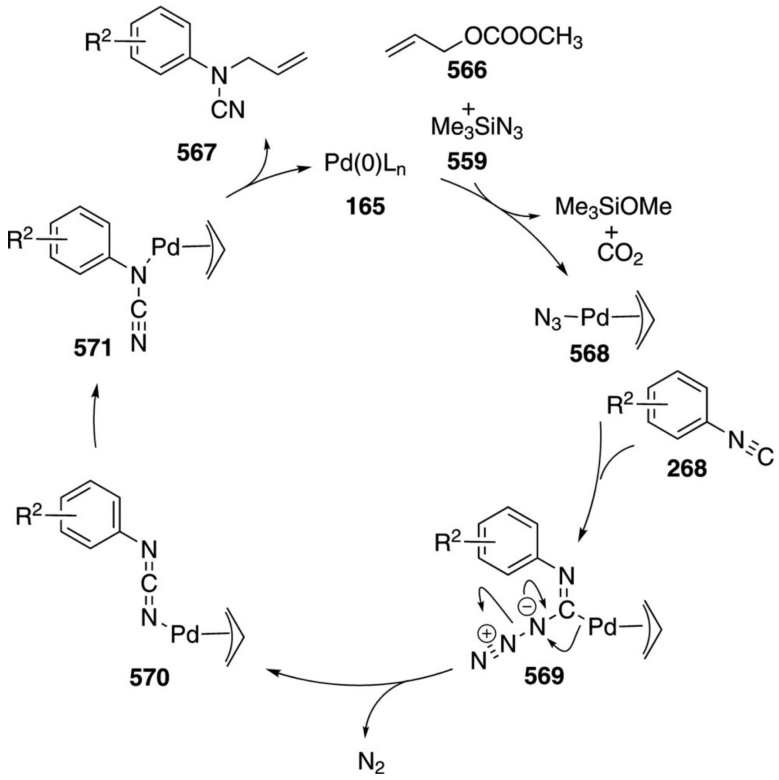


**Scheme 86.**
Palladium-catalyzed cyanamide synthesis.

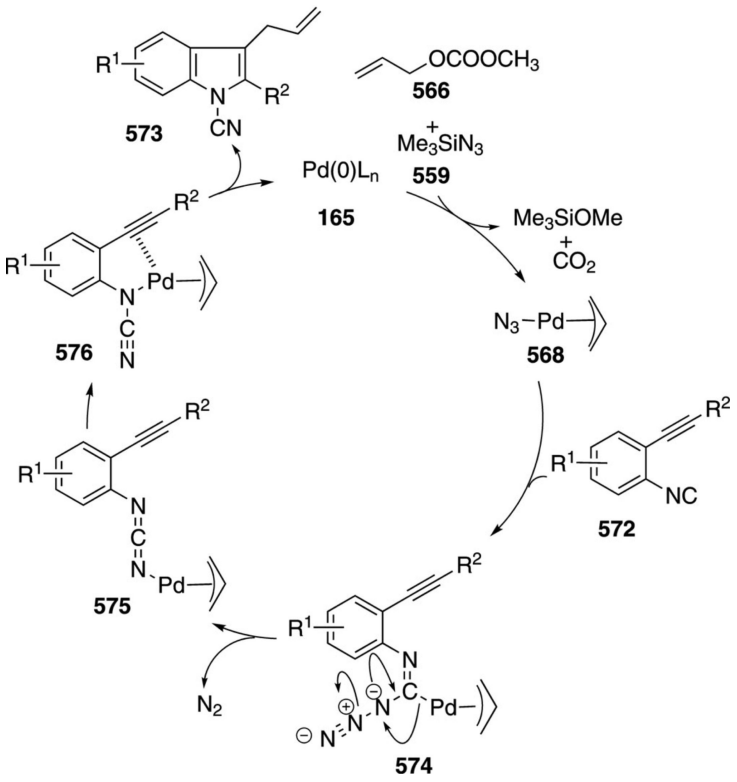


**Scheme 87.**
Palladium-catalyzed indole synthesis.

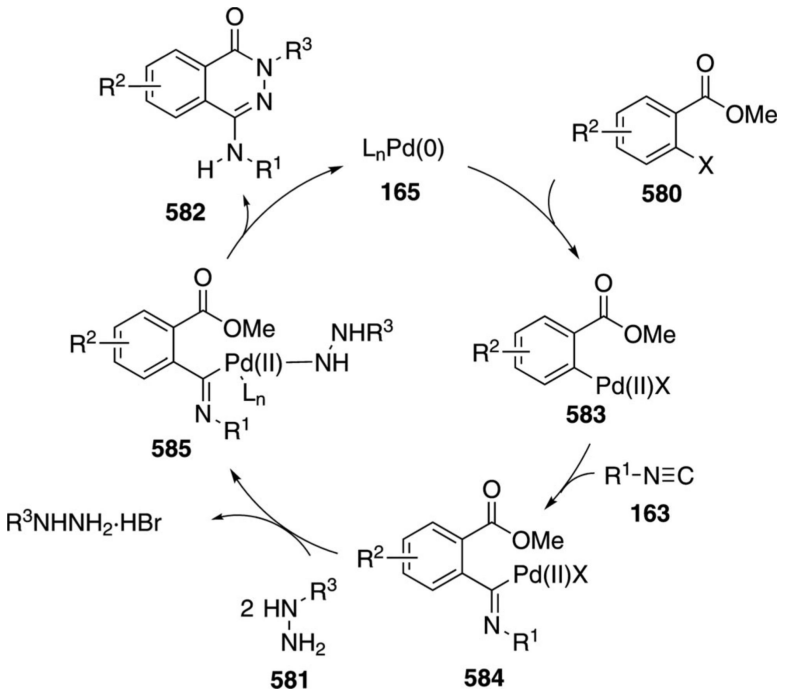


**Scheme 88.**
Palladium-catalyzed synthesis of aminophthaazin-1(2H)-ones.

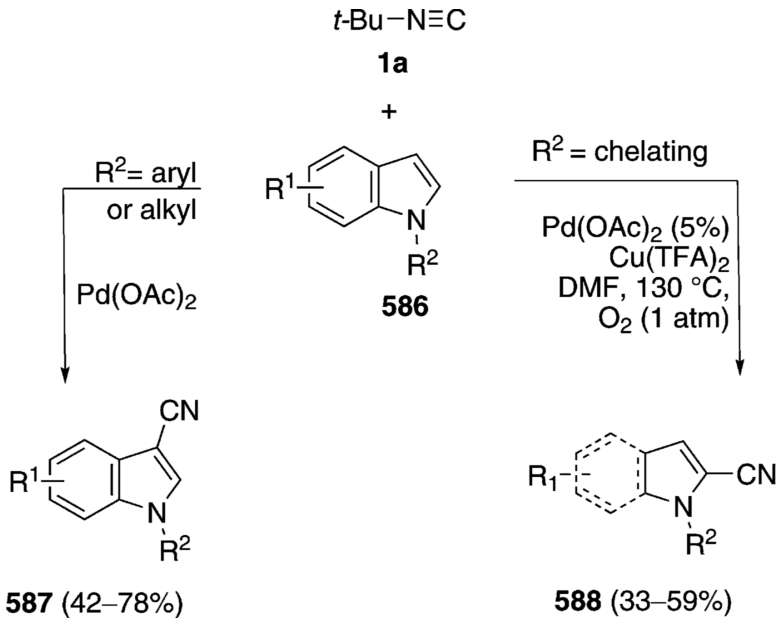


**Scheme 89.**
Palladium-catalyzed cyanations.

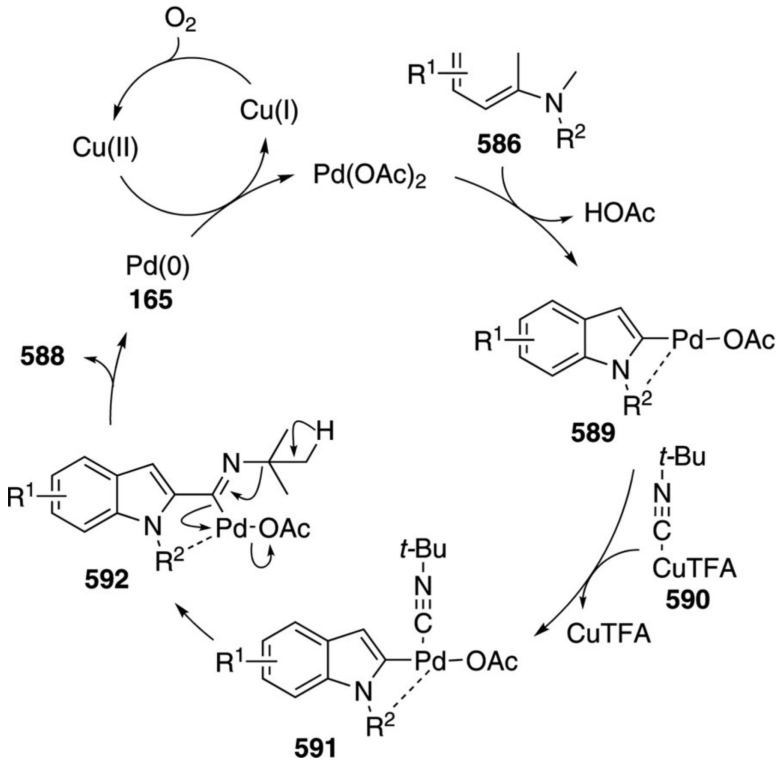


**Scheme 90.**
Palladium-catalyzed cyanation of indoles.

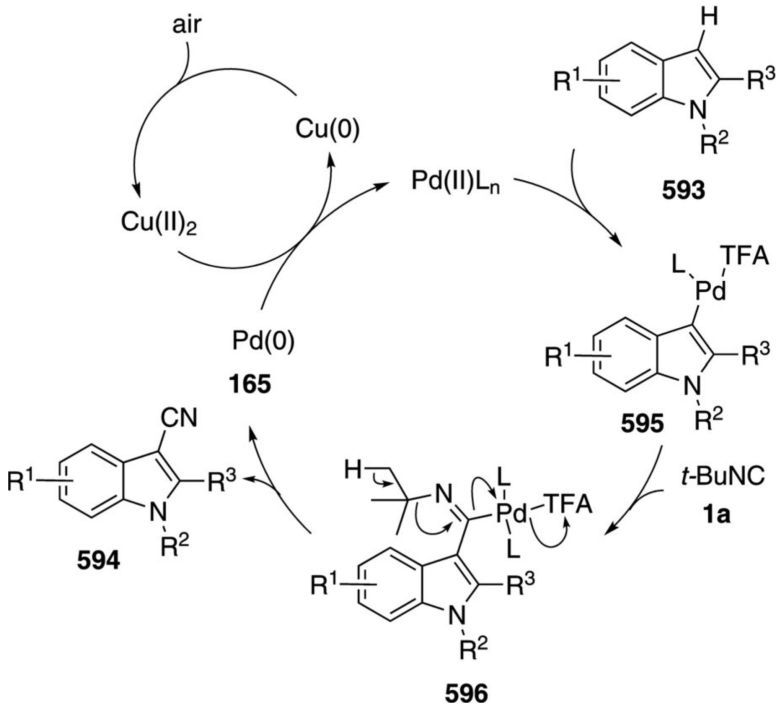


**Scheme 91.**
Palladium-catalyzed cyanation of 2-alkylindoles.

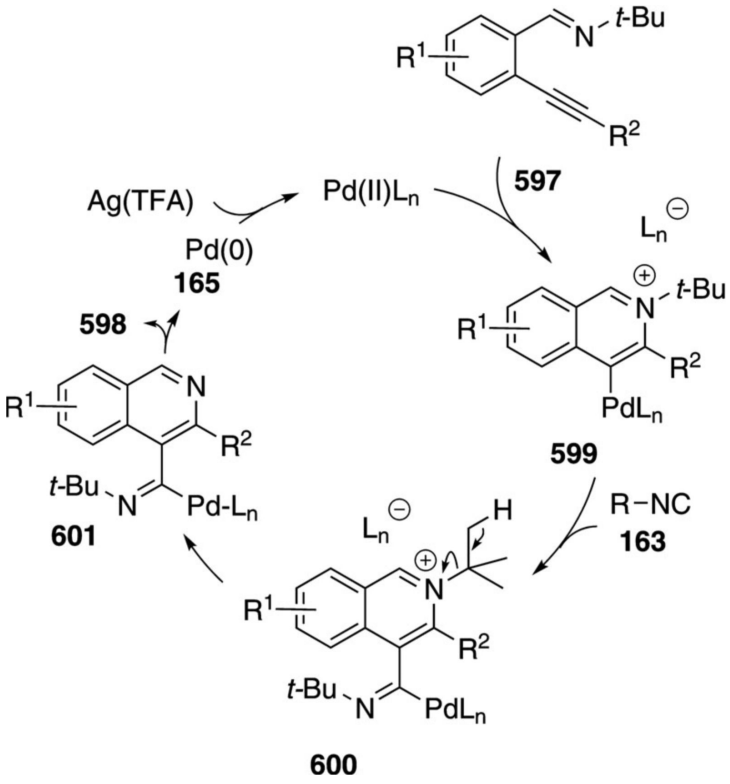


**Scheme 92.**
Palladium-catalyzed cyanation of 2-alkynylbenzaldimines.

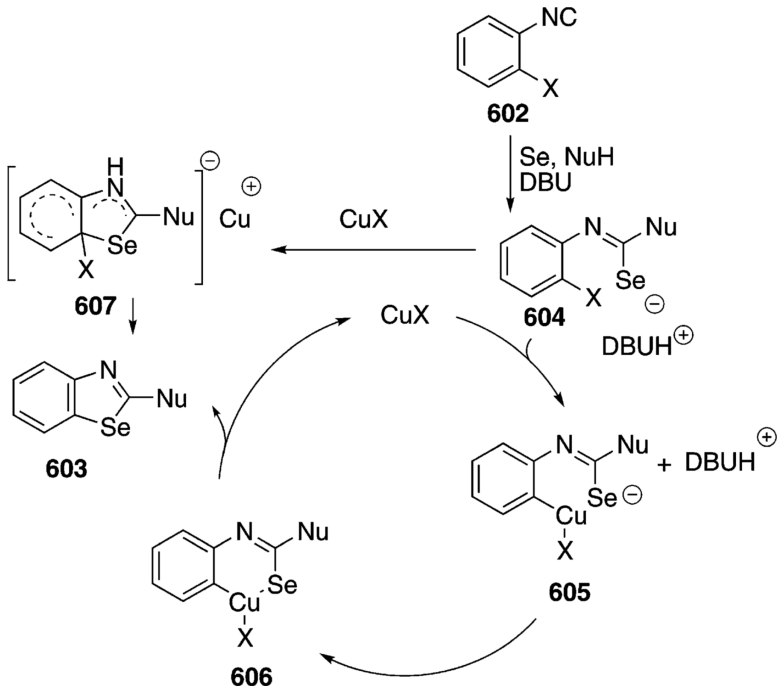


**Scheme 93.**

Copper-catalyzed synthesis of 1,3-benzeneselenazoles.

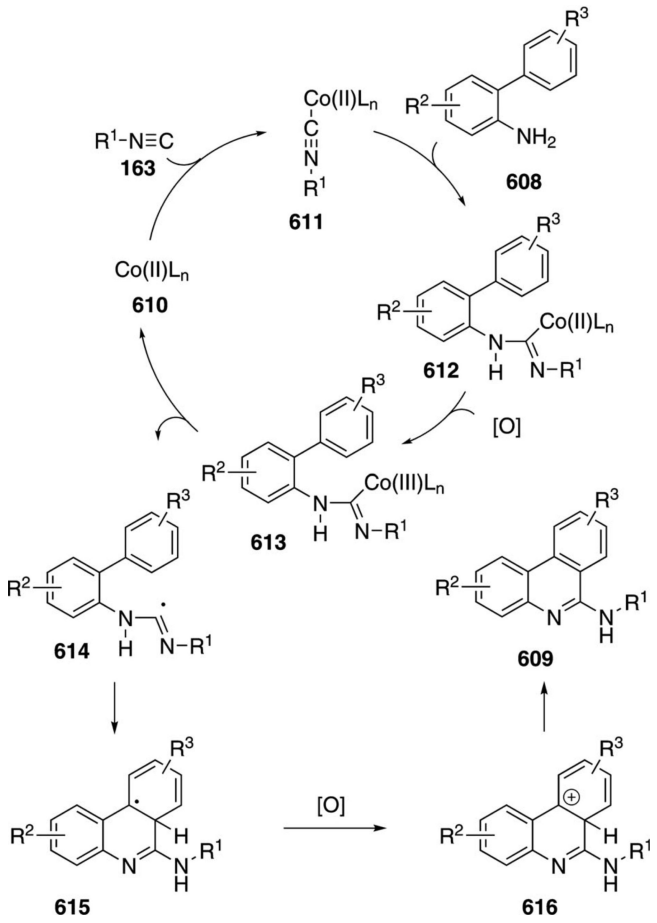


**Scheme 94.**
Cobalt-catalyzed synthesis of diiminofurans.

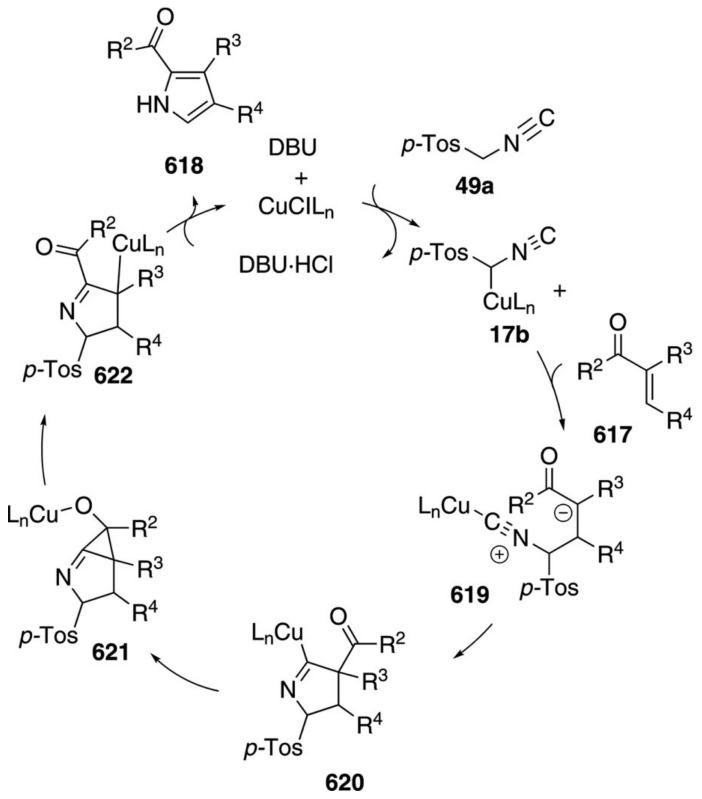


**Scheme 95.**
Copper-catalyzed pyrrole synthesis.

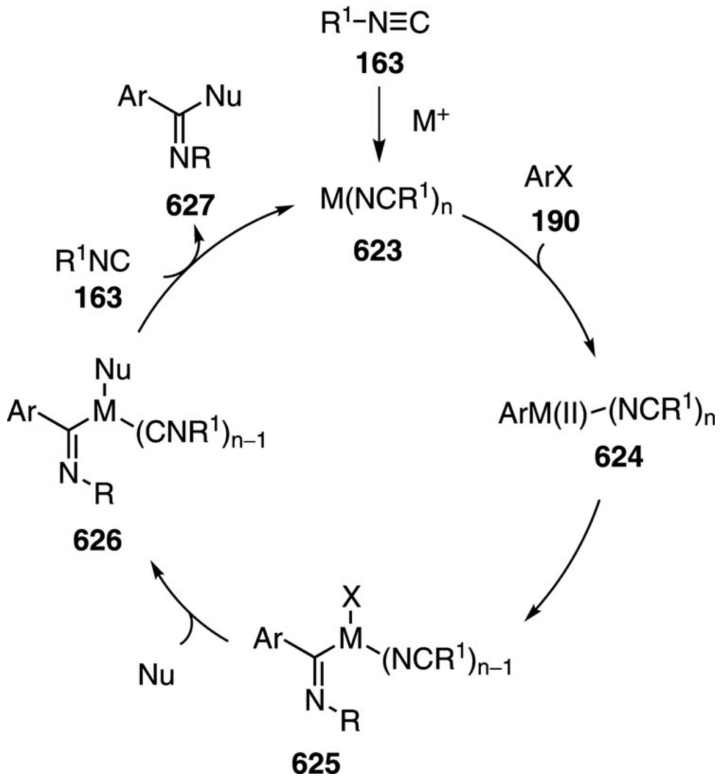


**Scheme 96.**
General isonitrile insertion mechanism.